THE USE OF CHITOSAN BEADS FOR THE ADSORPTION AND REGENERATION OF HEAVY METALS

PETER OGBEMUDIA OSIFO

Thesis submitted for the degree Philosophiae Doctor
in Chemical Engineering at the North-West University

Promoter: Prof. H.W.J.P. Neomagus
Co-promoter Dr. M.A. van der Gun

January 2007
Potchefstroom

DECLARATION

The material incorporated in this thesis is my own work, except where indicated to the contrary.

This material has not been submitted to another university for any other degree.

Signed

.....

P.O. Osifo

Student number: 12602981

Date: January 2007

Place: Potchefstroom

ACKNOWLEDGEMENTS

I wish to express my sincere gratitude to the following people and institutions for their assistance in the completion of this thesis:

Prof. Hein Neomagus for being my supervisor and Dr. Marius van der Gun for co-supervising this work.

Prof. L.R. Tiedt for all the Microscope analysis.

Mr. Jan Kroeze, for constructing my column.

Mr. Peter Cable from ROHM and HAAS, France; for donating Cation Exchange resin materials.

My wife for the patience and tolerance she showed through the years I took to complete this work.

My colleagues Collen Nkalanga and Hein van der Merwe for their encouragement throughout the period it take to complete this work.

My good friends Sampson Erevbenagie Osadolor, Solomon Obosogie, Gavin Eweka, Frank Ogagba and Modupe Ogunronbi for their prayers and encouragement.

Water Research Commission, South Africa for their financial support.

ABSTRACT

This work studied the removal of heavy metals from wastewater through the use of South African chitosan beads produced from locally available raw materials. For this purpose, chitosan beads were prepared from chitosan flakes that were synthesized from the chitin derived from the exoskeleton of the *Jasus lalandii*. The molecular weight and degree of deacetylation of the chitosan flakes were $9.4 \cdot 10^4$ g/mol and 83% respectively. When the flakes were converted into non-cross-linked beads, the molecular weight decreased slightly to $7.8 \cdot 10^4$ g/mol. Different beads were prepared ranging in size from 0.9 to 3.8 mm and the amount of glutaraldehyde used to crosslink the beads was varied between 0 and 4 vol%, in order to obtain beads with a different degree of cross-linking.

The beads were used as an adsorbent for heavy metals and were characterized for equilibrium and kinetic adsorption studies. The amine concentration, which is in direct relation to the adsorption capacity of non-cross-linked beads was determined as 4.9 mmol/g. The amine concentration decreased with an increasing glutaraldehyde concentration and a decreasing bead size. Cross-linking was however necessary to make the chitosan stable in acidic media, and a degree of cross-linking larger than 18% made the chitosan beads insoluble at a pH of 2.

Two models, the Langmuir isotherm model and a pH-model were used to fit equilibrium adsorption data. Although the Langmuir model gave good fits, the obtained parameters were pH dependent. On the other hand, the pH-model, which was derived from: i) the adsorption equilibrium reaction between the chitosan and the metal; ii) the acid base properties of chitosan; and iii), a mass balance of the different forms of nitrogen in the chitosan, could satisfactory describe the adsorption using pH independent variables. When deriving the pH-model the effect of pH on the degree of protonation of the adsorbent was considered. The model was fitted with the maximum adsorption capacity, and the fitted values were in close agreement with the amine concentration. The desorption of the metal from the chitosan could also be predicted well with this model, indicating a reversible complexation of the metal on the chitosan, making the recovery and possible re-use of the metal possible.

The kinetics of the adsorption process were described with a shrinking core model, where an instantaneous adsorption reaction was assumed. From this model, effective diffusion coefficients were determined from batch experiments.

The adsorption was also studied in a column and the experiments were modeled with a CSTR's in series model, using the experimentally determined adsorption equilibrium data. The breakthrough curve could be described reasonably well with this model, and the fitted effective diffusion coefficient was close to the one determined in the batch experiments. The adsorption capacity of the locally sourced and produced chitosan beads was high in comparison to the values indicated in the literature for other adsorbents. It was also found to be higher than that of either the commercially produced chitosan or the ion-exchange resin. The regeneration of the metal from the chitosan was effective. Multiple adsorption/desorption experiments were also carried out, and it was found that the adsorption increased for the second and third cycle, but decreased for the fourth and fifth ones. After the fifth cycle, the chitosan was physically damaged and could not been used anymore. This degeneration of the beads across multiple adsorption/desorption cycles was found to be the major concern blocking the uptake of the studied chitosan beads in industrial applications.

OPSOMMING

Die studie bestudeer die verwydering van swaar metale uit industriele afvalwater deur gebruik te maak van Suid Afrikaans geproduseerde chitosan korrels. Die chitosan korrels is vervaardig uit afval material afkomstig van die omgewing. Die korrels is vervaardig uit chitosan vlokkies wat afkomstig is vanuit chitin, wat afkomstig is van *Jasus lalandii.* Die chitosan vlokkies het 'n molekulere massa van $9.4 \cdot 10^4$ g/mol en die graad van deasetylering van 83%. Met die verandering van die chitosan vlokkies na die chitosan korrels het die molekulere massa afgeneem na $7.8 \cdot 10^4$ g/mol. Die geproduseerde chitosan vlokkies se grootte varieer tussen 0.9 en 3.8 mm. Die konsentrasie glutaraldehied wat gebruik is om die korrels te kruisbind is gevarieer tussen 0 tot 4 vol% om sodoende verskilllende grade van kruisbinding te verkry.

Die chitosan korrels word as adsorbent vir swaar metale gebruik en word dus gekaraktiriseer in terme van die ewewigs en kinetiese adsorbsie studies. Die amien konsentrasie wat direk verband hou met die adsorbsie kapasiteit van swaar metale op ongekruisbinde korrels is bepaal as 4.9 mmol/g. Die amien konsentrasie neem af met die toename in kruisbinding en die afname van die korrel grootte. Kruisbinding met glutaraldehied is egter noodsaaklik om te verseker dat die korrels stabiel is in 'n suur omgewing. 'n Graad van kruisbing groter as 18% verseker die onoplosbaarheid van die chitosan korrels by 'n pH van 2.

Die ewewigs adsorbsie data is beskryf deur twee modelle, die Langmuir isoterm model en die pH-model. Alhoewel die Langmuir model 'n goeie passing lewer is die parameters verkry van die data pH afhanklik. Die pH-model, wat afgelei is van: i), die adsorbsie ewewigs reaksie tussen die chitosan en die metaal; ii), die suur basis eienskappe van die chitosan; en iii), verkillende vorms van die stikstof massabalans in die chitosan, beskryf die adsorpsie voldoende deur gebruik te maak van pH onafhanklike veranderlikes. Die model is gepas deur gebruik te maak van die maksimum adsorpsie kapasiteit, die model pas die experimentele waardes en korrelleer goed met die amien konsentrasie. Die herwinning van die metaal vanaf die chitosan word ook deur die model beskryf en toon die omgekeerde komplekëring van die metaal op die chitosan wat die herwinning en hergebruik van die metaal moontlik maak.

Die adsorbsie kinetieka word beskryf deur die kern verkleinings model wat dit moontlik maak om aan te neem dat 'n oombliklike adsorbsie reaksie bestaan. Vanaf die model kan die effektiewe diffusie koeffisiënte bepaal word.

Die adsorbsie is ook bestudeer deur gebruik te maak van kolom studies en die eksperimente is dan gemoduleer deur gebruik te maak van die Tenk Gemengde Reaktor reeks model. Die model beskryf die deurbreek kurwe redelik goed en die passings effektiewe diffusie koeffisiënt is baie naby aan die koeffisient bereken gedurende die enkellading eksperimente. Die adsorpsie kapasiteit vir die Suid Afrikaans geproduseerde chitosan is hoër as die adsorpsie kapasiteite getoon in die literatuur vir ander adsorpsie materiale. Dit is ook bewys dat die adsorpsie kapasiteit hoër is as vir kommersiele chitosan en ioon-uitruilings harse. Die herwinning van die metale is effektief. Gekombineerde adsorpsie/herwinnings experimente toon aan dat die adsorpsie toeneem vir die tweede en derde siklus, maar afneem vir die vierde en vyfde siklus. Die chitosan korrels is meganies onstabiel na die vyfde siklus en kan nie verder gebruik word nie. Die eienskap word gesien as 'n negatiewe punt wat die industriele aanwending van chitosan korrels beperk.

TABLE OF CONTENTS

LIST OF TABLES

LIST OF FIGURES

GLOSSARY

Adsorption capacity: The amount of the adsorbed metal in mg per unit mass of dry chitosan measured in gram.

Adsorption column: Column packed with chitosan beads that is used for metal adsorption.

Bed-volume: The volume of the packed beads in the column excluding the void space between the beads in the bed.

Cross-linking: The chemical binding of two chitosan polymer chains by glutaraldehyde

Deacetylation: The removal of acetyl group from chitin to produce chitosan.

Degree of cross-linking: The fraction of the amine group that is used for cross-linking in the chitosan polymer chain.

Degree of deacetylation: The fraction of the amine group in the chitosan polymer chain.

Demineralization: The process of removing minerals, in the form of mineral ions, to purify the chitin.

Deproteinization: the process of removing protein from the raw lobsters to purify the lobsters shell for chitin production.

Mass fraction of water in the beads: The mass of water in the beads divide by the total mass of the beads.

Mass fraction of chitosan in the beads: The mass of chitosan in the beads divide by the total mass of the beads.

Maximum adsorption capacity: The maximum amount of adsorbed metal in mg per gram of dry chitosan.

Chapter 1 Introduction

1.1 Motivation

Water conservation and management are of global importance in attempts at meeting peoples water requirements. South Africa, situated in an arid area, lacks sufficient useable water to meet the needs of the people, especially those in the rural areas. In South Africa, the majority of people obtain water from streams and wells, which are often polluted. This pollution is partly the result of the increased industrial activity of the past few decades. This activity has produced different physical and chemical pollutants that find their way into water bodies. This has led to the amendment of the Environmental Conservation Act and Regulation, Act No 73 of 1998 and the Water Services Act and Regulation, Act No 108 of 1997, to more stringently regulate the types of effluent that should be allowed in the environment. These acts impose the following measures:

- The purification of effluent to a predetermined standard before discharge to the original water source, as stipulated in Table A-1, Appendix A;
- The requirement of a permit to use certain quantities of water;
- The requirement that effluent purification become an integral part of the industrial process;
- The requirement of a permit for the erection or enlargement of water care works.

The Acts attempt to maintain a balance between the demand for water and its deterioration in quality by imposing duties on the users, and by reducing the exemptions upon industrial users of water. Two of the more significant duties are first, to purify the effluent and second, to return the water and effluent to the point of origin. These duties play an important role in pollution control as the responsibility falls upon the user to provide evidence to the Department of Water and Forestry (DWAF) that requirements have been complied with, thereby promoting self regulation on the part of the industry.

The World Summit on Sustainable Development held in Johannesburg (South Africa, 2002) stressed the impact of industrial effluents on the sustainability of water resources. This prompted governments to be more stringent in dealing with these problems. Table A-2 (Appendix A) presents the highlights of the South African environmental legislation on wastewater emissions and health and safety in the industries.

In South Africa, the primary contribution to water pollution is the effluent from electroplating facilities, mining industries, and other process industries. The major contaminants arising in the effluents of metal finishing industries are heavy metals, associated salts, cleaning acids, and solvents (Cowan, 1998). Table A-3 (Appendix A) illustrates the principal constituents and concentrations in the untreated effluent from metal finishing processes (Buckley, 1987).

Heavy metals, even in trace amounts, are toxic and are not biodegradable. They must thus be removed from the wastewater to meet the stipulated environment requirements. The effects of heavy metals on the environment and on human health are illustrated in Appendix A, Table A-4 (DWAF, 1998).

The removal of trace metals from effluent water by way of precipitation, ion exchange, membrane separation, desalination and distillation are sometimes difficult, because of the inefficiency of the processes. Adsorptions processes have by comparison been shown to be promising alternatives for the removal of these trace metals (Muzarrelli, 1974). Treatment processes by adsorption have been achieved with activated carbon (Dastgheib and Rockstraw, 2002), corncobs (Vaughan *et al.*, 2001), marine algae (Yu and Kaewsarn, 1999), chitosan (Huang *et al.*, 1996), and activated sludge (Atkinson *et al.*, 1998). However, a review by Bailey *et al.* (1999), on the potential of using low-cost adsorbents for heavy metals, shows that chitosan has the highest adsorption capacity for most heavy metals. Adsorption capacity values of 796 mg Pb/g chitosan, 92 mg Cr(III)/g chitosan and 558 mg Cd/g chitosan were reported. Chitosan has the added advantage to be transformable into flakes, beads, membranes and hollow fibers for the removal of trace metal ions from aqueous solutions (Guibal, 2004).

Chitosan, a derivative of chitin, the second largest biopolymer material found in nature, can be extracted from fungi, and in large quantities, from the exoskeleton of crustaceans such as crabs, prawns, shrimps, krill and crawfish. Bailey *et al.* (1999) show that approximately 40,000 tons of chitin is produced from the crustacean waste of fisheries annually. This can be used for the many different applications listed in Table A-5 (Appendix A). In the manufacturing of chitosan, flakes are normally obtained, but this formulation is not efficient in adsorption processes due to its relative poor adsorption characteristics. Also, flaky materials can readily clog adsorption columns causing a large drop in pressure and hence high operation costs. To

overcome the problems of adsorption performance and clogging, flakes are transformed into gel beads.

Cross-linking of the adsorbent has been found to be another essential step toward metal recovery because non-crosslinked chitosan beads are soluble at low pH. Different cross-linking agents, such as glutaraldehyde and glycerol-polyglycidylether have been proposed for this purpose (Becker *et al.*, 1999).

Most of the research done on the use of chitosan, either as beads or flakes, are batch studies (*e.g.* Rorrer *et al.*, 1993; Juang *et al.*, 1997; Erosa *et al.*, 2001). Relatively few studies have been reported on continuous dynamic systems using an adsorption column (*e.g.* Guibal *et al.*, 1999; Gao *et al.*, 2000). For practical applications, however, the use of a fixed bed column is encouraged because it can be operated in a continuous mode, can treat large volumes of wastewater, and the adsorbent can be easily recycled after use without too much loss in mass of the adsorbent.

In this study, the exoskeleton of Cape rock lobster (*Jasus lalandii*) is used because of its large availability in South Africa. The chitin extracted from the crustacean is successively converted to chitosan flakes and then to chitosan beads used for removing heavy metals from aqueous streams. In the adsorption of heavy metals onto chitosan, it is known that pH influences the adsorption parameters, and the effects of pH on the mechanism of copper uptake are investigated. Batch studies are conducted to determine equilibrium and kinetic adsorption parameters with a pH-model from adsorption and desorption data. The parameters are used to describe column operations, which is the practical assessment of the chitosan material. Finally, the study of multiple cycles of adsorption and desorption in a column are performed, which has not yet been presented in the open literature.

1.2 Objectives

The overall objective is to investigate the suitability of chitosan beads, derived from the *Jasus lalandii*, for the adsorption and recovery of heavy metals from wastewater.

The specific objectives in this study are defined as follows:

- To prepare and characterize cross-linked chitosan beads;

- To investigate the metal-adsorbent binding mechanism;
- To develop and validate a thermodynamic model that includes the effect of pH;
- To relate the thermodynamic and kinetic properties with the physical characterization of chitosan;
- To develop and validate a chitosan adsorption column, including equilibrium and kinetic adsorption data;
- To asses the efficiency of a chitosan loaded adsorption column operated with multiple cycles of adsorption and desorption.

1.3 Scope of the Project

This thesis reports on the use of chitosan beads derived from *Jasus lalandii* for the removal of heavy metals from wastewater. Chapter 1 introduces and motivates this process.

In Chapter 2, the preparation of the different chitosan beads is given, and in Chapter 3, the manufactured beads are characterized thoroughly by different physical and chemical methods.

In Chapter 4, an advanced equilibrium adsorption model is presented and validated with a large number of experimental results. The results are compared with literature and a comparison is made between the adsorption equilibrium results and the characterization results, as given in Chapter 3.

Chapter 5 deals with the kinetics of the adsorption process, and presents a particle model based on the shrinking core theory. This model is validated with batch studies, in which the adsorption loading of the chitosan beads is measured in time. Based on the batch kinetic studies, a chitosan bead adsorption column is modeled and tested with experimental breakthrough results. Finally, the efficiency of the beads in multiple adsorption and desorption cycles are measured and discussed.

General conclusions and recommendations are given in Chapter 6 and a critical evaluation of the obtained results in conjunction with the practical applicability of chitosan beads for the removal of heavy metals from wastewater is made.

References

Atkinson, B.W., Bux, F. & Kasan, H.C. 1998. Waste activated sludge remediation of metal-plating effluents. *Water SA*, 24 (4), 355-359.

Bailey, S.E., Olin, T.J., Bricka, R.M. & Adrian, D. 1999. A review of potentially low-cost sorbent for heavy metals. *Water Research*, 33 (11), 2469-2479

Becker, T., Schlaak, M. & Strasdeit, H. 2000. Adsorption of nickel(II) , Zinc(II) and Cadmium(II) by new chitosan derivatives. *Reactive and Function Polymers*, 44, 289-298.

Buckley, C. 1987. An investigation into the water management and effluent treatment in the processing (i) pulp and paper (ii) metals (iii) fermentation products and (iv) pharmaceutical products. *WRC Report No 106/2/87*, By Pollution Research Group Department of Chemical Engineering University of Natal.

Cowan, J.A.C. 1998. The development of management strategies and recovery systems for heavy metal wastes. *WRC Report No 589/1/98.*

Dastgheib, S.A. & Rockstraw, D.A. 2002. Systematic study and proposed model of the adsorption of binary metal ion solutes in aqueous solution onto activated carbon produced from pecan shells. *Carbon*, 11 (40), 1853-1861.

Department of Water Affairs Forestry (DWAF). 1998. Quality of domestic water supplies, Assessment Guide. Volume 1. 2nd Edition. The Department of Water Affairs and Forestry, Department of Health and Water Research Commission.

Erosa, D.M.S., Medina, T.I.S., Mendoza, R.N., Rodriguez, M.A. & Guibal, E. 2001. Cadmium sorption on chitosan sorbents: Kinetic and equilibrium studies, *Hydrometallurgy*, 61, 157-167.

Gao, Y., Lee, K-H., Oshima, M. & Motomizu, S. 2000. Adsorption behavior of metal ions on crosslinked chitosan and the determination of oxoanions after pretreatment with a chitosan column. *Analytical Science,* 116, 1303-1308.

Guibal, E. Milot, C. & Roussy, J. 1999. Molybdate sorption by cross-linked chitosan beads: Dynamic studies. *Water Environment Research,* 71, 1-17.

Guibal, E. 2004. Interaction of metal ions with chitosan-based sorbents: a review. *Separation and Purification Technology*, 38, 43-74.

Huang, C., Chung,Y. & Lion, M. 1996. Adsorption of Cu(II) and Ni(II) by pelletized biopolymer. *Journal of Hazardous Materials*, 45: 265-277.

Juang, R.S., Tseng, R-L., Wu, F.C. & Lee, S-H. 1997. Adsorption behavior of reactive dyes from aqueous solution on chitosan. *Journal of Chemical Technology. Biotechnology,* 70, 391-399.

Muzzarelli, R.A.A. 1974. Natural chelating polymers: Alginic acid, chitin and chitosan. Pergamon press.

Rorrer, G.L, Hein, T. & Way, D.J. 1993. Synthesis of porous-magnetic chitosan beads for removal of cadmium ions from waste water. *Industrial Engineering Chemical Research,* 32, 2170-2178.

Vaughan, T., Seo, C.W. & Marshall, W. 2001. Removal of selected metal ions from aqueous solution using modified corncobs. *Bioresource Technology*, 78, 133-139.

Yu, Q. & Kaewsarn, P. 1999. Binary adsorption of copper(II) and cadmium(II) from aqueous solutions by biomass of marine alga *Durvillaea Potatorum. Separation Science and Technology*, 34(8), 1595-1605.

Chapter 2 Preparation of chitosan beads

2.1 Introduction

In this chapter, the preparation of chitosan beads and the consecutive crosslinking of the beads are presented. In Section 2.1.1, the sources of chitin and its structure are given and in Section 2.1.2, the chitosan structure and its preparation methods are discussed. A brief literature survey concerning the preparation of chitosan is presented in Section 2.2 and in Section 2.3 the experimental procedures for the formulation of beads are described.

2.1.1 Chitin

Although chitosan itself is found in some fungi and can be isolated from their cell walls, it is predominantly prepared from chitin, a linear, high molecular weight, crystalline polysaccharide consisting of β-(1-4) linked N-acetyl-D-glucosamine units having acetamide groups at the C-2 position as circled in Figure 2.1. A major source of chitin are the shells of arthropods (exoskeletons), which contain 20-50% chitin on a dry weight basis (Kurita, 2001).

The shells of crustaceans, such as crabs and shrimps, are easily available as waste from seafood processing industries and are used for the commercial production of chitin *e.g.* by Biopolymer Engineering, USA and France Chitine, France. Other sources for chitin include insects, krill, crayfish, jellyfish and algae (Muzarrelli, 1974).

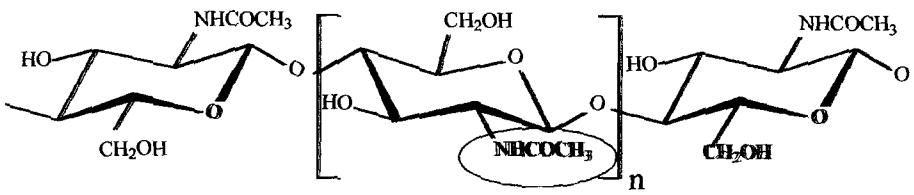

Figure 2.1: Structure of chitin.

2.1.2 Chitosan

An alkaline treatment is used to convert chitin into chitosan, a linear β-(1-4) linked D-glucosamine unit with the characteristic features of the amine group in the polymer chain as depicted in Figure 2.2.

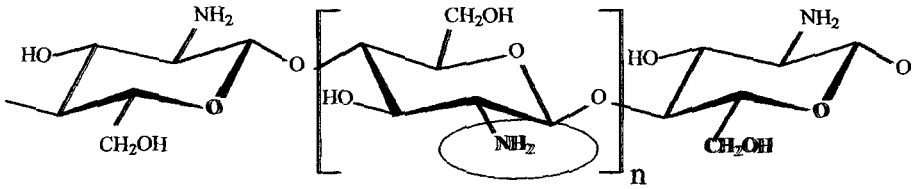

Figure 2.2: Structure of chitosan.

Other reaction methods for the preparation of chitosan such as the use of hydrochloric acid have been described. This reaction treatment is however associated with a degradation of the polymer chain (Muzzarelli, 1974) and is therefore not desirable. Chitosan prepared from chitin is a solid material that is obtained in the form of flakes or powder. It has been shown that in these forms the material is highly crystalline. This makes flakes and powder less suitable as an adsorbent as they are less hydrophilic in aqueous systems resulting in an increase in mass transfer resistance. Chitosan's solubility in acetic acid is used to reduce the crystallinity by converting flakes into gel beads. This modification is used to expand the polymer network which has been found to improve the adsorption kinetics and the adsorption capacity (Rorrer *et al.*, 1993; Guibal, 2004).

2.2 Literature survey

The literature covers the preparation of chitosan flakes starting from chitin recovery, moving through the deacetylation of chitosan flakes, the production of chitosan beads from flakes, and finally, the cross-linking of chitosan beads.

2.2.1 Extraction of chitin from shell waste

Different methods for the extraction of chitin from shell waste have been described (*e.g.* Muzzarelli, 1974; No and Meyer, 1997). In these methods, the extraction is achieved in three

basic steps; i) protein separation, ii) calcium carbonate separation and iii) removal of color pigments. The first step involves the removal of proteins by treatment with an aqueous 5% NaOH solution at 100° C for 1-6 h. After deproteinization the shells are decalcified with 1 N hydrochloric acid (1:15 ratio w/v) at room temperature, for 1-2 h, to dissolve the calcium carbonate as calcium chloride.

Decoloration is carried out with ethyl ether and ethanol to remove the pigments from chitin. During the preparation of chitin some chain degradation can occur, depending on the conditions of preparation, and also the deacetylation reaction to form chitosan takes place, but only at a low conversion (<10%).

2.2.2 Chitin deacetylation

Researchers have shown that it is possible to deacetylate chitin both in acidic and alkaline solutions. Alkaline deacetylation of chitin is predominantly used because it produces chitosan with a longer chain length (*e.g.* Muzzarelli, 1974). Sodium or potassium hydroxide (40-50%) is normally used at 100°C to convert the acetyl groups of chitin to amine groups of chitosan (Muzarrelli, 1974; Kurita, 2001). The reaction treatment time and temperature have been found to affect the degree of deacetylation (Muzzarelli, 1974; Rege and Block, 1999; Kurita, 2001), and therefore, different processing conditions may produce chitosan with different characteristics. In most cases, a time of 30-60 minutes is used as that will sufficiently deacetylate chitin into chitosan. The degree of deacetylation of chitosan reported in literature is normally less than 95% (Juang & Shao, 2002; Rhazi *et al.*, 2002), but higher deacetylation degrees can be achieved through repeated deacetylation steps.

2.2.3 Formulation of chitosan beads

The hydrophobic nature, and the resistance to mass transfer of chitosan flakes sometimes discourage its uses for metal adsorption in aqueous solutions. In adsorbing uranyl ions, Piron and Domard (1997) hydrated chitosan flakes by stirring in distilled water for 12 h before the adding of metal ions. This method reduces the crystallinity of the flakes and improves the adsorption kinetics.

In some cases, the mass transfer rate is increased by reducing the size of the material, but small particle flakes have been found to be unsuitable for use in column systems because they cause column clogging and high pressure drops. Chitosan flakes are therefore often transformed into gel beads to improve adsorption capacity and kinetics (Guibal *et al.*, 1999; Guibal, 2004).

Different size beads have been formulated, and their sorption properties towards metal ions reported. Rorrer *et al.* (1993) and Guibal *et al.* (1999) used different diameter beads for metal adsorption studies. They found that the initial rate of metal uptake with the smaller bead is faster but at equilibrium, the capacity of both beads is the same.

2.2.4 Cross-linking of chitosan

There are different cross-linking agents that are used for chitosan modifications, *e.g.* N, N, N', N'-tetra-acetic acid (Alam *et al.*, 1998) and glycerol-polyglycidylether (Becker *et al.*, 2000). The bi-functional chemical glutaraldehyde is however the most widely used agent, because it does not diminish the adsorption capacity too much (Becker *et al.*, 2000; Wan Ngah *et al.*, 2002). Figure 2.3 shows chitosan, and chitosan cross-linked with glutaraldehyde, as given by Rorrer *et al.* (1993).

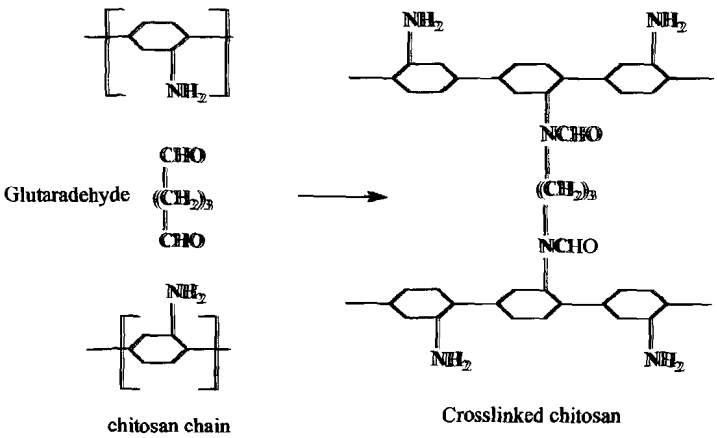

Figure 2.3: Chitosan cross-linked with glutaraldehyde.

Rorrer *et al.* (1993) prepared cross-linked chitosan beads using 1.5 mL of a 2.5% glutaraldehyde solution per gram of beads for 24 h. Monteiro and Airoldi (1999) investigated the effects of chitosan-glutaraldehyde interactions in a homogeneous system. In this case the solution of chitosan in an acetic acid was directly coagulated in glutaraldehyde solution for 1 h.

Ruiz *et al.* (2001) performed heterogeneous cross-linking, by adding chitosan flakes directly into glutaraldehyde solution, for metal adsorption. In this method chitosan flakes were directly mixed with 0.42 to 4.15 mol of glutaraldehyde per mol amine for 16 h.

2.3 Experimental

The production of chitosan beads was carried out at the School of Chemical and Minerals Engineering laboratories, North-West University, Potchefstroom. Chitin isolated from Cape rock lobsters (*Jasus lalandii*) *was* deacetylated to chitosan flakes. The flakes were transformed into chitosan beads and then cross-linked with glutaraldehyde. In Section 2.3.1, the materials used for the preparation are given, and the different procedures that were used to produce chitosan beads from chitin are presented in sections 2.3.2-2.3.4.

2.3.1 Chemicals

Acetic acid of analytical grade (>99%) was purchased from Saarchem UnivAR. Glutaraldehyde (50 wt % in water), HCl (>99%), and NaOH (>99%) were purchased from Aldrich Chemicals. Distilled water was produced with a Pure Water distiller (Ultima 888 water distiller). Solution pH was measured with a pH meter (Hanna HI 8421 or Corning Scholar 425). The chitin material used was extracted from the Cape rock lobster (*Jasus lalandii)*, and purchased from BioSpec (Cape Town, South Africa). Commercial chitosan (CC) flakes, extracted from the chitin of Squat Lobster (*Pleuroncodes monodon)* were purchased from Biopolymer Engineering, USA and used as received.

2.3.2 Preparation of chitosan flakes

The deacetylation of the chitin was carried out in a batch mode. A reactor containing a 50% NaOH solution at a temperature of 120°C was charged with dry chitin flakes. The deacetylation reaction was carried out for 1 h, after which the reactor was drained. The partially deacetylated chitin flakes were separated from the NaOH solution by filtration over a woven nylon filter. The flakes were drained for 30 minutes and then added to a freshly made NaOH heated solution, followed by three exposures of 2 h each to the NaOH solution. The flakes were thoroughly washed with demineralised water in order to remove the NaOH, and

were filtered and dried for 12 h at 70°C. The dried flakes were then stored in plastic bags at –20°C. For a more detailed description of this procedure, see Van der Merwe (2006).

2.3.3 Preparation of chitosan beads

For the formation of beads, the method outlined by Rorrer *et al.* (1993) was applied. A 7.0% (w/w) chitosan solution was made by dissolving 75.3 g of chitosan flakes in 1 L of 3.0% (v/v) acetic acid solution. The dissolved chitosan solution was filtered through a polystyrene sieve with a mesh size of 100 μm to remove impurities.

The filtered chitosan solution was pumped with a peristaltic pump (Watson Marlow 313S) through a 140 mm glass pipette having a 25 mm long draw-out capillary tip with an inner diameter of 0.9 mm, into 2 L of a 1.0 M NaOH solution. Upon contact with the hydroxide solution, the anti-solvent NaOH induced the formation of gel beads. The chitosan beads and aqueous NaOH solutions were stirred continuously for 12 h, after which the beads were washed with distilled water to reach a constant neutral pH. The experimental set-up is schematically given in Figure 2.4.

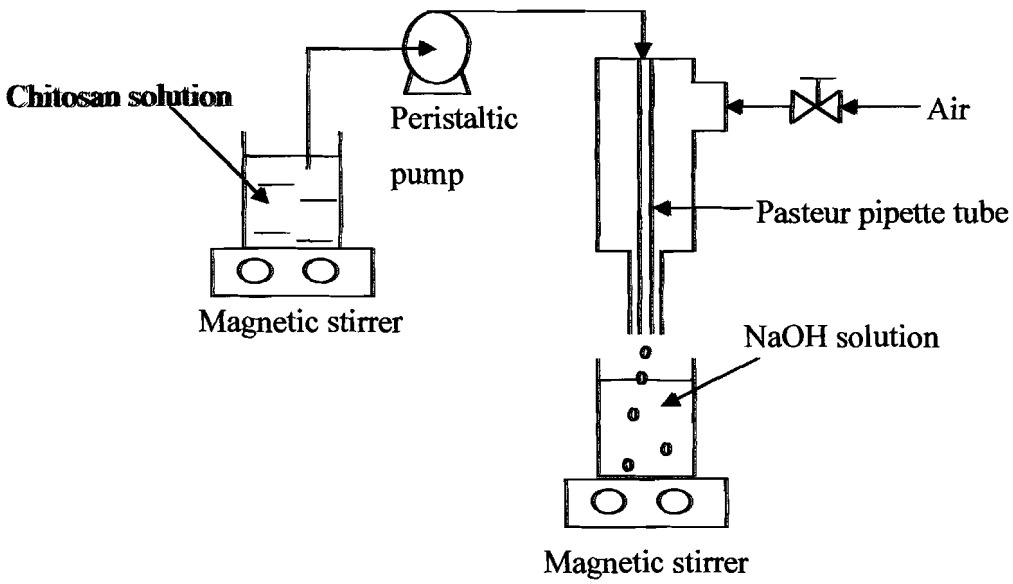

Figure 2.4: Experimental set-up for the production of chitosan beads.

The bead size was controlled by blowing air along the base of the nozzle in order to force the bead to fall down into the anti-solvent bath before its reaches its critical volume and weight. Since the bead size has a pronounced effect in the practical application of column operation, three different sizes of beads were manufactured: 0.9, 1.8 and 3.8 mm. The 3.8 mm diameter beads were produced from operation without blowing air through the annular space, and the 0.9 and 1.8 mm beads were produced by blowing air through the annular space operations at different velocities.

When chitosan beads were produced from commercial flakes using the procedures above, non-spherical beads with a tail were formed. This was as a result of the relative fast bead formation rate in the concentrated sodium hydroxide solution. This problem was overcome by reducing the concentration of chitosan solution to 6.4% (w/w) and the coagulation bath concentration to 0.5 M NaOH.

2.3.4 Cross-linking of chitosan beads

A fraction of the beads prepared according the process described in Section 2.3.3 was cross-linked with a 0.5, 2.5 and 4% glutaraldehyde solution. 1.5 mL of the glutaraldehyde solution was used per gram of gel beads. The cross-linking reaction was carried out for 24 h at room temperature and, after the cross-linking operation the beads were extensively rinsed with distilled water to remove any un-reacted glutaraldehyde. The beads were then stored in distilled water. Table 2.1 gives a summary of the different sizes of beads produced and cross-linked. The code given in the last column of this table will be used throughout this thesis.

Table 2.1: Classification of beads according to source, size and preparation method.

Chitosan	Diameter of bead (mm)	Glutaraldehyde (%w/w)	Code
Local chitosan	0.9	2.5	LC(0.9)(2.5)*
Local chitosan	1.8	2.5	LC(1.8)(2.5)
Local chitosan	3.8	2.5	LC(3.8)(2.5)
Local chitosan	3.8	0.5	LC(3.5)(0.5)
Local chitosan	3.8	4.0	LC(3.8)(4.0)
Local chitosan	3.8	0.0	LC(3.8)(0.0)
Commercial chitosan	3.8	2.5	CC(3.8)(2.5)
Commercial chitosan	3.8	0.0	CC(3.8)(0.0)

**LC(0.9)(2.5) indicates a bead-diameter of 0.9 mm and a glutaraldehyde concentration of 2.5% prepared from local chitosan*

Abbreviations

DCL	degree of cross-linking
DDA	degree of deacetylation
LC	local chitosan
CC	commercial chitosan

References

Alam, M.S., Inuoe, K. & Yoshizuka, K. 1998. Ion exchange/adsorption of rhodium(III) from chloride media on some anion exchangers. *Hydrometallurgy*, 48, 213-227.

Becker, T., Schlaak, M. & Strasdeit, H. 2000. Adsorption of Nickel(II) , Zinc(II) and Cadmium(II) by new chitosan derivatives. *Reactive and Function Polymers*. 44: 289-298.

Guibal, E. 2004. Interaction of metal ions with chitosan-based sorbents: a review. *Separation and Purification Technology*, 38, 43-74.

Guibal, E., Milot, C. & Roussy, J. 1999. Molybdate sorption by cross-linked chitosan beads: Dynamic studies. *Water Environment Research*. 71, 1-17.

Juang, R.S. & Shao, H.J. 2002. A simplified model for the sorption of heavy metal ions from aqueous solutions on chitosan. *Water Research*, 36, 299-3008.

Kurita, K. 2001. Controlled functionalization of the polysaccharide chitin. *Progress in Polymer Science*, 26, 1921-1971.

Monteiro, O.A.C. & Airoldi, C. 1999. Some studies of cross-linking chitosan-glutaraldehyde interaction in a homogeneous system. *International Journal of Biological Macromolecules*, 29, 119-128

Muzzarelli, R.A.A. 1974. Natural chelating polymers: Alginic acid, chitin and chitosan. Pergamon press.

No, H.K. & Meyer. S.P. 1997. Preparation of chitin and chitosan. Chitin Hand Book. Edited by Muzzarilli, RAA and Peter, MG. European chitin society. 475-489.

Piron, E. & Domard, A. 1997. Interaction between chitosan and uranyl ions. Part 1. role of physicochemical parameters on the kinetics of sorption. *International Journal of Biological Macromolecules*. 21, 327-335.

Rege, P.R. & Block, L.H. 1999. Chitosan processing: influence of process parameters during acidic and alkaline hydrolysis and effect of the processing sequence on the resultant chitosan's properties. *Carbohydrate Research*, 321, 235-245.

Rhazi, M., Desbrieres, J., Tolaimate, A., Rrnaudo, M., Vottero, P. & Alagui, A. 2002. Contribution to the study of the complexation of copper by chitosan and oligomers. *Polymer*, 43, 1267-1276.

Rorrer, G.L, Hein, T. & Way, D.J. 1993. Synthesis of porous-magnetic chitosan beads for removal of cadmium ions from waste water. *Industrial Engineering Chemical Research,* 32, 2170-2178.

Ruiz, M., Sastre, A.M. & Guibal, E. 2000. Palladium sorption on glutaraldehyde-crosslinked chitosan. *Reactive and Functional Polymers*, 45, 155-173.

Van der Merwe, H. C. 2006. Chitosan membranes for removal of zinc from simulated wastewater. PhD Thesis, School of Chemical and Minerals Engineering, North-West University, SA.

Wan Ngah, W.S. Endud, C.S. & Mayanar, C.S.E. 2002. Removal of copper(II) ions from aqueous solution onto chitosan and cross-linked chitosan beads. *Reactive and Functional Polymers*, 50, 181-190.

Chapter 3 Characterization of chitosan beads

3.1 Introduction

The characterization of chitosan beads is an essential step in this study since chitosan produced from different chitin sources and under different processing conditions have been shown to differ in physical and chemical properties (Kurita, 2001 and Guibal, 2004). From a review report on chitosan by Guibal (2004), the three most important properties that affect metal adsorption are: i) the degree of deacetylation, ii) the degree of cross-linking and iii) the crystallinity.

The degree of deacetylation (DDA) of chitosan, as reported by Huang *et al.* (1996), is directly related to its adsorption capacities because the amine group in chitosan is considered to be the most important feature in the adsorption of metal ions. Many methods have been reported for determining the DDA including elemental analysis, dye adsorption, titration of free amine groups, enzymatic degradation and spectroscopic methods such as IR, UV and NMR. The merits and drawback of these analytical methods have been discussed in detail else where (Tan *et al.*, 1998; Kurita, 2001; Khan *et al.*, 2002). For practical use, titration of the free amine groups, dye absorption and IR spectroscopy, which has been found to be fast and reliable, are proven techniques (Roberts, 1997).

Non-crosslinked chitosan is easily soluble in some acidic media, which is from a practical viewpoint, one of the serious drawbacks of its use for metal collection and concentration. Cross-linking makes chitosan insoluble in acidic media. As a result, several types of chemical cross-linking have been proposed and their adsorption properties examined. Only limited literature on the quantitative determination of the degree of cross-linking (DCL) is available (*e.g.* Kawamura *et al.*, 1997).

The amine groups of chitosan have been shown to be involved in the cross-linking, and according to Guibal (2004) chitosan cross-linked at lower concentrations of glutaraldehyde adsorbed more metals than those cross-linked at higher concentrations. Monteiro and Airoldi (1999) performed a study on cross-linked chitosan-glutaraldehyde interactions in a homogeneous system in which various instrumental analyses were used to characterize the interaction of chitosan with glutaraldehyde including ^{13}C NMR, IR spectroscopy and scanning

electron microscopy. The ^{13}C NMR revealed the peaks of double ethylenic and imine bonds. From IR spectroscopy measurements, a selected band at 1655 cm^{-1} reveals an imine bond and the band at a wavelength 1562 cm^{-1} reveals the ethylenic double bond. It was concluded that the free pendant amine groups of the chitosan polymer interact with the aldehydic group of glutaraldehyde to form stable imine bonds due to the resonance established with adjacent double ethylenic bonds. Elemental analysis revealed a decrease in the nitrogen as the concentration of glutaraldehyde used for cross-linking increases.

Guibal (2004) reported on the advantages of using glutaraldehyde cross-linked chitosan beads for adsorption over non-cross-linked beads and chitosan flakes. The cross-linked beads have a higher specific surface area (180-250 m^2/g) compared to the flakes (2-30 m^2/g). The pore size of the non-cross-linked beads was determined to be between 30 and 50 nm and in the case of glutaraldehyde cross-linked chitosan beads the pore size increased to 56-90 nm, which significantly increased the diffusion rate.

A large fraction of chitosan beads consists of water. Many researchers have used drying methods to determine the water content and arrived at values ranging between 90 and 96% (Erosa *et al.*, 2001 and Guibal *et al.*, 1999a). When chitosan beads are cross-linked it is possible that the volume of water in the beads will decrease as cross-linking agents occupy additional space within the volume structure.

The molecular weight of the polymer is another important property. Although it does not influence adsorption characteristics, it can significantly influence the polymer modification. For example, the ability of the polymer to form a gel is strongly affected by its molecular weight and its molecular weight distribution (Kotze *et al.*, 2001). Van der Merwe (2006) found an increase in viscosity and dissolution time with molecular weight when chitosan was dissolved in an acetic acid solution. Several methods are used to estimate the molecular weight of chitosan, of which viscometry and size exclusion chromatography (SEC) are proven and reliable techniques that are most often used. In the case of SEC, the molecules are separated according to their molecular sizes, and the molecular weight distribution is obtained. Table 3.1 presents the average molecular weights of chitosan for various methods of determination and, the values range from 84-410 kg/mol.

Table 3.1: Molecular weights of chitosan as reported in literature.

Method employed	Mw (kg/mol)	Author
Viscometry	410	Juang & Shao (2002)
Viscometry	84	Rhazi *et al.* (2002)
SEC	120	Guibal *et al.* (1999b)
Light scattering	120	Muzzarelli (1974)

In this chapter, chitosan beads, as prepared according to the procedure presented in Section 2.3 are characterized. In Section 3.2, the experimental procedures are given, and in Sections 3.3 and 3.4 the result, discussion and conclusions are presented respectively.

3.2 Experimental Methods

Experiments are performed with chitosan beads in order to determine the:

- Average molecular weight with SEC;
- DDA with IR spectroscopy and with UV spectrophotometry;
- Amine concentration, degree of protonation (α) and DCL with titration;
- Stability of the beads in acid solution;
- Fraction of water in the bead, and;
- Distribution coefficient for metal ions.

3.2.1 Chemicals

Acetic acid was purchased from Saarchem UnivAR of analytical grade (>99%). HCl (>99%), NaOH (>99%), ammonium acetate (>98%), ethanol (>99%) and the dye material; C.I. Acid orange 7 [range II; 4-(2-hydroxy-1-naphthylazo) benzenesulphonic acid, sodium salt] were purchased from Aldrich Chemicals. Distilled water was produced with a Pure Water distiller (Ultima 888 water distiller). Solution pH was measured with a pH meter (Hanna HI 8421 or Corning Scholar 425). Before analysis, the beads were vacuum filtered for 10-15 minutes and at these conditions, are termed wet beads.

3.2.2 Molecular weight measurements

The molecular weight distribution of the LC and CC flakes and that of non-cross-linked beads were determined using SEC. This is a unique analytical method because it is an absolute method. It was also chosen because of its capacity to determine a wide range of molecular weights, its accuracy and reproducibility. The molecular weight of cross-linked beads could not be determined with this method, because they are not soluble at the pH at which characterization takes place.

Preparation of eluent: A 0.2 M ammonium acetate solution was prepared, and the pH was adjusted with acetic acid from pH ±6.7 to 4.5 to form a stable buffer. The solution was filtered through cellulose nitrate filters with a mesh size of 0.22 μm, and was used as a mobile phase and solvent in the analysis.

Preparation of samples: The wet beads were freeze-dried over night at -20°C and the flakes sieved through a mesh size of 100 μm before being added to the sodium acetate solution. 25 mg of the sample was added to 5 mL of 0.2 M ammonium acetate to give a solution of 5 mg/L. The sample solution was placed in a Labcon incubator set at 25 ± 0.5°C and shaken for 12 h to dissolve. 0.8 mL of the sample was collected and filtered through a membrane filter with a mesh size 0.2 μm into a sample vial.

Analysis: The experimental set-up consisted of an HP 1100 vacuum degasser, isocratic pump and auto sampler connected to a TSK-guard PWH (Toso Haas, Japan) in line column. The size exclusion columns were TSK G6000 PW (Toso, Japan; ID 7.5 mm, length 30 cm, particle size > 17 μm, pore size > 100 nm) and TSK G500 (Toso Haas, Japan; ID 7.5 mm, length 30 cm, pore size 100 nm) connected in series. The samples of the chitosan solutions (100 μm) were injected at a flow rate of 0.8 mL/min and were analyzed with a laser beam (He/Ne laser, λ = 633 nm) and a refracting index detector. The data from the laser photometer and the detector were interpreted with Astra for MS-Windows (Wyatt Technology Corporation, USA).

3.2.3 Degree of deacetylation measurements

Dye absorption method using UV spectrophotometer

In this analysis, the method of Roberts (1997) was used. The dye material; C.I. Acid orange 7 [range II; 4-(2-hydroxy-1-naphthylazo) benzenesulphonic acid, sodium salt] was purified by re-crystallization with 80 % aqueous ethanol and dried in an oven at 45-50°C before use.
Detailed information on sample preparation and analysis is given in Appendix B.

Infrared spectroscopy method

For the characterization of the degree of deacetylation, the baseline method proposed by Baxter *et al.* (1992) was applied. This analysis was used to confirm the influence of cross-linking on chitosan. The following procedure was followed;

- About 10 g of wet beads were air dried by spreading them on tissue paper.
- The dried beads were ground into a fine powder with a mortar and pestle.
- The fine chitosan powder was stored in an oven at 50 ± 0.5°C overnight for further drying.

Analysis: Exactly 2.000 mg of chitosan powder was weighed and mixed with 300.0 mg of dry KBr (stored open at 100°C in the oven). The mixture of chitosan and KBr was then pressed at 200 kg/cm^2 to form a pill. The pills were then left to dry for 12 h at 100°C, to remove all the water before analysis. The pills were analyzed with IR immediately after removing them from the oven. The IR spectra analysis was carried out with a NICOLET MAGNA-IR500 Series II connected to a computer using the Omnic FTIR software package. The DDA was determined using the following expression (Roberts, 1997):

$$\%\text{DDA} = 100 - \left(\frac{A_{1655}}{A_{3450}}\right)115 \qquad 3.1$$

where A_{1655} and A_{3450} are the fractions of infra-red absorbance at wave-numbers 1655 cm^{-1} and 3450 cm^{-1}, respectively.

3.2.4 Determination of bead stability in acid solution

The solubility of the various beads manufactured in acid solution was measured in 100 mL of 10^{-5} to 0.1 M HCl or acetic acid solutions. Exactly 10.0 g of wet beads was put in each of several 250 mL flasks containing solutions with different acid concentrations. The flasks were placed in a Labcon incubator for 24 h (25 ± 0.5 °C and 120 rpm). The content of each flask was filtered and the mass of the remaining beads determined. The beads were termed soluble when the mass loss is >5% and insoluble when the mass loss is <5%.

3.2.5 Determination of the DCL, amine concentration and the degree of protonation

A standard titration method was used to determine the amine concentration, the pK_a, the degree of protonation (α) and the DCL in the chitosan. Both non-cross-linked and cross-linked chitosan solutions were titrated with standard hydrochloric acid solution. Exactly 10.000 g of wet chitosan beads were weighed into a 30 mL glass tube and ground with an 18 mm Teflon pestle fitted to a three-jaw keyless chuck with 240V variable electric motor (3000-4000 rpm) purchased from Cole-Parmer. A 100 mL suspension was prepared using distilled water. The suspension was continuously stirred with a magnetic stirrer during titration with a 1.0 M HCl solution. The pH of the solution was recorded after set time intervals. Titration studies were done for all the beads in Table 2.1 and the experiment was repeated with LC(3.8)(2.5) beads aged for 360 days in order to check if the properties beads are affected with age. The data obtained from the titration results were used to determine the amine concentration, and the DCL was calculated using the following expression:

$$[-NH_2] = [-NH_2]_T (1 - DCL) \qquad 3.2$$

In which $[-NH_2]_T$ is the amine concentration for non-cross-linked chitosan.

3.2.6 Influence of grinding

Unground beads were used in titration experiments to determine chitosan properties as in Section 3.2.5. Exactly 10.000 g of LC(3.8)(2.5) beads were placed in each of several 250 mL Erlenmeyer flasks and acidic solutions of 100 mL of 0.0001 to 0.1 M HCl were added to the

flasks, and placed in a Labcon incubator for 24 h (25 ± 0.5°C, 120 rpm). After 24 h, the pH of the solution with unground beads was measured.

3.2.7 Determination of mass fraction of chitosan in beads

The mass fraction of chitosan in the beads was determined from the wet and dry weight of beads. The dry weight of beads was determined after heating in a ventilated oven at 80°C for a period of 24 h. The mass fraction of water in the bead was calculated from:

$$X_b = \frac{m_{wb} - m_{dw}}{m_{wb}} \qquad 3.3$$

where m_{wb} is the mass of the wet beads and m_{db} is the mass of the dried beads. The mass fraction of chitosan in the bead (X_{cb}) is calculated as:

$$X_{cb} = 1 - X_b \qquad 3.4$$

3.2.8 Determination of distribution coefficient for metal ion

In order to find the appropriate diffusion coefficient in the kinetic experiments, it is essential to determine the metal ion distribution coefficient. For this purpose, sodium is used because alkaline metals are not adsorbed onto chitosan. This was found by Muzzarelli (1974) and was confirmed by tests on chitosan flakes. However, physical adsorption of sodium onto the water of the beads can occur, a feature that is used to determine the distribution coefficient of the metal between the aqueous and the bead phase.

A 25 mL Na_2SO_4 solution (1000 mg Na^+/L) was prepared and added to 16.70 g of the wet beads in a 250 mL Erlenmeyer flask. The Erlenmeyer was placed in an incubator and after 24 h (25 ± 0.5°C, 120 rpm), a 20 mL sample was taken and put in a 50 mL volumetric flask. A 25 mL of KCl solution (4000 mg K^+/L) was also prepared and added to all samples, blanks and standards to suppress ionization. The volumetric flask was than filled up with distilled water. The sodium concentration was measured with an atomic absorption spectrometer (Varian SpectraAA-10). The beads were dried in an oven for 24 h at 80°C and weighed. The final concentration of sodium in the beads was determined from a sodium mass balance:

$$[Na^+]_{w,i}V_{w,i} = [Na^+]_{w,f}V_{w,f} + [Na^+]_{b,f}V_{w,b} \quad 3.5$$

The volume of the solution does not change significantly, therefore $V_w = V_{w,i} = V_{w,f}$, and solving for the concentration of sodium in the beads gives:

$$[Na^+]_{b,f} = \frac{V_w([Na^+]_{w,i} - [Na^+]_{w,f})}{V_{w,b}} \quad 3.6$$

The total volume of water in beads, $V_{w,b}$, is calculated from the difference in the beads' dry and wet mass according to:

$$V_{w,b} = \frac{m_{wb} - m_{db}}{\rho_{H_2O}} \quad 3.7$$

It was assumed that the density of water in the beads is the same as that of pure water. The sodium distribution coefficient is determined from the ratio of the sodium concentration in the beads to the concentration of sodium in water according to:

$$k_d = \frac{[Na^+]_{b,f}}{[Na^+]_{w,f}} \quad 3.8$$

3.3 Results and discussion

In this section the results of the experimental work with respect to the:

- Molecular weight of chitosan (Section 3.3.2);
- DDA (Section 3.3.3);
- DCL (Section 3.3.4);
- Amine concentration (Section 3.3.5) and the DOP (Section 3.3.6);
- Stability of the beads in acid solution (Section 3.3.7);

- Fraction of water in the bead (Section 3.3.8), and;
- Fraction of water in the bead that is accessible for ion diffusion (Section 3.3.9), are presented and discussed.

3.3.1 Molecular weight of chitosan

The molecular weights determined by SEC of different chitosan materials are presented in Table 3.2. The weight-average molecular weight (M_w) of the flakes and beads from the same material source was found to differ slightly. In the case of local chitosan material, the molecular weight was found to be $7.8 \cdot 10^4$ g/mol for the flakes and $9.4 \cdot 10^4$ g/mol for the beads. Similar trends were found for the CC beads with the flakes having a molecular weight of $7.1 \cdot 10^4$ g/mol and for the beads the molecular weight was $1.1 \cdot 10^5$ g/mol. Still, the calculated average molecular weight for LC material ($8.6 \cdot 10^4$ g/mol) and CC material ($9.1 \cdot 10^4$ g/mol), are in the range of the values reported in literature shown in Table 3.1.

Table 3.2: Molecular weight values from SEC.

Sample	M_w (g/mol)
Local chitosan	
LC(3.8)(0.0)	$9.4 \cdot 10^4$ (±4%)
Flakes	$7.8 \cdot 10^4$ (±4%)
Commercial chitosan	
CC(3.8)(0.0)	$1.1 \cdot 10^5$ (±6%)
Flakes	$7.1 \cdot 10^4$ (±5%)

3.3.2 Degree of deacetylation (DDA)

In finding the DDA, two methods were employed: the dye absorbance method as given by Roberts (1997) and the IR spectroscopy method as given by Baxter *et al.* (1992). In the case of dye absorbance techniques, the extent of adsorption was measured by UV-vis spectroscopy at 484 nm. The degrees of deacetylation by these methods are given in Table 3.3. The DDA obtained from both methods do not differ significantly. The average value of the DDA is 80 (±5)% for the LC and 76 (±3)% for the CC.

Table 3.3: DDA values from different methods

Chitosan	Dye absorbance	IR
Local	83 (±5)%	78 (± 3)%
Commercial	80 (± 5)%	72 (± 3)%

3.3.3 Stability of beads in acid solution

Table 3.4 gives the solubility of chitosan beads at a pH between 2 and 4 and pH 5 in both hydrochloric and acetic acid solutions. The non-cross-linked beads and the beads cross-linked at 0.5 wt% glutaraldehyde were found to be soluble at a pH between 2 and 4 and insoluble at pH 5. The beads that were cross-linked with a concentration > 2.5 wt% glutaraldehyde were stable at all levels of acid concentration.

Table 3.4: Solubility of beads in acid solutions.

Chitosan bead	DCL	Hydrochloric acid		Acetic acid	
	(%)	pH 2-4	pH 5	pH 2-4	pH 5
LC(3.8)(0.0)	0.0	Soluble	Insoluble	Soluble	Soluble
LC(3.8)(0.5)	8.2	Soluble	Insoluble	Soluble	Soluble
LC(3.8)(2.5)	18.4	Insoluble	Insoluble	Insoluble	Insoluble
LC(3.8)(4.0)	34.7	Insoluble	Insoluble	Insoluble	Insoluble

3.3.4 Determination of chitosan dissociation constant, amine concentration and DCL

Figure 3.1 shows the IR spectra of the samples from LC(3.8)(0.0) and LC(3.8)(2.5). From the analysis of these spectra for the cross-linked and non-cross-linked chitosan, more absorbance was revealed in the region of 1655 cm^{-1} for the cross-linked chitosan which is a characteristic of amide I (the C=O from aldehyde). This proves the presence of glutaraldehyde which is involved in chitosan cross-linking (Monteiro and Airoldi, 1999; Guibal *et al.*, 1999b; Jeon and Holl, 2003).

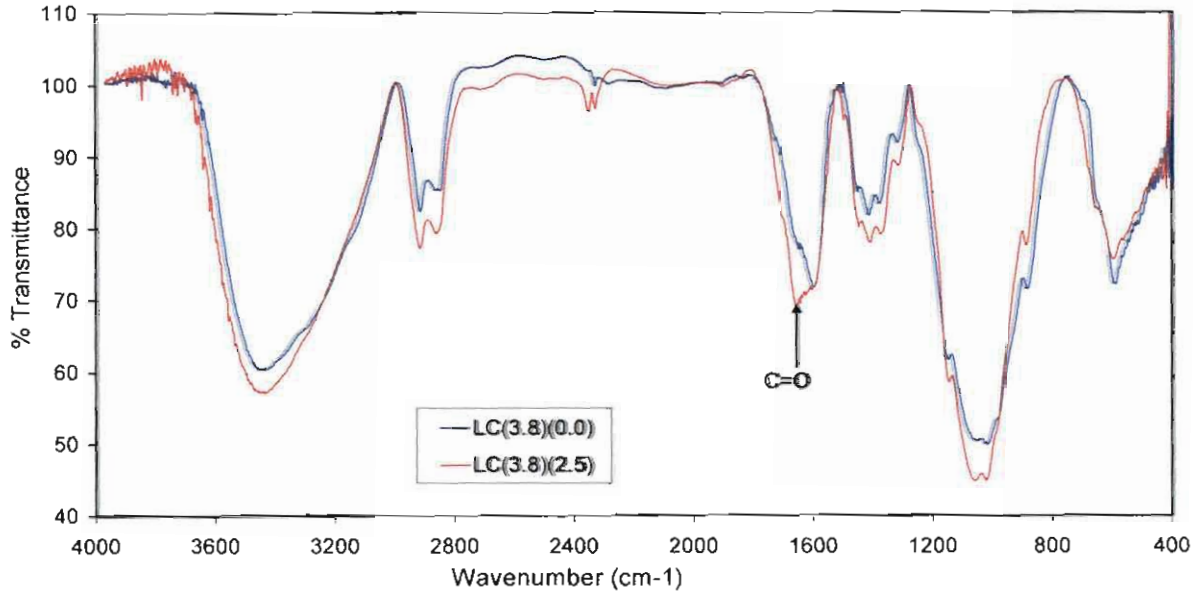

Figure 3.1: IR spectra of non-cross-linked and cross-linked chitosan beads

When a weak base is titrated with an acid, the point of inflection, as described by Skoog *et al.* (1996) can be used to locate the base dissociation constant. This point on the curve of the non-cross-linked beads was used to determine the pK_a as 6.0 (Figure 3.2). For the case of cross-linked beads, the pK_a was 4.7 (also shown in Figure 3.2). The titration curve of chitosan was compared with a weak base with constant pK_a and a good agreement was found as shown by the solid line in Figure 3.2. The results of titration with other modified beads are summarized in Table 3.5.

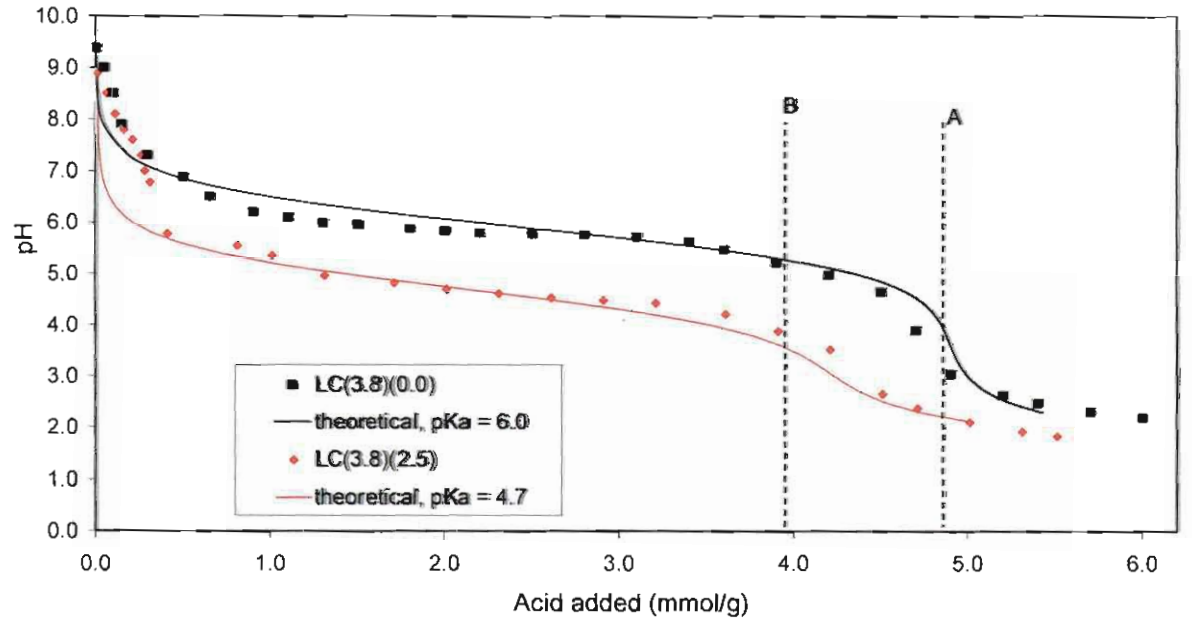

Figure 3.2: Titration curves for non-cross-linked and cross-linked chitosan beads.

Figure 3.3 shows the effect of glutaraldehyde concentration on the pK_a. As can be seen, a linear relationship was observed between the pK_a and glutaraldehyde concentration. The pK_a was found to decrease with an increase in glutaraldehyde concentration.

Table 3.5: Measured pK_a of chitosan beads.

Beads	pK_a	Beads	pK_a
LC(3.8)(0.0)	6.0 (±0.2)	LC(0.9)(2.5)	4.3 (±0.2)
LC(3.8)(0.5)	5.3 (±0.2)	LC(1.8)(2.5)	4.3 (±0.2)
LC(3.8)(2.5)	4.7 (±0.2)	CC(3.8)(0.0)	6.2 (±0.2)
LC(3.8)(4.0)	4.3 (±0.2)	CC(3.8)(2.5)	3.8 (±0.2)

The methods described by Skoog *et al.* (1996) for the determination of an equivalent amount of acid needed to neutralize the base was also used to determine the amine concentration in the chitosan. For the case of non-cross-linked beads, the equivalent amount of acid used was determined at the inflection point indicated with dotted line A in Figure 3.2. From this figure, the equivalent point was determined as being equal to 4.9 (±0.1) mmol of acid per grams of chitosan. Similar procedures were also applied to LC(3.8)(2.5) beads shown in Figure 3.2 with dotted line B and the equivalent amount of acid per gram of chitosan was 4.0 (±0.1) mmol.

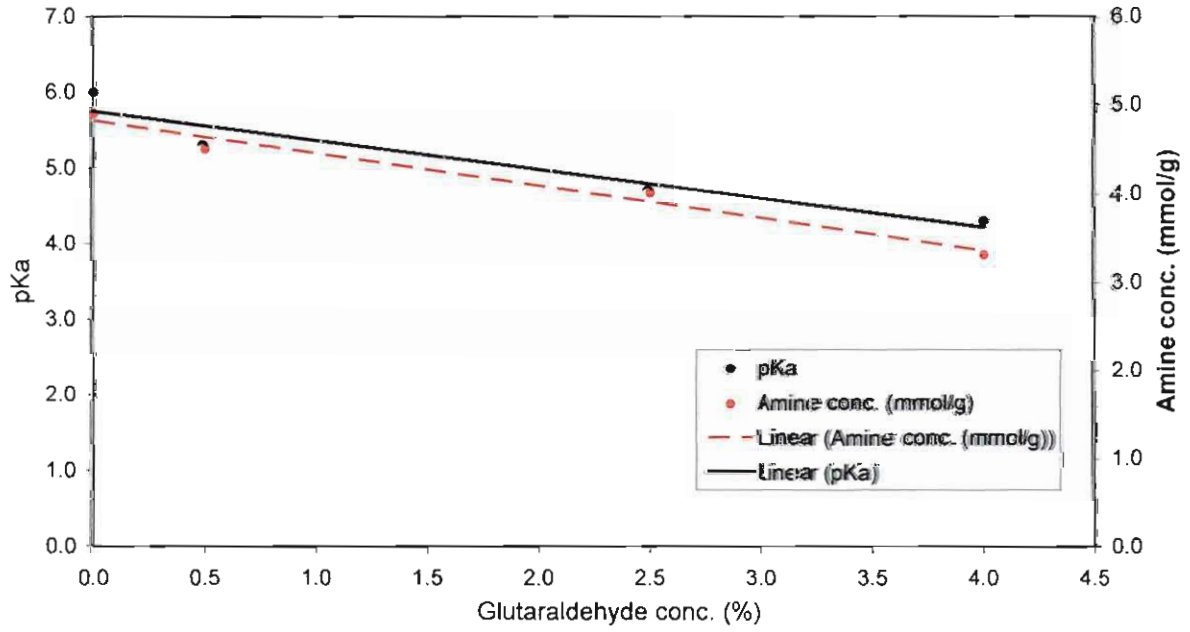

Figure 3.3: Relationships between amine concentrations, chitosan dissociation constant and DCL

This procedure was also employed to determine the amine concentration for other modified beads. The results are given in Table 3.6. Also, there was a linear relationship between glutaraldehyde concentration and amine concentration as shown in Figure 3.3, which decreases with increasing cross-linking concentration. In the case of LC(3.8)(0.0), the amine concentration decreased by about 18% when cross-linked with 2.5 % glutaraldehyde. For commercial chitosan beads, the concentration of amine found for the non-cross-linked and 2.5% glutaraldehyde cross-linked beads were 3.6 (±0.1) and 3.0 (±0.1) mmol/g chitosan respectively.

Table 3.6: Measured amine ($-NH_2$) concentrations of beads.

Beads	[$-NH_2$] (mmol/g)	Beads	[$-NH_2$] (mmol/g)
LC(3.8)(0.0)	4.9 (±0.1)	LC(0.9)(2.5)	3.3 (±0.1)
LC(3.8)(0.5)	4.5 (±0.1)	LC(1.8)(2.5)	3.4 (±0.1)
LC(3.8)(2.5)	4.0 (±0.1)	CC(3.8)(0.0)	3.6 (±0.1)
LC(3.8)(4.0)	3.2 (±0.1)	CC(3.8)(2.5)	3.0 (±0.1)

The results in Table 3.6 also show a decrease in amine concentration with a decrease in bead size. It has been documented that smaller size particles have a shorter diffusion path (Wu *et al.*, 2001; Guibal, 2004), and for this situation smaller beads have relatively more of their amine sites exposed for cross-linking. In a situation where different glutaraldehyde concentrations were used for the same bead size, the amine concentration was found to decrease with an increasing glutaraldehyde concentration. This is in agreement with what was reported by Monteiro and Airoldi (1999).

The data obtained from the titration results were also used to determine the DCL. The DCL was calculated using Equation (3.2) and the values for the DCL for the modified beads are given in Table 3.7. As the concentration of cross-linking reagent increases, the DCL decreases. Therefore, cross-linking with glutaraldehyde can reduce amine concentration; this has also been reported by Guibal *et al.* (1999b). A similar trend was observed between the DCL and bead diameter with the DCL decreasing relative to increases in bead diameter.

Table 3.7: Calculated degrees of cross-linking (DCL) of beads.

Beads	DCL (%)	Beads	DCL (%)
LC(3.8)(0.0)	0.0	LC(0.9)(2.5)	32.7
LC(3.8)(0.5)	8.2	LC(1.8)(2.5)	30.6
LC(3.8)(2.5)	18.4	CC(3.8)(0.0)	0.0
LC(3.8)(4.0)	34.7	CC(3.8)(2.5)	16.7

Physical observation of the cross-linked beads after 90 days in distilled water revealed color changes from whitish to grayish. Beads remained that color over the longer period. The titration curve for the freshly made cross-linked beads was compared to the curve of the beads after 360 days. The curves are shown in Figure 3.4 and from the profiles of the curves it can be concluded that the pK_a does not change significantly with time.

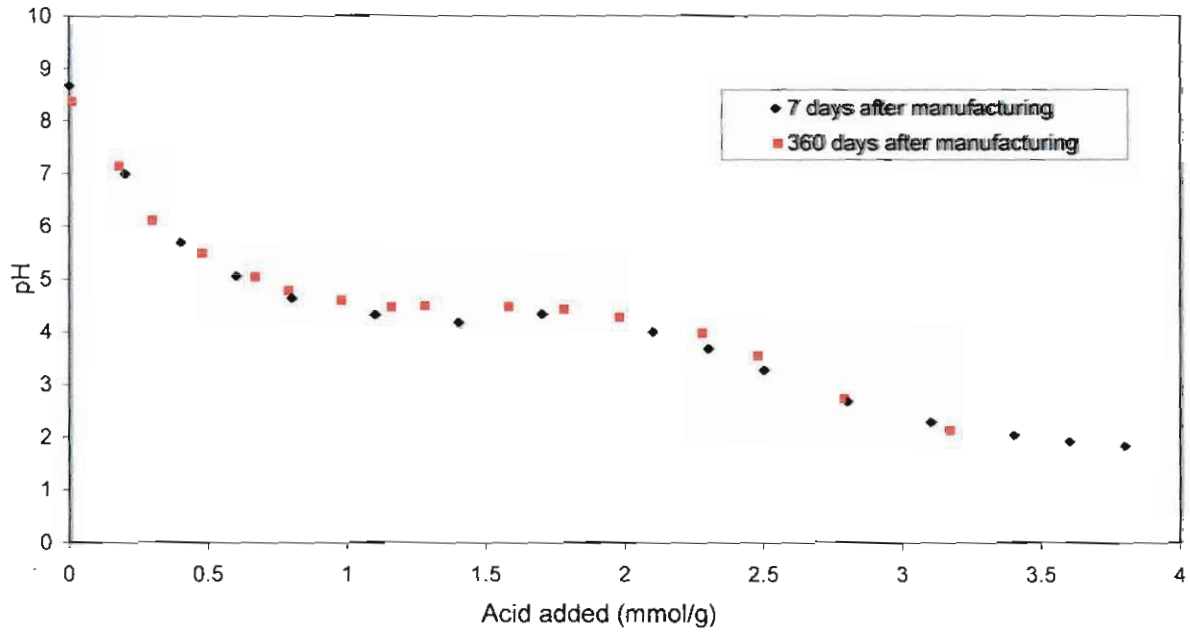

Figure 3.4: Comparison of titration curves for LC(1.8)(2.5) beads.

3.3.5 Influence of grinding

Figure 3.5 shows the titration curve of unground beads and ground beads when titrated with an aqueous HCl solution. The dissociation constants and the chitosan concentrations were determined to be the same for both particle types. This shows that the amine sites in the unground beads are as available as are those in the ground beads.

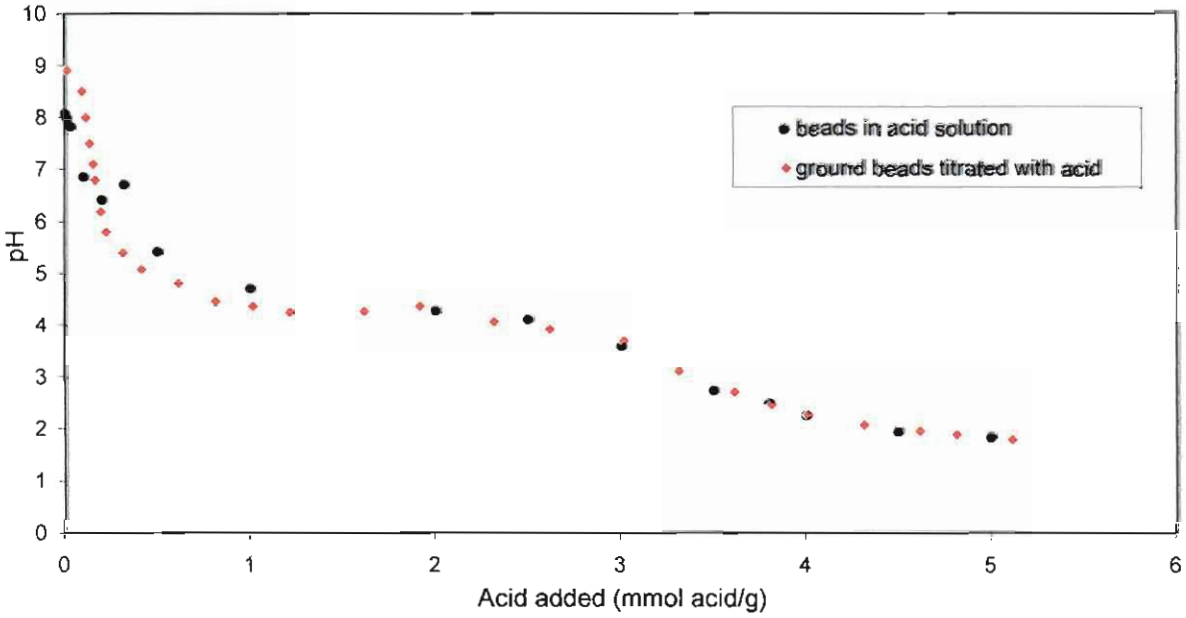

Figure 3.5: Comparison of pH for LC(1.8)(2.5) beads.

3.3.6 Degree of protonation

The degree of protonation (α) was calculated from the titration data. Figure 3.6 illustrates the α for cross-linked beads, as calculated from titration results (shown as data points) compared to α determined from the theoretical pK_a of 4.3 (shown as line). The procedure for the determination of α is given in Appendix C and Table D-1 (Appendix D) gives the values of the titration results and the calculated α.

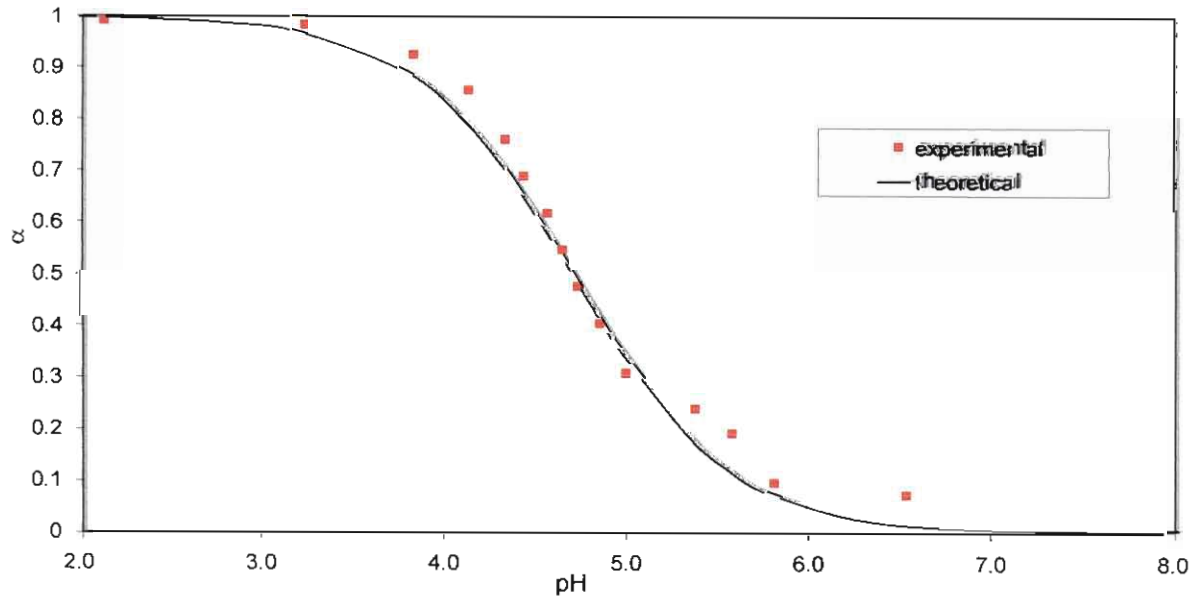

Figure 3.6: Degree of protonation obtained from experimental data for LC(1.8)(2.5) beads.

3.3.7 Mass fraction of chitosan in beads

Table 3.8 shows the determined water contents in the beads. From the table it can be concluded that the beads consist of a large fraction (90-96 wt %) of water. It was found that the water content decreased with increasing cross-linking time and bead diameter. The percentage water relates well with the DCL, in that the percentage water in the beads decreases with increasing DCL.

Table 3.8: Average mass of water determined from modified beads.

Beads	X_b (wt%) in beads*	DCL(%)
LC(3.8)(0.0)	96.0 (± 0.1)	0.0
LC(3.8)(2.5)	94.9 (± 0.1)	18.4
LC(1.8)(2.5)	93.4 (± 0.1)	30.6
LC(0.9)(2.5)	90.1 (± 0.1)	32.7
LC(3.8)(0.5)	95.1(± 0.1)	8.2
LC(3.8)(4.0)	90.0 (± 0.1)	34.7

**Based on an average of 5 independent experiments*

3.3.8 Distribution coefficient

Equation (3.8) was used to determine the distribution coefficient for sodium and the coefficient was calculated as the ratio of sodium in the bead to that in solution. The average value of the coefficient was found to be 1.01 (±0.02). This result shows that the metal is equally distributed between the aqueous and gel bead phases.

3.4 Conclusions

The molecular weight of the chitosan biopolymer was $9.4 \cdot 10^4$ and $7.8 \cdot 10^4$ g/mol for the flakes and beads respectively. These values do not differ significantly from the commercial chitosan. The degree of deacetylation was 83%, which also did not differ significantly from the commercial chitosan.

The most important characteristics of the chitosan beads are summarized in Table 3.9. It was found that the amine concentration in the beads decreased with an increasing glutaraldehyde concentration and a decrease in bead diameter. The beads were all stable at a pH of 2, except for the largest beads that were not cross-linked or cross-linked with 0.5% glutaraldehyde.

Table 3.9: Summary of the results of characterized chitosan beads.

Beads	[-NH_2] (g/mol)	DCL (%)	pK_a	Solubility at pH = 2	X_b (wt%) in beads
LC(3.8)(0.0)	4.9	0.0	6.0	Soluble	96.0 (± 0.1)
LC(3.8)(2.5)	4.0	18.4	4.7	Insoluble	94.9 (± 0.1)
LC(1.8)(2.5)	3.4	30.6	4.3	Insoluble	93.4 (± 0.1)
LC(0.9)(2.5)	3.3	32.7	4.3	Insoluble	90.1 (± 0.1)
LC(3.8)(0.5)	4.5	8.2	5.3	Soluble	95.1(± 0.1)
LC(3.8)(4.0)	3.2	34.7	4.3	Insoluble	90.0 (± 0.1)

The pK_a of the local and commercial non-cross-linked chitosan was 6.0 and 6.2 respectively, and were similar to values in the literature. The pK_a of the LC decreased with an increase in cross-linking. The beads consist predominantly of water, with mass fractions larger than 90% for all the beads, and the percentage water in the beads decreased with an increase of the DCL. Using the inert metal sodium, it was shown that the distribution coefficient between the water in the beads and the water surrounding the beads, was close to unity.

List of symbols and abbreviations

k_d	distribution coefficient (-)
m_{wb}	mass of wet beads (g)
m_{db}	mass of dry beads (g)
Mw	molecular weight of chitosan (g/mol)
$[Na^+]_{b,f}$	sodium concentration in beads (mol/L)
$[Na^+]_{w,i}$	initial sodium concentration (mol/L)
$[Na^+]_{w,f}$	final sodium concentration (mol/L)
[-NH_2]	amine concentration (mol/g)

$[-NH_2]_T$	total amine concentration of non-cross-linked beads (mol/g)
ρ_{H2O}	density of water (g/L)
V_w	volume of the solution (L)
$V_{w,i}$	initial volume of sodium solution (L)
$V_{w,f}$	final volume of sodium solution (L)
$V_{w,b}$	volume of water in bead (L)
ΔV	change in the volume of acid added to base at interval of titration (mL)
X_{cb}	mass fraction of chitosan in bead
X_b	mass fraction of water in bead
α	degree of protonation (-)
DCL	degree of cross-linking (-)
DDA	degree of deacetylation (-)
LC	local chitosan
CC	commercial chitosan

References

Baxter, A., Dillon, M. & Anthony Taylor, K. D. 1992. Improved method for IR determination of the degree of N-acetylation of chitosan. *International Journal of Biological Macromolecules*, 14, 166-169.

Erosa, D.M.S., Medina, T.I.S., Mendoza, R.N., Rodriguez, M.A. & Guibal, E. 2001. Cadmium sorption on chitosan sorbents: Kinetic and equilibrium studies, *Hydrometallurgy*, 61, 157-167.

Guibal, E. 2004. Interaction of metal ions with chitosan-based sorbents: a review. *Separation and Purification Technology*, 38, 43-74.

Guibal, E., Milot, C. & Roussy, J. 1999a. Molybdate sorption by cross-linked chitosan beads: Dynamic studies. *Water Environment Research*, 71, 1-17

Guibal, E., Milot, C., Eterradossi, O., Gauffier, C. & Domard, A. 1999b. Study of molybdate ion sorption on chitosan gel beads by different spectrometric analyses. *International Journal of Biological Macromolecules*, 24, 49-59.

Huang, C., Chung,Y. & Lion, M. 1996. Adsorption of Cu(II) and Ni(II) by pelletized biopolymer. *Journal of Hazardous Materials*, 45: 265-277.

Jeon, C. & Holl, W. H. 2003. Chemical modification of chitosan and equilibrium study for mercury ion removal. *Water Research*, 37, 4770-4780.

Juang, R.S. & Shao, H.J. 2002. A simplified model for the sorption of heavy metal ions from aqueous solutions on chitosan. *Water Research*, 36, 299-3008.

Kawamura, Y., Yoshida, H., Asai, S., Kurahashi, I. & Tanibe, H. 1997. Effects of chitosan concentration and precipitation bath concentration on the material properties of porous cross-linked chitosan beads. *Separation Science and Technology*, 32, 1959-1974.

Khan, A. K., Peh, K. K. & Ch'ng, H. S. 2002. Reporting degree of deacetylation values of chitosan: the influence analytical methods. *Journal Pharmacy and Pharmaceutical Sciences*, 5(3), 205-212

Kotze, J.S., Vosloo, H.C.M. & Vorster, S.W. 2001. Characterization of chitosan by size exclusion chromatography using a MALLS detector. Masters dissertation North-West University, SA.

Kurita, K. 2001. Controlled functionalization of the polysaccharide chitin. *Progress in Polymer Science*, 26, 1921-1971.

Monteiro, O.A.C. & Airoldi, C. 1999. Some studies of cross-linking chitosan-glutaraldehyde interaction in a homogeneuous system. *International Journal of Biological Macromolecules*, 29,119-128

Muzzarelli, R.A.A. 1974. Natural chelating polymers: Alginic acid, chitin and chitosan. Pergamon press.

Rhazi, M., Desbrieres, J., Tolaimate, A., Rrnaudo, M., Vottero, P. & Alagui, A. 2002. Contribution to the study of the complexation of copper by chitosan and oligomers. *Polymer*, 43, 1267-1276.

Roberts, G. A. F. 1997. Determination of degree of N-acetylation of chitin and chitosan. Chitin Handbook. Edited by: Muzzarelli, R.A.A and Peter, M.G. *European chitin society,* 129-136.

Skoog, DA., West, D.M. & Holler, F.J. 1996. Fundamentals of analytical chemistry. Seventh edition, Saunders College Publisher, 159-244..

Tan, S. C., Khor, E., Tan, T. K. & Wong, M. S. 1998. The degree of deacetylation of chitosan: advocating the first derivative UV-spectrometry method of determination. *Talanta*, 45, 713-719.

Van der Merwe, H. C. 2006. Chitosan membranes for removal of zinc from simulated wastewater. PhD Thesis, School of Chemical and Minerals Engineering, North-West University, SA.

Wu, F-C., Tsang, R-L. & Juang, R-S. 2001. Kinetic modeling of liquid-phase adsorption of reactive dyes and metal ions on chitosan. *Water Resaerch*, 35 (3), 613-608.

Chapter 4 Adsorption of heavy metals on chitosan beads: a thermodynamic study

4.1 Introduction

Although the adsorption of heavy metals onto chitosan has been studied for more than 20 years, there is still no conclusive mechanism of adsorption presented in literature. The nature of the metal species and the pH of the solution are the most significant parameters that influence the metal uptake mechanism. The pH influences the adsorption properties of chitosan in two ways: i) due to its basic character, the free amine groups are a function of pH; and ii) the speciation of the metal in solution depends on the pH.

Traditionally, the adsorption parameters are determined at a fixed pH and therefore also only valid for that certain pH, and only a few models have been presented in literature that takes the effect of pH on adsorption into account (*e.g.* Chu, 2002; Juang and Shao, 2002; Rhazi *et al.*, 2002a).

In this chapter, adsorption-desorption studies were performed and the results were used to verify an equilibrium model that takes the effect of pH into consideration. In addition, this model was used to verify the effects on the equilibrium parameters of; i) bead sizes, ii) bead modifications through cross-linking, and iii) solution ionic strength. In this work, the main focus was on Cu, but the metals Zn, Cd, and Pb were also studied. In Section 4.2, the theoretical background of metal adsorption on chitosan is presented with consideration of the various effects of pH, while in Section 4.3 the adsorption equilibrium model is discussed. The experimental work is presented in Section 4.4 and the results and discussion are given in Section 4.5. Finally, the conclusions are listed in Section 4.6.

4.2 Literature survey

The amine group in chitosan is considered to be the most important feature in the adsorption of metal ions, especially those of transition metals (Muzzarelli, 1974). This has been verified with mercury(II), copper(II), uranyl(II), vanadium(IV), palladium(II), zinc(II) and cadmium(II) by several authors (*e.g.* Jansson-Charrier *et al.*, 1996; Ruiz *et al.*, 2000; Rhazi *et al.*, 2002a,b; Jeon and Holl, 2003), and the lone-pair-electron on the nitrogen of the amine group has often been characterized as a chelating site in the adsorption. According to Muzarrelli (1974), this

electron pair forms a coordinate bond with the transition metal ions and, because of the basic nature of the functional group it can also adsorb anionic complexes.

In many cases, the chitosan-metal interaction has been reported to be influenced by the pH of the solution. Ruiz *et al.* (2000) indicated two key parameters affecting the adsorption of several metal ions on chitosan: i) the speciation of the metal ions in solution; and ii) the degree of protonation of chitosan. The speciation forms of the metal salt in aqueous solution, which is dependent on the pH of the solution, controls the metal uptake capacity. Copper adsorption is for example favorable at a pH 5-6 and in this range, copper is mainly present as copper(II) ions (Rhazi *et al.*, 2002a and Chu, 2002). A study on cadmium adsorption on cross-linked chitosan by Rorrer *et al.* (1993) indicated that at a pH of 6, where most cadmium species exist as cadmium(II) ions, a maximum adsorption was found. Jeon and Holl (2003) studied the effect of a pH value between 2 and 9 on mercury(II) adsorption onto modified chitosan, and found that mercury(II) was mostly adsorbed at a pH of 7 because at this pH, mercury(II) ion is the dominant specie in solution.

A standard acid-base theory was used by Rhazi *et al.* (2002a) to describe the nature of chitosan in aqueous solutions, and it was observed that at near neutral pH, most of the sites are unprotonated and the adsorption of metal cations is favored. The effect of the pH on chitosan adsorption characteristics can be nicely illustrated at low pH, where the majority of the amine groups of chitosan are protonated. This was studied by Guibal *et al.* (1999) who reported on the adsorption of molybdate species in the form of anions at a pH of 3. Similar results were obtained by Wu *et al.* (2001) who found high uptakes of $Cu(EDTA)^{2-}$ at a pH 3-4. At these pH conditions, the metal-chitosan interaction has been described to be electrostatic attraction, and most of the amine sites of the chitosan are protonated, carrying a positive charged ion that can attract anions (Guibal, 2004).

Domard (1987) had studied the mechanism of metal-chitosan interaction by varying the pH of the solution. He performed a potentiometric experiment with copper below a pH of 6.1 to propose a coordination mechanism between copper and chitosan of the complex $[CuNH_2(OH)_2]^0$. Jha *et al.* (1987) studied the adsorption of cadmium(II) onto chitosan at a pH between 6 and 7, also to suggest a coordination bonding. Rhazi *et al.* (2002a) performed a similar potentiometric experiment to that of Domard (1987), but in this case, the pH and copper(II) to amine ratio were varied. They deduced a coordination mechanism and, proposed

two complexes at two different pH values. The complex $\{[Cu(-NH_2)]^{2+}, 2OH^-, H_2O\}$ is formed at a pH of between 5 and 5.8 while the other complex $\{[Cu(-NH_2)]^{2+}, 2OH^-\}$ is formed at a pH of above 5.8. An X-ray photoelectron spectroscopy method was used by Dambies *et al.* (2001) to study the mechanism of metal-chitosan interactions. They found that at a pH of 4.5 and 6.9, copper is bonded to the amine functional group and that the copper is not reduced, remaining in its 2+ oxidation state.

In the quantitative description of the adsorption of heavy metals onto chitosan beads, researchers have tried to fit experimental data to a model which includes the pH. A popular, and frequently used, model for the adsorption of metal ions on chitosan is the Langmuir isotherm model (*e.g.* Wu *et al.*, 2001; Chu, 2002):

$$q_e = \frac{q_m b C_e}{1 + b C_e} \qquad 4.1$$

The Langmuir isotherm parameters, the maximum capacity q_m and specifically, the affinity coefficient b are pH-dependent so each set of equilibrium values is only valid for a particular pH. A more sophisticated Langmuir-Freundlich model, was used by Chu (2002) in order to fit equilibrium data from copper(II) adsorption onto partly deacetylated chitin. The model is based on 5 adjustable parameters that are pH-independent and is able to account for the adsorption of copper(II) ions at various pH values.

Juang and Shao (2002) formulated a series of equilibrium reactions to predict the adsorption of divalent metal ions; nickel(II), copper(II), and zinc(II) in batch systems. A good fit between model and experiments was obtained for a single metal ion but failed in binary solutions. Jeon and Holl (2003) used a similar equilibrium reaction as Juang and Shao (2002) to successfully predict the adsorption of mercury(II) ion onto modified chitosan beads.

In summary, the adsorption of most transition metal ions is pH dependent but only a few models in the literature are able account for this. For a good understanding of the adsorption mechanism and for a good quantitative prediction of the adsorption characteristics, a generalized model involving the effect of pH is needed. In this work, an equilibrium model is proposed in which adsorption, and also desorption data are considered, in order to investigate

the competitive adsorption between protons and metal ions. From the model, pH-independent parameters are determined and used to describe equilibrium isotherms at various pH.

4.3 Equilibrium model

This model is similar to the equilibrium model as given by Juang and Shao (2002) but is derived from two equilibrium reactions and a nitrogen mass balance. In most cases, metal complexation through coordination has been proposed as the adsorption mechanism for chitosan, and the following equilibrium reaction is used, with the chitosan adsorption sites denoted as $-NH_2$ (Juan and Shao, 2002; Rhazi *et al.*, 2002a):

$$M_{(aq)}^{2+} + n(-NH_2) + mH_2O \leftrightarrows [M(-NH_2)_n,(OH^-)_m]^{(2-m)+} + mH^+ \qquad 4.2$$

Where n is the number of amine and m is the number of hydroxide ions in the complex per metal. If $[M(-NH_2)_n,(OH^-)_m]^{(2-m)+}$ is denoted as [M*], the corresponding equilibrium constant is given by:

$$K_{ads} = \frac{[M^*][H^+]^m}{[-NH_2]^n[M_{(aq)}^{2+}]} \qquad 4.3$$

In addition to the adsorption equilibrium reaction, chitosan can also react according to:

$$-NH_2 + H^+ \leftrightarrows -NH_3^+ \qquad 4.4$$

Traditionally, this reaction is described by an acid base constant ($pK_a = \log K_a$). For chitosan, the pK_a varies according to the source of chitosan and the process of its modification as was discussed in Section 3.3.4 (Guibal *et al.*, 1999; Gao *et al.*, 2000). An experimental titration curve was also traditional used to describe the acid-base constant. From these experiments, the degree of protonation, α, defined as the ratio of the protonated amine groups to the total amine groups that are not complexed with a metal, is derived:

$$\alpha = \frac{[-NH_3^+]}{[-NH_2]+[-NH_3^+]} \qquad 4.5$$

The total amine group concentration is equal to the sum of the concentration of the free (un-reacted) amine groups [-NH_2], the protonated amine groups [-NH^+_3], and the metal loaded amine groups (n·[M*]):

$$[-NH_2]_T = [-HN_2] + [-NH_3^+] + n[M^*] \qquad 4.6$$

Combining Equations (4.5) and (4.6) gives:

$$[-NH_3^+] = \alpha([-NH_2]_T - n[M^*]) \qquad 4.7$$

Substituting for [R-NH^+_3] in Equation (4.6) gives:

$$[-NH_2] = ([-NH_2]_T - n[M^*])(1-\alpha) \qquad 4.8$$

where [M*] is the amount of metal adsorbed by the adsorbent at equilibrium, which is conventionally termed q_e.

If all the amine sites are available for adsorption, the total amine concentration has a direct relation with the maximum capacity, q_{max} and n, according to:

$$q_{max} = \frac{[-NH_2]_T}{n} \qquad 4.9$$

which results in:

$$[-NH_2] = n(q_{max} - q_e)(1 - \alpha) \qquad 4.10$$

Substituting Equation (4.10) into Equation (4.3) gives:

$$K_{ads} = \frac{q_e[H^+]^m}{[n(1-\alpha)(q_{max} - q_e)]^n C_e} \qquad 4.11$$

where C_e is the equilibrium metal concentration in solution. Equation (4.11) is now in terms of measurable quantities that can be used to determine the equilibrium constant. Taking the log of both sides of Equation (4.11) gives (after re-arrangement):

$$\log \frac{q_e}{[n(1-\alpha)(q_{max} - q_e)]^n C_e} = \log K_{ads} - m \log[H^+] = \log K_{ads} + m\,pH \qquad 4.12$$

With q_e, C_e and α known from experimental measurements, q_{max} can be fitted in the plot of the left hand side of Equation (4.12) against equilibrium pH. Previous studies have different results about the number of amine groups bonding metal ions (Juan and Shao, 2002; Rhazi *et al.*, 2002a). In this work, the value of n is chosen for some discrete number of cases (n = ½, 1, 1½, and 2). The value of K_{ads} is determined from the intercept of the straight line on the y-axis and the slope of the line is used to determine m.

In a specific situation where n and m are equal to one, Equation (4.11) can be re-arranged to a Langmuir type equation:

$$q_e = \frac{q_{max} b C_e}{1 + b C_e} \qquad 4.13$$

Where:

$$b = \frac{(1-\alpha) K_{ads}}{[H^+]} \qquad 4.14$$

4.4 Experimental

4.4.1 Introduction

Equilibrium adsorption and desorption studies were carried out with copper(II), zinc(II), cadmium(II), and lead(II) ions on beads produced and characterized as presented in chapters 2 and 3 respectively.

4.4.2 Chemicals

The following metal salts were used in the experiments; anhydrous $CuSO_4$, (>99.9%, Merck), $Pb(NO_3)_2$, (>99.9%, Aldrich), $CdSO_4$ (>99.9%, Aldrich), and hydrated $ZnSO_4.7H_2O$ (>99%, Aldrich). Acetic acid (>99%) and sodium acetate (>99%) were both purchased from Saarchem UnivAR of analytical grade. Hydrochloric acid (>99%), sodium hydroxide (>99%), sodium nitrate (>99.9) and ammonium acetate (>98%) were all purchased from Aldrich Chemicals. Distilled water was produced in the laboratory with a Pure Water distiller (Ultima 888 water distiller). The pH of solution was measured with a pH meter (Hanna HI 8421 or Corning Scholar 425). The LC and CC beads presented in Table 2.1 were used for the adsorption studies. Cation exchange resin beads, Amberlite 200CNa having a diameter of 0.5 mm (supplied by ROHM and HAAS, France), were used as a reference adsorbent to the chitosan beads.

4.4.3 Adsorption

Two sets of equilibrium experiments were conducted depending on the type of pH control:

Set I: metal adsorption experiments at controlled equilibrium pH.
Set II: metal adsorption experiment at controlled initial pH, without adjusting the pH during adsorption. Table E-1 (Appendix E) gives detailed set out of Set I and Set II experiments.

The Set I experiments were used to fit the traditional models, like Langmuir and Freundlich, while the Set II experiments were used to determine the different constants in the model as derived in Section 4.3. Successively, this model was used to describe the Set I experiments.

Beads to the amount of 0.2-6.0 g were added to 10-250 mL metal solution in 50 or 500 mL Erlenmeyer flasks. The concentration of metal in the solution varied between 0.16 and 5.04 mmol/L (10 and 320 mg/L for Cu) prepared from a 7.87-15.74 mmol/L (500-1000 mg/L for Cu) stock solution. To establish equilibrium, the Erlenmeyer flasks were placed in a Labcon incubator for 24 h (25 ± 0.5°C, 120 rpm). After equilibrium, the pH of the solution was measured and also a clear metal solution was collected and analyzed with atomic absorption spectrometry (Varian SpectrAA-10). The wet beads were vacuum filtered through Whatman-glass filters (Grade GF/C), and then rinsed with distilled water before being dried in the oven at

80°C for 24 h to obtain the dry mass of chitosan. A material balance on the metal components in the liquid phase was used to determine metal removed and, the adsorption loading capacity was calculated as the amount of solute removed per mass of the dry adsorbent using Equation (4.15).

$$q_e = \frac{(C_i - C_e)V}{m_d} \qquad 4.15$$

The influence of ionic strength on equilibrium adsorption onto chitosan beads was experimented by adding 0.001, 0.01, 0.1, and 0.25 M sodium nitrate to different sets of copper solution. In this experiment, it was assumed that sodium is not adsorbed as discussed in Section 3.3.8. The metal adsorption capacity was determined according to Equation (4.15).

4.4.4 Desorption

After adsorption, the metal loaded chitosan beads were vacuum filtered into a 250 mL Erlenmeyer flask and weighed. A volume of 50 mL of 0.001-0.1 M HCl prepared from a 1.0 M HCl standard solution was added. The Erlenmeyer flask was placed in a Labcon incubator shaken for 24 h (25 ± 0.5°C, 120 rpm) to reach equilibrium for desorption. After equilibrium, the pH of the metal ion solution was measured and a clear metal solution was collected and analyzed with atomic absorption spectrometry (Varian SpectrAA-10). The wet beads, in the remaining solution were vacuum filtered through Whatman-glass filters (Grade GF/C), and then rinsed with distilled water before being dried in the oven at 80°C for 24 h to obtain the dry mass of chitosan.

4.5 Results and discussion

4.5.1 Adsorption in the presence of a buffer

During metal adsorption, pH control has been found to be essential in avoiding metal precipitation. This depends on the range of metal concentration used. In many situations, a buffer has been used to keep the solution pH at the desired range. Sometimes a large concentration of buffer is required, which may affect equilibrium parameters because of metal

complex formation. For example when an acetic acid/sodium acetate buffer was used, the uptake capacity was lower as illustrated in Figure 4.1.

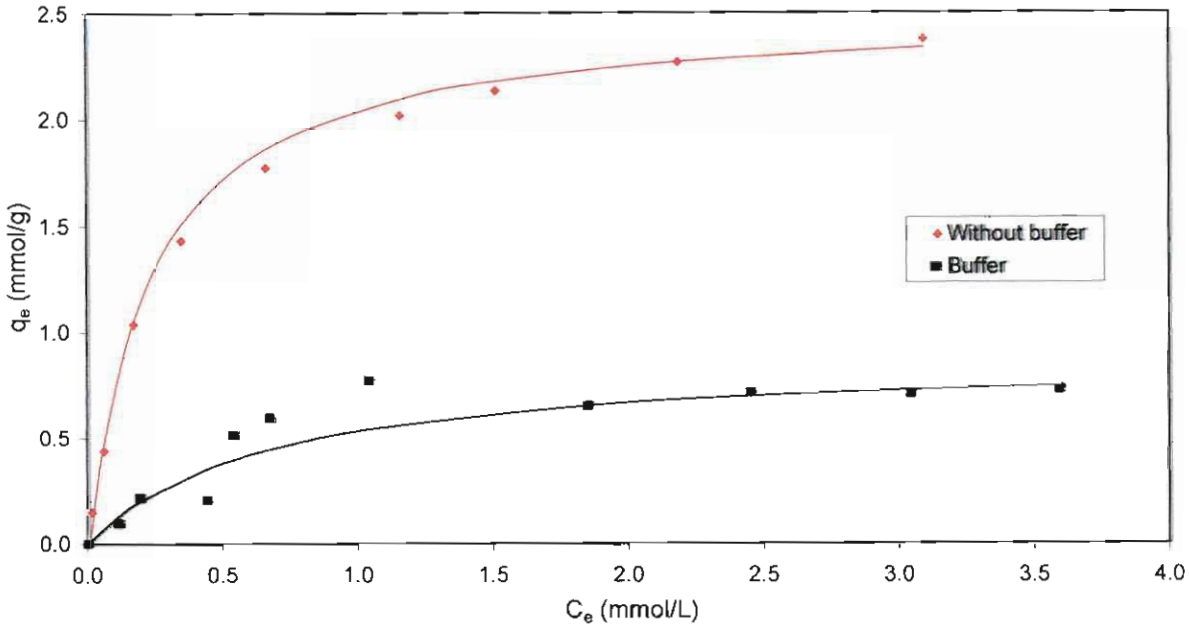

Figure 4.1: Adsorption isotherm of copper(II) ion adsorbed on chitosan beads in the presence and absence of a 0.025 M acetic acid and 0.36 M sodium acetate buffer.

4.5.2 Alkaline properties of chitosan

The alkaline properties of chitosan were investigated in a batch system. In this experiment, beads were place in flasks containing a solution of distilled water and copper sulfate. Before the beads were added to the flask, the pH of the solution was adjusted to 4.9. As shown in Figure 4.2, after the beads were added to the copper solutions, the pH increased to 6.3 and remained constant. This increase in pH is due to the basic characteristics of chitosan. For the case of beads in distilled water, a higher final pH was measured. This increase in pH is caused by the increase in available free amine sites that produce more hydroxide ions. This is in contrast to a solution of copper where fewer hydroxide ions are produced because copper ions are also competing for vacant amine sites. This finding is in agreement to the result obtained by Jeon and Holl (2003) for chitosan beads left in distilled water and in a mercury(II) solution.

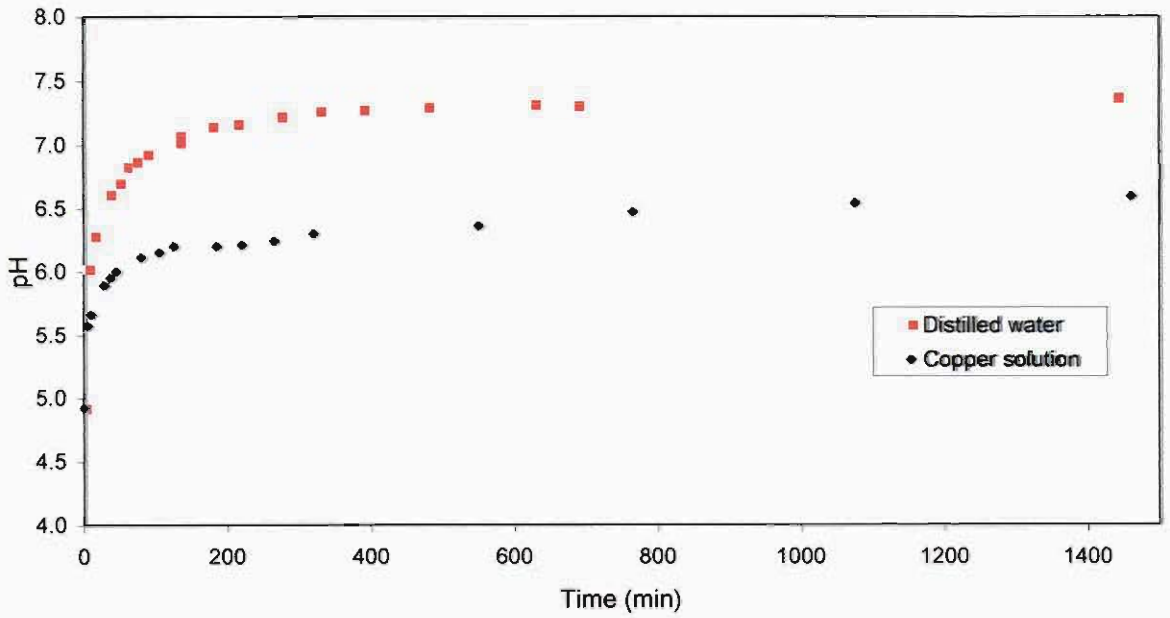

Figure 4.2: Change over time of chitosan beads in distilled water and in 1.57 mmol/L copper(II) solution.

4.5.3 Adsorption results

Sections 4.5.1 and 4.5.2 showed that for a controlled equilibrium pH either a buffer or pH control using *e.g.* nitric acid/sodium hydroxide is needed. Although the pH adjustment with nitric acid/sodium hydroxide is experimentally troublesome and time consuming, it was preferred in this study because the use of a buffer has shown to affect the adsorption performance significantly (Figure 4.1).

Two models, the Langmuir model and the model as given in Section 4.3 (from now on called the pH-model) were used to study metal adsorption properties on chitosan beads. The Langmuir model was use to fit the Set I adsorption data in which the equilibrium pH values were at 5, 5.5 and 6. For the case of applying the pH-model, the equilibrium constant is determined from Set II equilibrium data and then used to describe Set I experimental data.

4.5.3.1 Equilibrium parameters

The Set I experimental data, as given in Tables F-1, F-2, F-3, and F-4 (Appendix F), were fitted to the Langmuir model and Figure 4.3 shows the isotherms of copper adsorption on cross-

linked and non-cross-linked beads at different pH values. The fitted Langmuir model describes the measured data well and the calculated Langmuir parameters are given in Table 4.1. The non-cross-linked beads show a higher uptake capacity, which was also found by Monteiro and Airoldi (1999) to be the case when copper was adsorbed on cross-linked and non-cross-linked chitosan gels. The parameter b was found to increase and q_m was found to differ with solution pH.

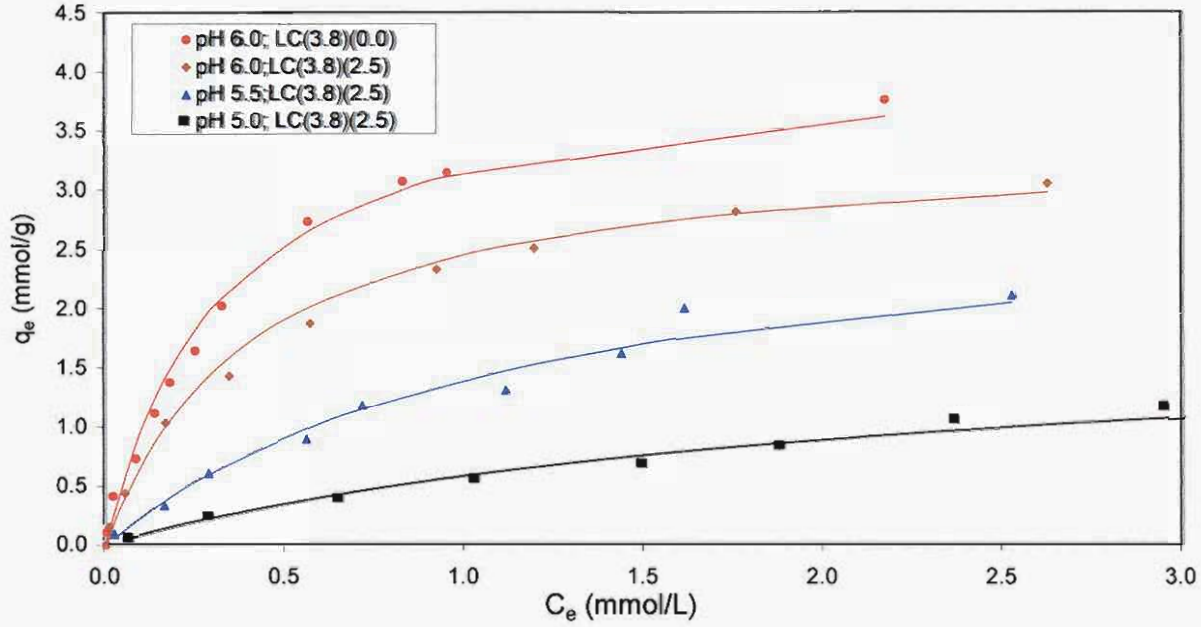

Figure 4.3: Effect of pH on copper adsorption onto chitosan beads: Langmuir model fit.

In the range of equilibrium studied, the calculated adsorbent capacities were found to be in the range of 2.1-3.4 mmol/g. Similar findings were reported by Chu (2002) and Jeon and Holl (2003) when copper and mercury were adsorbed onto chitosan.

Table 4.1: Langmuir isotherm parameters for copper adsorption on cross-linked chitosan beads at different pH values.

Beads	LC(3.8)(2.5)	LC(3.8)(2.5)	LC(3.8)(2.5)	LC(3.8)(0.0)
pH (±0.05)	5.0	5.5	6.0	6.0
q_m (mmol/g)	2.08	3.32	3.40	4.20
b (L/mmol)	0.39	0.71	2.70	3.39
R^2	0.94	0.94	0.99	0.98

From the results, it can be concluded that the effect of pH is significant and cannot be explained by the Langmuir isotherm. The Langmuir isotherm does predict the experiments well, but the fitted parameters cannot be explained from a physical background which is illustrated by the values of q_m, which changes with pH. Since metal ions and hydronium ions compete for the same sites in chitosan, it will be appropriate to apply a model that takes this competition into account. This pH model is given in Equations (4.2) – (4.14), and the model parameters were obtained by fitting the Set II experiments. After this, the pH-model was used to describe the Set I experiments and the comparison is discussed.

4.5.3.2 pH model

The pH-model is used to describe the equilibrium data of copper adsorption on LC and CC beads. It is also used to study the influence of bead size, DCL and the solution ionic strengths on copper(II) ion adsorption performance on LC beads. In addition, the model is used to describe experimental data from cadmium(II), lead(II), and zinc(II) adsorbed on LC(3.8)(2.5) beads.

Determination of equilibrium constant and capacity

The Set II experimental results as presented in Appendix G (Tables G-1 – G-6), were fitted with the pH-model; this involves the plotting of the left hand side of Equation (4.12) against equilibrium pH. Results for the non-cross-linked (LC(3.8)(0.0)) and cross-linked beads (LC(3.8)(2.5)) are presented in Figure 4.4. Desorption results are included for the cross-linked beads and also for the construction of Figure 4.4. It was found that both adsorption and desorption could be described by the same model. Within the proposed range of n, n = 1 resulted in the best fit ($R^2 > 0.95$). The fitted q_{max} was 4.2 and 5.3 mmol/g for cross-linked and non-cross-linked beads respectively. The q_{max} was found to be comparable to the amine concentration calculated from the titration results (Table 4.2), and demonstrates that that the amine groups are primarily involved in copper complexation.

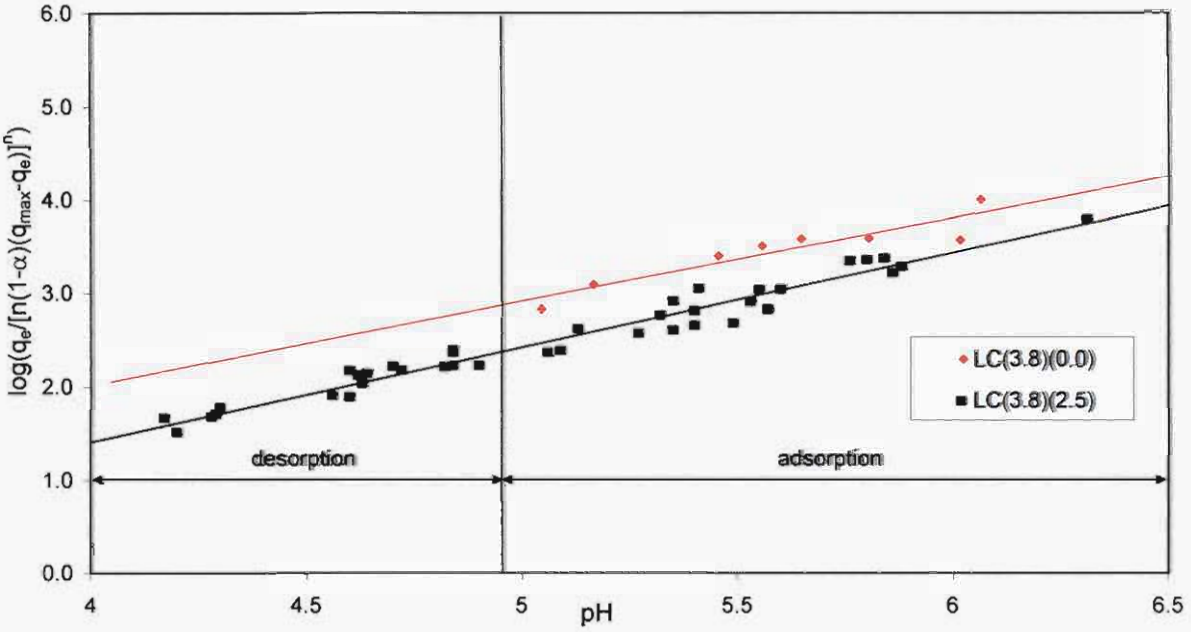

Figure 4.4: Equilibrium constant measurements for copper adsorption on cross-linked and non-cross-linked beads.

The parameter m and K_{ads} were determined from the slope and intercept of Figure 4.4, and values are given in Table 4.2. The value of K_{ads} for LC(3.8)(2.5) beads was found to be lower than that of the LC(3.8)(0.0) beads. The value of *m* was found to be close to unity which shows that one $-NH_2$ group, one OH^- group and two water molecules are involved in the complex (see Equation (4.2)).

Table 4.2: Equilibrium constant values for copper-chitosan interactions.

Beads	m	$K_{ads} \cdot 10^{-3}$	q_{max} (mmol/g)	$[-NH_2]$* (mmol/g)	R^2
LC(3.8)(0.0)	0.98 (±0.02)	7.58 ($\pm 5.0 \cdot 10^{-4}$)	5.3	4.9	0.95
LC(3.8)(2.5)	1.00 (±0.02)	2.71 ($\pm 5.0 \cdot 10^{-4}$)	4.2	4.0	0.97

**From Section 3.3.4*

The values of K_{ads} and q_{max} were used in Equation (4.13) to fit experimental data of Set I (Figure 4.3) as presented in Tables F-1, F-2, F-3, and F-4 (Appendix F). As shown in Figure 4.5, the experimental (data points) and the model calculations (solid lines) correlate very well. Here the maximum capacity q_{max} was assumed to be constant and pH-independent.

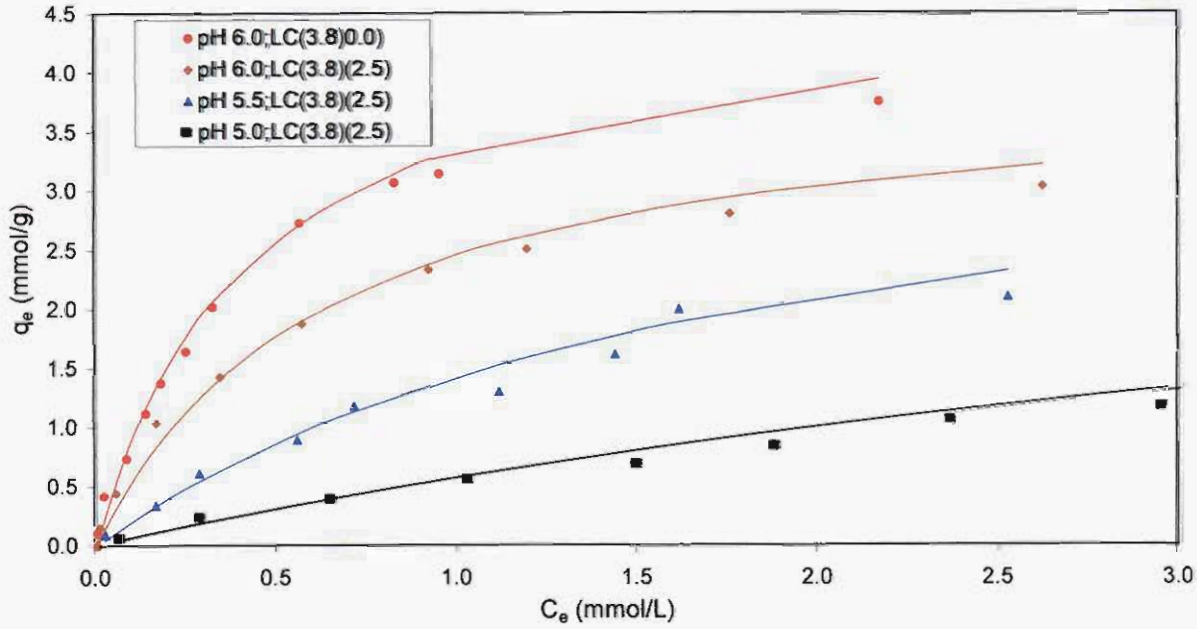

Figure 4.5: Effect of pH on copper adsorption onto chitosan beads: Proposed model fit.

Influence of bead size on equilibrium properties

The effect of bead diameter (D) was examined with 0.9, 1.8 and 3.8 mm diameter LC beads cross-linked with 2.5% (v/v) glutaraldehyde solution. The adsorption data is available in Appendix G. Figure 4.6 and Table 4.3 show the influence of particle size on the equilibrium constant. Once more, the value of n =1 gave the best fit and the calculated m was again found to be one. The K_{ads} values were in the range $(1.02\text{-}2.71)\cdot10^{-3}$ and increased slightly with decreasing bead size. These slight changes might be attributed to the DCL as it has been observed in Section 3.3.4 that the DCL increases with a decrease in the bead size.

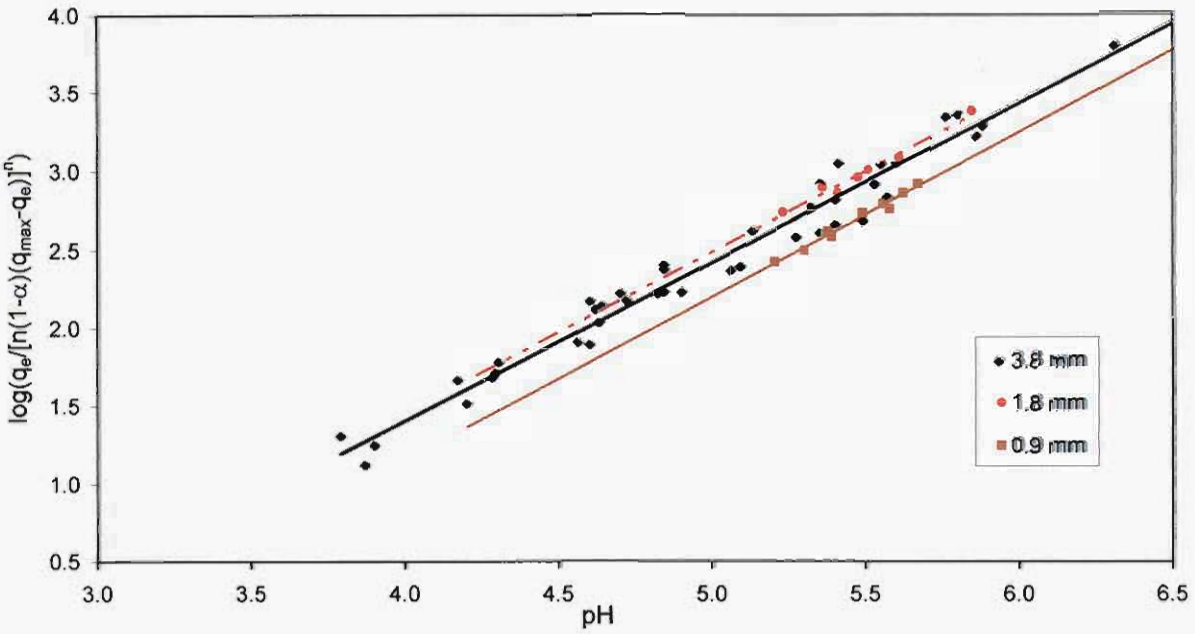

Figure 4.6: Influence of particle sizes on equilibrium constant values.

The calculated q_{max} of the adsorbents are in range of 3.8-4.2 mmol/g and they are comparable to those values determined from the titration (Section 3.3.4). This is in agreement with the findings of Guibal *et al.* (1997), that when molybdate was adsorbed onto chitosan beads, there was no difference in adsorption capacity for the different size beads.

Table 4.3: Equilibrium parameters for copper adsorption on different LC beads.

Beads	LC(0.9)(2.5)	LC(1.8)(2.5)	LC(3.8)(2.5)
q_{max} (mmol/g)	3.8	3.8	4.2
$K_{ads} \cdot 10^{-3}$	1.14 ($\pm 7.0 \cdot 10^{-4}$)	2.49 ($\pm 5.0 \cdot 10^{-4}$)	2.71 ($\pm 5.0 \cdot 10^{-4}$)
m	1.05 ($\pm$0.02)	0.99 ($\pm$0.02)	1.00 ($\pm$0.02)
[-NH_2] (mmol/g)*	3.3	3.4	4.0
DCL (%)*	32.7	30.6	18.4

From Section 3.3.4

Influence of DCL on equilibrium properties

Figure 4.7 shows the effects of the DCL on the adsorption equilibrium properties, and the determined equilibrium parameters q_{max} and K_{ads} are given in Table 4.4. The DCL was found to affect K_{ads}, with an increase in the DCL resulting in a decrease of K_{ads}.

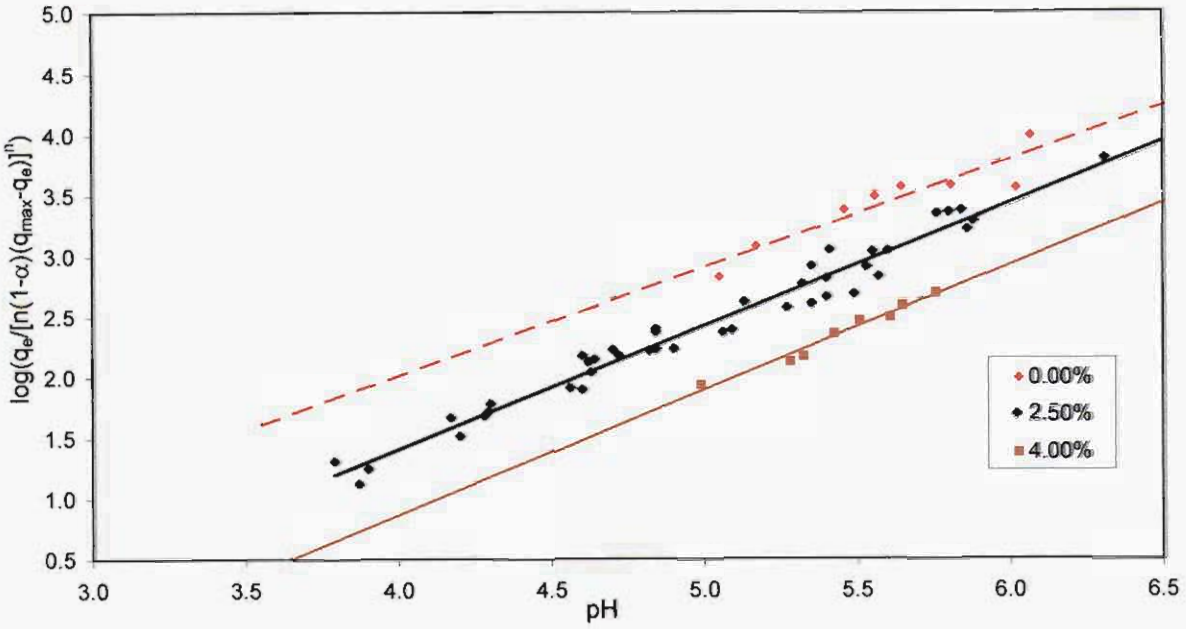

Figure 4.7: Influence of glutaraldehyde concentration on equilibrium constant values.

Table 4.4: Effect of cross-linking on equilibrium properties for copper adsorption on beads.

Beads	LC(3.8)(0.0)	LC(3.8)(2.5)	LC(3.8)(4.0)
q_{max} (mmol/g)	5.3	4.2	3.8
$K_{ads} \cdot 10^{-3}$	7.58 ($\pm 5.0 \cdot 10^{-4}$)	2.71 ($\pm 5.0 \cdot 10^{-4}$)	1.02 ($\pm 5.0 \cdot 10^{-4}$)
DCL (%)*	0.0	18.4	34.7
[-NH_2] (mmol/g)*	4.9	4.0	3.2

**From Section 3.3.4*

The Set I experiments carried out at a pH 6 with beads having different DCL is shown in Figure 4.8. The parameters in Table 4.4 were used to fit the equilibrium curves. The adsorbent capacity (q_{max}) varies between 3.8 and 5.3 mmol/g. The LC(3.8)(0.0) has more adsorption loading compared to LC(3.8)(2.5) and LC(3.8)(4.0). This observation is similar to the findings of Monteiro and Airoldi (1999) for chitosan gel cross-linked with different percent glutaraldehyde solutions. They found that an increase in the amount of cross-linking reduces copper uptake capacity.

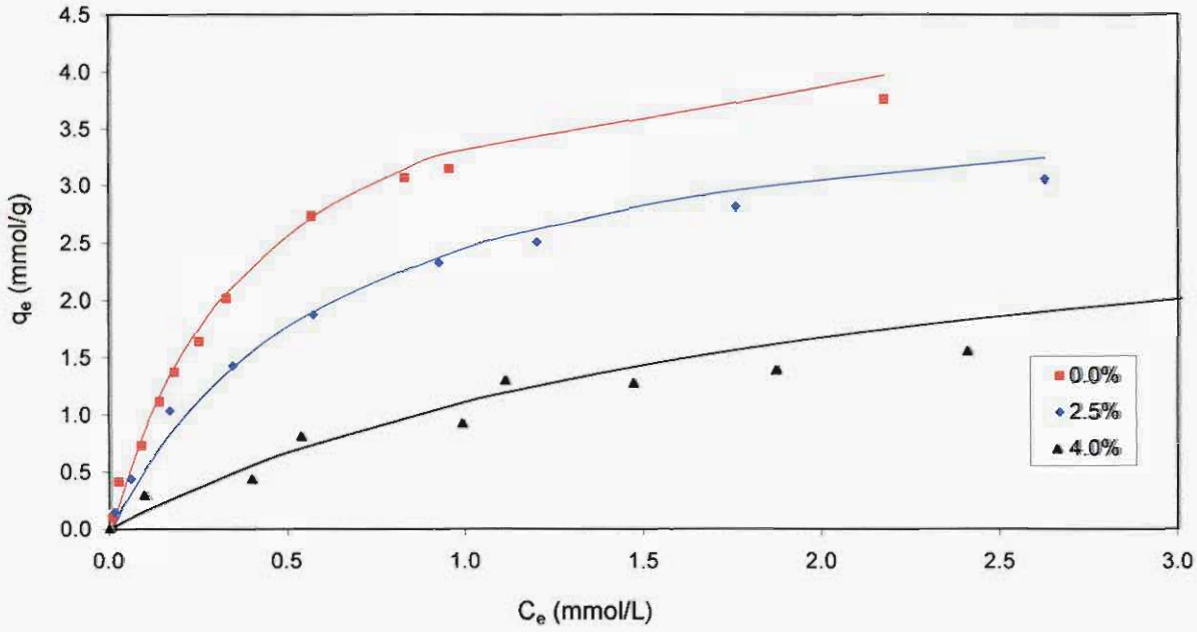

Figure 4.8: Effect of cross-linking on adsorption equilibrium at a pH value of 6.

Figure 4.9 nicely illustrates the effect of DCL on q_{max} and K_{ads}. The calculated q_{max} drops sharply after cross-linking and remain nearly constant at different cross-linking concentrations that were used for this study. The addition of a new molecule to chitosan during cross-linking may change the way chitosan interact with metals. This can be seen from the significant change in the value of K_{ads} before and after cross-linking as presented in Figure 4.9. Also, after cross-linking K_{ads} may be considered the same as the values are slightly different and are within the same margin of error.

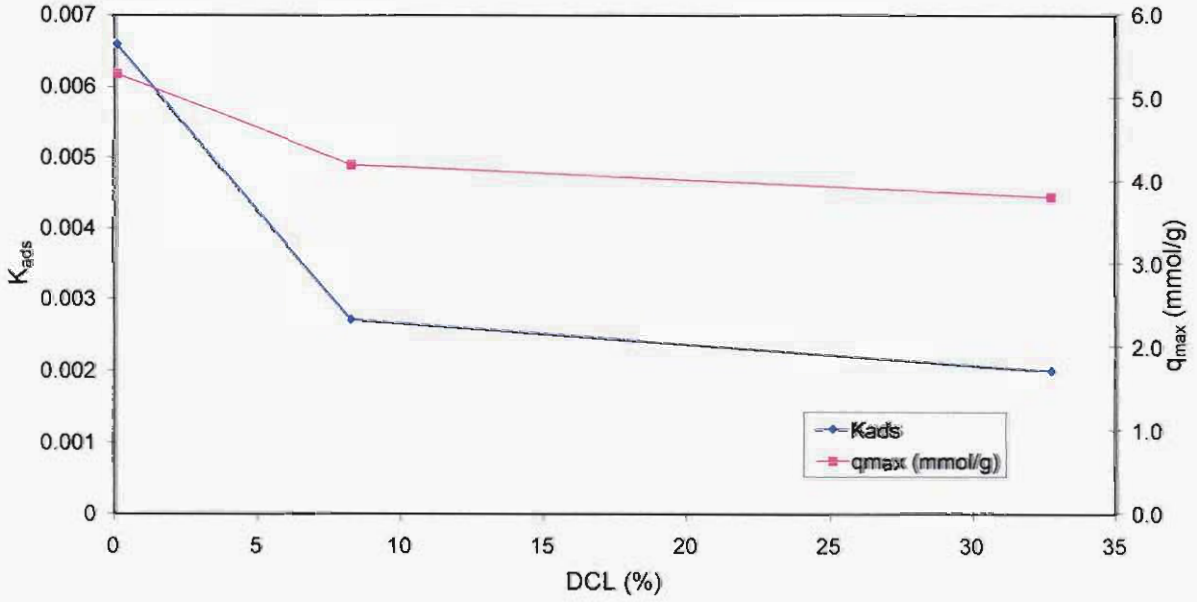

Figure 4.9: Effect of DCL on q_{max} and K_{ads} for copper adsorption on chitosan beads.

Influence of ionic salt on equilibrium properties

Figure 4.10 shows the influence of ionic strength on adsorption equilibrium properties. The equilibrium constant determined was in the range of $(0.8\text{-}2.7)\cdot10^{-3}$ when 0-0.1 M sodium nitrate was added (See experimental data in Appendix G, Tables G-6 – G-9). Below 0.1M sodium nitrate, the K_{ads} is not affected by ionic strength. A decrease in K_{ads} by a factor of 3 was found if the solution contained 0.1 M sodium nitrate salt.

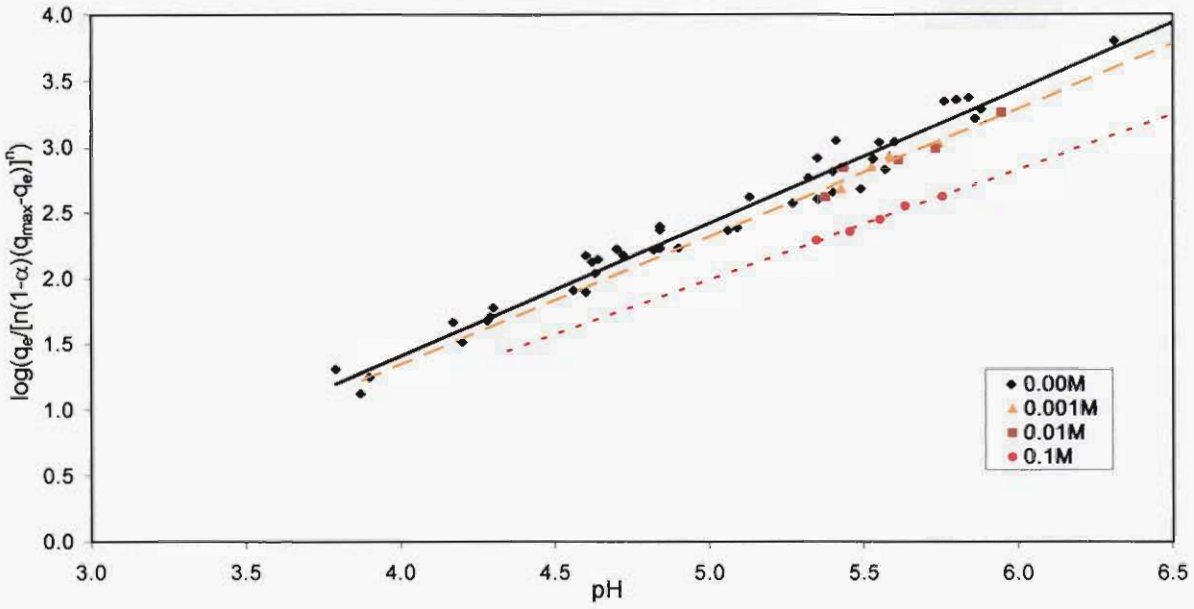

Figure 4.10: Influence of salt concentration on equilibrium constant.

Figure 4.11 shows the effect of salt ion concentration on the equilibrium isotherm curve for adsorption taking place at a constant pH of 6. The parameters obtained from Figure 4.10 were used to fit the curves with adsorbent capacity of 4.2 mmol/g beads. The uptake capacity was not affected at low salt concentrations (<0.01 M). A slightly lower copper uptake was however found for a salt concentration of above 0.1 M sodium nitrate. This agrees with the findings of Hsien and Rorrer (1995) that ionic strength has no influence on the adsorption of cadmium(II) onto chitosan within a concentration range of 0.0-0.15 M sodium nitrate. Jha *et al.* (1987), observed a 22% decrease in capacity for cadmium adsorption on chitosan at a concentration of 0.1 M sodium perchlorate. The results are also confirmed by Piron and Domard (1997), who examined the effects of sodium nitrate on the influence of uranyl ions onto chitosan. At equilibrium, they found that the uptake capacity remains the same when the concentration of salt is increased from 0.01-0.06 M sodium nitrate.

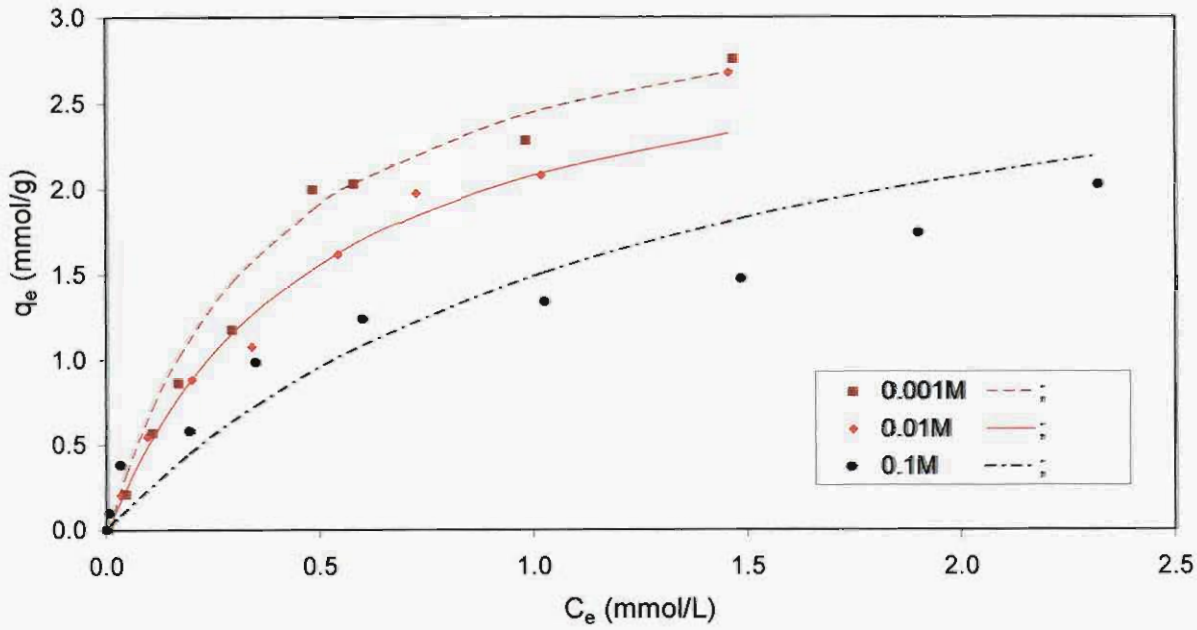

Figure 4.11: Curves of copper adsorption onto beads in the presence of ionic salts at a pH 6.

Equilibrium constant from CC beads

The equilibrium results from adsorption studies for the commercial chitosan beads prepared as presented in Section 2.3.3 is shown in Table 4.5. The results show a similar trend to that of the LC beads (see Appendix G, Table G-10 and G-11)). Best fits were also obtained when $n = 1$ was chosen and the value of m was approximately one. The equilibrium constant for copper adsorption when CC(3.8)(0.0) beads were used is $2.93 \cdot 10^{-3}$ and was larger than for CC(3.8)(2.5) beads with equilibrium constant of $2.26 \cdot 10^{-3}$. The equilibrium constant for LC and CC beads were compared as shown in Table 4.5. The K_{ads} of the LC beads were found to be larger than the equilibrium constant for non-cross-linked CC beads.

Table 4.5: Equilibrium parameters for copper adsorption on beads made of commercial grade chitosan.

Bead	CC(3.8)(0.0)	LC(3.8)(3.8)(0.0)	CC(3.8)(2.5)	LC(3.8)(2.5)
q_{max} (mmol/g)	3.8	5.3	3.6	4.2
$K_{ads} \cdot 10^{-3}$	2.93 ($\pm 5.0 \cdot 10^{-4}$)	7.58 ($\pm 5.0 \cdot 10^{-4}$)	2.26 ($\pm 5.0 \cdot 10^{-4}$)	2.71 ($\pm 5.0 \cdot 10^{-4}$)
m	1.01 (±0.02)	0.98 (±0.02)	0.91 (±0.02)	1.00 (±0.02)
[$-NH_2$] (mmol/g)	3.6	4.9	3.0	4.0

4.5.4 Comparison with other adsorbents

A conventional adsorbent, cation exchange resin Amberlite 200CNa, recommended by ROHM and HAAS, France, was used to adsorb copper. Figure 4.12 shows the equilibrium characteristics of the cation resins as compared to the LC at a pH of 5.5. Their equilibrium properties are listed in Table 4.6, and it is shown that chitosan beads have a larger adsorption capacity.

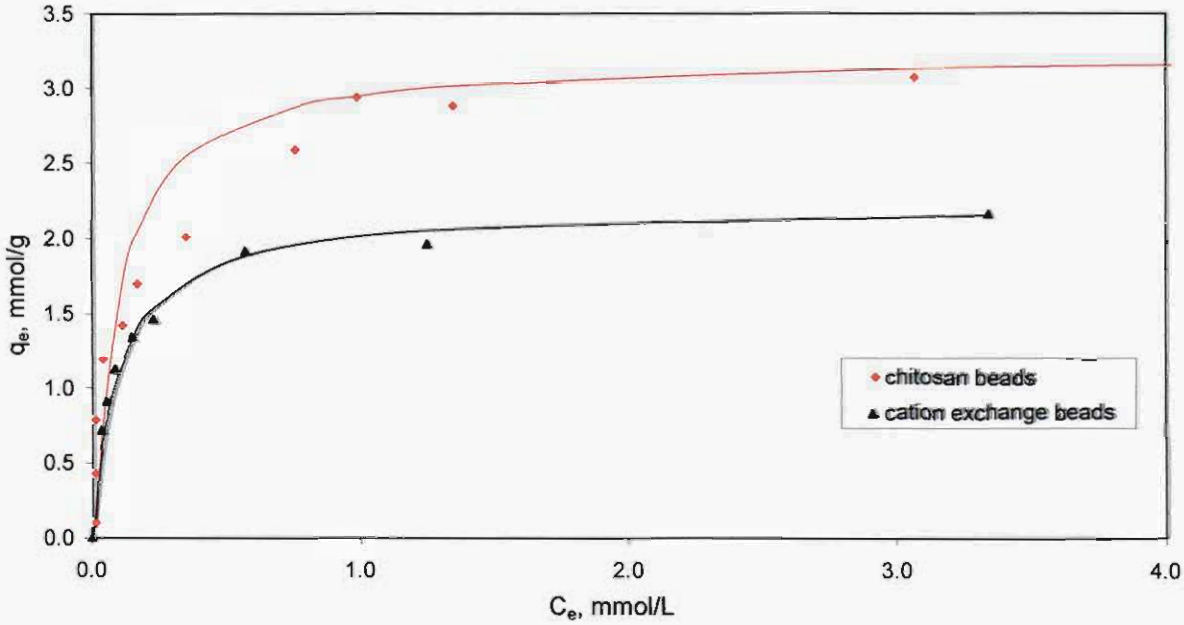

Figure 4.12: Equilibrium isotherm curves for chitosan beads and cation resins beads fitted to Langmuir for adsorption carried out at a pH 5.5.

Table 4.6 also shows the equilibrium properties found in literature for copper adsorption on different adsorbents. The calculated values of b from the pH-model (Equation (4.14)) for the LC and CC beads are in the same range when compares with values for other adsorbent. Within the experimental conditions used for these studies, it can be seen that the LC beads displayed a high adsorption capacity for copper.

Table 4.6: Comparison of adsorption capacities of different adsorbents for copper.

Adsorbent	q_{max} (mmol/g)	b (L/mmol)	pH	Sources
Chitosan beads (LC)	3.8-5.3	0.43-3.39	4-6	This work
Chitosan beads (CC)	3-3.6	0.11-0.89	5-5.5	This work
Flakes (shrimp)	1.9	6.98	6	Wu *et al.* (2001)
Prawn shells	0.13-0.27	1.19-5.29	3-6	Chu (2002)
Ion exchange (Amberlite 200)	2.0	2.54	5.5	This work
Pecan shell Activated carbon	1.9	-	4.5	Dastgheib and Rockstraw (2002)

4.5.5 Adsorption properties of cadmium(II), lead(II) and zinc(II)

The pH model was also fitted to equilibrium results from zinc(II), cadmium(II), and lead(II) adsorbed on LC(3.8)(2.5) beads. The best-fits are shown in Figure 4.13 and the calculated equilibrium parameters are given in Table 4.7. The capacity of the adsorbent that was used to predict equilibrium parameters of Figure 4.13 was 4.2 mmol/g for all metals, a value that was in good agreement with the capacity found from titration results as presented in Section 3.3.4. The value of n = 1 again gave the best fit, and the determined values of m for the case of zinc(II), cadmium(II), and lead(II) are close to one, indicating that one amine group ($-NH_2$) and one hydroxide ion are involved in the complex.

The calculated equilibrium constants vary according to the different types of metal adsorbed onto the beads. The order of increase of K_{ads} is copper(II)>lead(II)>zinc(II)>cadmium(II). This sequence was also found by Bassi *et al.* (2000) when these metals were adsorbed onto chitosan flakes.

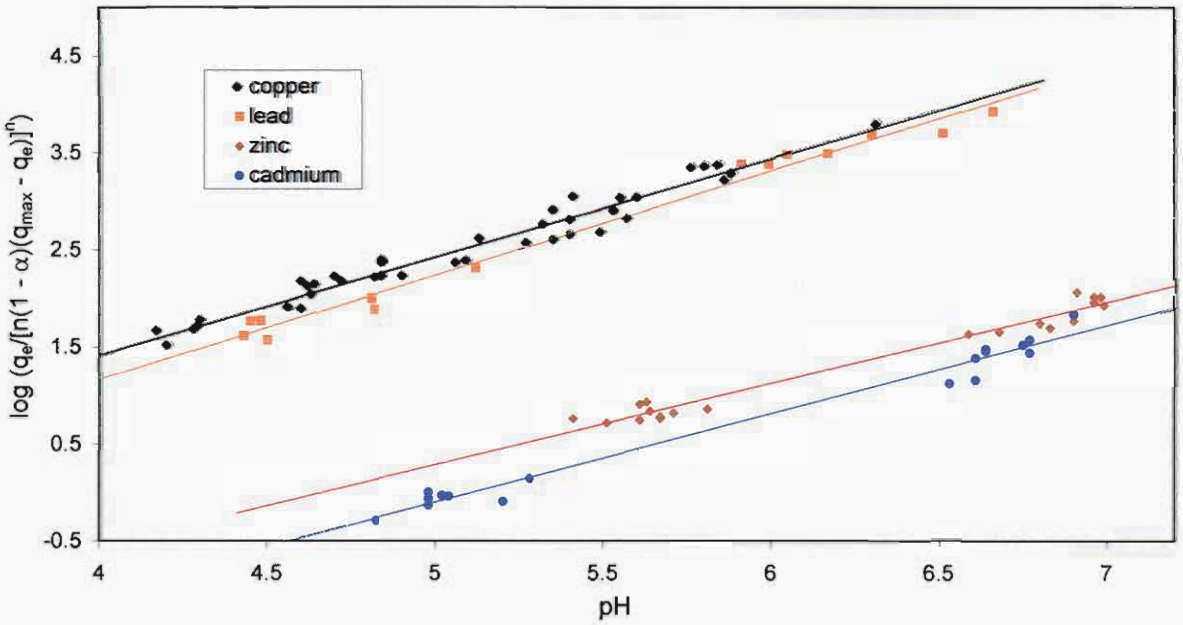

Figure 4.13: Equilibrium constant measurements for lead, cadmium, zinc and copper.

Table 4.7: Equilibrium values for metal-chitosan interactions.

Metals	m (±0.02)	K_{ads} ($\pm 5.0 \cdot 10^{-4}$)	q_{max} (mmol/g)	R^2
Zinc(II)	0.9	$9.55 \cdot 10^{-3}$	4.2	0.964
Cadmium(II)	0.8	$4.79 \cdot 10^{-3}$	4.2	0.937
Lead(II)	0.9	$2.22 \cdot 10^{-3}$	4.2	0.912
Copper(II)	1.0	$2.58 \cdot 10^{-3}$	4.2	0.968

4.6 Conclusions

The pH equilibrium model was shown to successfully describe the adsorption of copper(II), lead(II), cadmium(II) and zinc(II) onto chitosan beads. The model was derived from two equilibrium equations, one describing the acid-base properties of the chitosan bead, and the other describing the adsorption of the metal onto the chitosan bead, and a mass balance of the different forms of nitrogen in the beads. For solving the model, the maximum adsorption capacity was fitted and was found to be closely related to the amine concentration of the chitosan beads. The number of amine groups and hydroxide groups that were involved in the metal complexation were both found to be one for all types of beads. The model could also accurately describe the desorption of the metals from the chitosan, indicating the reversible

nature of the metal chitosan bond, and making an effective recovery of the metal possible (further study is given in Chapter 5). The equilibrium constant (K_{ads}) for copper adsorption is in the range of $(1.02\text{-}7.58)\cdot10^{-3}$ and decreases with an increase in the DCL. The ionic strength of the solution did not have a significant effect on the adsorption characteristics if the concentration of the added sodium nitrate was below 0.01 M, while the adsorption constant decreased by a factor 3 at a concentration of 0.1 M.

The adsorption capacity of the LC beads was found to be higher than most adsorbents reported in the literature, and the adsorption constant for different metals decreased in the range copper(II) > lead(II) > zinc(II) > cadmium(II).

List of symbols

b	affinity between adsorbent and adsorbate in Langmuir equation (L/mg)
C_i	initial solution concentration (mol/L)
C_e	final (equilibrium) solution concentration (mol/L)
D	diameter of bead (m)
$[H^+]$	concentration of hydrogen ion (mol/L)
K_a	acid dissociation constant (mol/L)
K_{ads}	adsorption constant (-)
m	number of hydroxide ion involve in the complex (-)
m_d	mass of dry beads (g)
$M^{2+}_{(aq)}$	metal ion in aqueous solution (mol/L)
[M*]	concentration of metal adsorbed (mol/g)
$[\text{-}NH_2]$	free amino concentration (mol/g)
$[\text{-}NH_2]_T$	total amino groups available for adsorption (mol/g)
$[\text{-}NH^+_3]$	protonated amino concentration (mol/g)
n	number of amine group complexing with metal (-)
q_e	equilibrium adsorption capacity (mol/g)
q_m	pH dependent maximum adsorption capacity (mol/g)
q_{max}	pH independent maximum adsorption capacity (mol/g)
α	degree of protonation (-)
V	volume of solution (L)

References

Bassi, R., Prasher,.S.O. & Simpson, B.K. 2000. Removal of selected metal ions from aqueous solutions using chitosan flakes. *Separation Science and Technology,* 35(4), 547-560.

Chu, K. H. 2002. Removal of copper from aqueous solution by chitosan in prawn shell: adsorption equilibrium and kinetics. *Journal of. Hazardous Materials,* B90, 77-95.

Dambies, L., Guimon, S. & Guibal, E. 2001. Characterization of metal ion interactions with chitosan by X-ray photoelectron spectroscopy. *Colloids and Surfaces A*, 177, 203-214

Domard, A. 1987. pH and c.d. measurements on a fully deacetylated chitosan: application to copper(II)-polymer interactions. *International Journal of Biological Macromolecules,* 9, 98-104.

Gao, Y., Lee, K-H., Oshima, M. & Motomizu, S. 2000. Adsorption behavior of metal ions on crosslinked chitosan and the determination of oxoanions after pretreatment with a chitosan column. *Analytical Science,* 1 16, 1303-1308.

Guibal, E. 2004. Interaction of metal ions with chitosan-based sorbents: a review. *Separation and Purification Technology*, 38, 43-74.

Guibal, E., Milot, C. & Roussy, J. 1999. Molybdate sorption by cross-linked chitosan beads: Dynamic studies. *Water Environment Research,* 71, 1-17

Guibal, E., Milot, C. & Roussy, J. 1997. Chitosan gel beads for metal ion recovery, Chitin Handbook. Edited by: Muzzarelli, R.A.A and Peter, M.G. *European Chitin Society,* 423-429.

Hsien, T.Y. & Rorrer, G.L. 1995. Effects of acylation and cross-linking on the material properties and cadmium ion adsorption capacity of porous chitosan beads. *Separation Science and Technology*, 30, 2455-2475.

Jansson-Charrier, M., Guibal, E., Roussy, J., Delanghe, B. & Le Cloirec, P. 1996. Vanadium (IV) sorption by chitosan: Kinetics and Equilibrium. *Water Research,* 30 (2), 465-475.

Jeon, C. & Holl, W. H. 2003. Chemical modification of chitosan and equilibrium study for mercury ion removal. *Water Research,* 37, 4770-4780.

Jha, I.N., Iyengar, L. & Prabhakara-Rao, A.V.S. 1987. Removal of cadmium using chitosan. *Journal of Environmental Engineering,* 114 (4), 963-974.

Juang, R.S. & Shao, H.J. 2002. A simplified model for the sorption of heavy metal ions from aqueous solutions on chitosan. *Water Research,* 36, 299-3008.

Monteiro, O.A.C. & Airoldi, C. 1999. Some studies of cross-linking chitosan-glutaraldehyde interaction in a homogeneuous system. *International Journal of Biological Macromolecules*, 29,119-128

Muzzarelli, R.A.A. 1974. Natural chelating polymers: Alginic acid, chitin and chitosan. Pergamon press.

Piron, E. & Domard, A. 1997. Interaction between chitosan and uranyl ions. Part 1. role of physicochemical parameters on the kinetics of sorption. *International Journal of Biological Macromolecules*, 21, 327-335.

Rhazi, M., Desbrieres, J., Tolaimate, A., Rmaudo, M., Vottero, P. & Alagui, A. 2002a. Contribution to the study of the complexation of copper by chitosan and oligomers. *Polymer,* 43, 1267-1276.

Rhazi M., Desbrieres J., Tolaimate A., Rmaudo M, Vottero, P., Alagui, A. & El Meray, M. 2002b. Influence of the nature of metal ions on the complexation with chitosan. Application to the treatment of liquid waste. *European Polymer Journal*, 38, 1523-1530.

Rorrer, G.L, Hein, T. & Way, D.J. 1993. Synthesis of porous-magnetic chitosan beads for removal of cadmium ions from waste water. *Industrial Engineering Chemical Research,* 32, 2170-2178.

Ruiz, M., Sastre, A.M. & Guibal, E. 2000. Palladium sorption on glutaraldehyde-crosslinked chitosan. *Reactive and Functional Polymers*, 45, 155-173.

Wu, F-C., Tsang, R-L. & Juang, R-S. 2001. Kinetic modeling of liquid-phase adsorption of reactive dyes and metal ions on chitosan. *Water Research, 35* (3), 613-608.

Chapter 5 Adsorption of heavy metals on chitosan beads: a kinetic study

5.1 Introduction

In Chapter 4, the equilibrium properties of chitosan were discussed. For design purposes, however, quantitative information about the kinetics of adsorption is also required. In this chapter, the aim is to describe metal adsorption kinetics on cross-linked chitosan beads, with two modes of kinetic studies *i.e.*, batch and continuous. From the batch studies, the effects of adsorbent modification with respect to cross-linking and particle sizes, and the effects of copper concentration on the kinetic properties were investigated. Experimental data from these studies were fitted using a single particle model developed from the concepts of the shrinking core theory. The kinetics of adsorption onto cross-linked chitosan beads of cadmium(II), lead(II) and zinc(II) ions were also investigated. For the continuous (column) adsorption, experimental breakthrough curves were studied and compared to a column model that is based on the single particle model. The efficiency of the adsorbent with respect to its regeneration capacity was also studied.

In Section 5.2 a literature review on the kinetics of metal adsorption is presented. The kinetic models for the description of metal uptake are shown in Section 5.3 for the batch system and 5.4 for the continuous system. The experimental part is given in Section 5.5, and the discussion of the experimental results and conclusions are presented in Sections 5.6 and 5.7 respectively.

5.2 Literature survey

Different adsorbents have been applied to remove metals from wastewater, and a series of kinetic models have been postulated to study the rate determining step in mass transfer of adsorption of metal ions onto the particle (*e.g.* Jansson-Charrier *et al.* 1996; Guibal *et al.*, 1999; Ko *et al.*, 2001). In most cases, batch experiments were used to investigate the rate of metal adsorption. Erosa *et al.* (2001) studied the adsorption of cadmium(II) on cross-linked chitosan beads in a batch system, and found that the cadmium(II) uptake rate was described by a kinetic equation that includes both external mass transfer and intraparticle diffusion. In the range of

adsorbate concentrations studied by these authors, intraparticle diffusion was however found to introduce the largest resistance onto the adsorption process. The effective diffusion coefficient and the external mass transfer coefficients were determined as $(0.5\text{-}10)\cdot10^{-11}$ m^2/s and $(8\text{-}10)\cdot10^{-6}$ m/s respectively. Guibal *et al.* (1999) and Wu *et al.* (2001) also found the rate controlling step to be intraparticle diffusion. From the research by Guibal *et al.* (1998) on the kinetics of molybdate and vanadate adsorption onto chitosan beads, the effective diffusion coefficient was determined in the range of $(2\text{-}17)\cdot10^{-12}$ m^2/s under different experimental conditions.

Several kinetic properties have in addition been derived from column studies. In a continuous flow study, adsorbents are packed in a column and adsorbates flow through it. Starting at the inlet, the saturated solid adsorbent zone gradually extends through the column and the adsorbate eventually breaks through the column. The breakthrough curve can be determined from the effluent concentration of the column, and is usually S-shaped, where the slope of the curve is affected by the equilibrium sorption isotherm, mass transfer to and through the adsorbent and the fluid-flow operating parameters. Several models have been used to study the experimental breakthrough curves.

Da Silva *et al.* (2002) studied the effect of different concentrations for the adsorption of copper(II) ions on marine alga biomass. They used a diffusion model to describe the experimental breakthrough curves and found an effective diffusion coefficient of $(1.6\text{-}3.8)\cdot10^{-9}$ m^2/s. Guibal *et al.* (1999) studied the adsorption of molybdate on cross-linked chitosan gel beads in a column, where the effects of the superficial velocity on the breakthrough curves were also given. They found that at a low velocity, the external mass transfer coefficient $(5.1\text{-}8.1)\cdot10^{-6}$ m/s was significant and the intraparticle diffusion coefficient was $(1.7\text{-}8.0)\cdot10^{-13}$ m^2/s. Zulfadhly *et al.* (2001) used fungi's biomass to adsorb a multi-metal mixture in a fixed bed column and the performance of the column was modeled using a Semi-Empirical-Bed-Depth-Service-Time Model. The model was used to predict the external mass transfer coefficient and effective diffusion coefficient. The model gave a good prediction of the experimental breakthrough curves, with an effective diffusion coefficients for copper(II) of $5.4\cdot10^{-10}$ m^2/s and an external mass transfer coefficient of $3.3\cdot10^{-4}$ m/s. Hetzikioseyian *et al.* (2001) applied a simplified fixed bed model based on the concept of fast local equilibrium to simulate experimental breakthrough curves selected from literature. They developed a nonlinear

equation involving the equilibrium isotherm parameters and the overall apparent dispersion coefficient, and combining the flow characteristics and the mass transfer resistances in liquid and solid phases. This equation was used to fit the experimental breakthrough. Chen *et al.* (2003) used a fixed-bed model considering external mass transfer, pore diffusion, and radial and axial dispersions to describe experimental adsorption of copper onto activated carbon.

Furthermore, many metal adsorption studies have been described with models derived from the shrinking core theory. The adsorption of copper and cadmium onto bone char was successfully described by Ko *et al.* (2001) using a film-pore mass transport diffusion model that was based on the theory of the shrinking core, and the solid phase loading capacity which was used to correlate model and experimental data obtained from a mass balance of the experimental breakthrough. From their research, the equilibrium loading capacities for copper and cadmium were found to be 0.7 and 0.4 mmol/g respectively, and the effective diffusion coefficient for copper ($6.6 \cdot 10^{-11}$ m^2/s) and cadmium ($4.4 \cdot 10^{-11}$ m^2/s) were determined. A study by Swan *et al.* (1975) on the use of sulfuryl compound to remove mercurial substances from wastewater was carried out in a fixed-bed column. The kinetics of adsorption in the column was predicted with a model based on the fundamentals of the shrinking core theory. Nestle and Kimmich (1996) have also used a shrinking core model to describe the adsorption of heavy metals on alginate beads.

As is evident above, the shrinking core theory has been broadly applied to a wide range of adsorbent materials used for the adsorption of various metals, and it has been found to be more suitable than other transport models (Ko *et al.*, 2001). Consequently, this work applies a model based on the shrinking core theory to test experimental data from kinetic experiments. A kinetic model describing the adsorption of metals in batch and continuous processes is presented in Sections 5.3 and 5.4 respectively.

5.3 Kinetic model

5.3.1 Single particle model

A shrinking core model, which was based on the work put forward by Swan *et al.* (1975), was used in this study with only slight modifications. Figure 5.1 illustrates the shrinking core principle, in which the particle consists of an outer zone, where the adsorbate is already

adsorbed and an inner zone, the active core, where the adsorbate has not yet penetrated. During the adsorption process, the active zone shifts inwards, until the adsorbent is fully loaded.

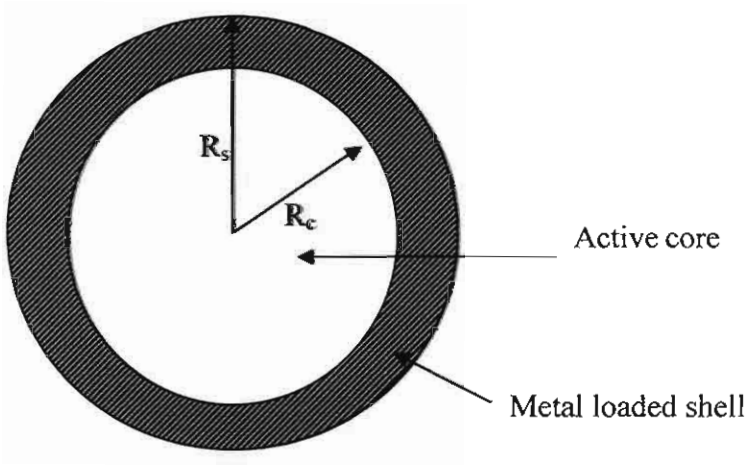

Figure 5.1: Concentration profile in a spherical chitosan bead.

In the model presentation, only the basic equations will be presented as the mathematical derivation of the particle model has been described extensively by Swan *et al.* (1975) (see Appendix H for more details). The model is based on the assumption that the rate of diffusion in the particle equals the rate of adsorption in the particle with diffusion as the rate limiting step. The model is derived from the adsorption into a spherical chitosan bead as follows;

The rate of diffusion (r_D) in the spherical chitosan core per unit mass is given by Fick's first law:

$$r_D = \frac{3D_{eff}R_S R_C(C_S - C_C)}{\rho R_S^3(R_S - R_C)} \qquad 5.1$$

The rate of adsorption in the inner core of the chitosan bead per unit mass is given by:

$$r_C = \frac{R_C^3 \eta_C k C_C}{R_S^3} \qquad 5.2$$

Each rate gives the net rate of adsorption and equating Equations (5.1) and (5.2) gives:

$$r_D = r_C = \frac{\partial q}{\partial t} = \frac{\eta_C k C_S}{\frac{R_S^3}{R_C^3} + \frac{3\eta_C \Phi_S^2 (R_S - R_C)}{R_C}} \qquad 5.3$$

where η_o is the effectiveness factor for fresh adsorbent, derived in a way similar to a heterogeneous catalysed first order reaction in a porous catalyst (Fogler, 1999):

$$\eta_O = \frac{1}{\Phi_s}\left(\frac{1}{\tanh 3\Phi_s} - \frac{1}{3\Phi_s}\right) \qquad 5.4$$

The effectiveness factor for the unloaded core, η_c, is similarly defined as:

$$\eta_C = \frac{1}{\Phi_C}\left(\frac{1}{\tanh 3\Phi_C} - \frac{1}{3\Phi_C}\right) \qquad 5.5$$

The parameter Φ is the Thiele modulus, dimensionless, and is defined based on the adsorbent particle radius as:

$$\Phi_S = \frac{R_S}{3}\left(\frac{k\rho}{D_{eff}}\right)^{1/2} \qquad 5.6$$

and based on the active core of the bead as:

$$\Phi_C = \frac{R_C}{3}\left(\frac{k\rho}{D_{eff}}\right)^{1/2} \qquad 5.7$$

The following dimensionless equation is defined:

$$1 - \theta = \frac{R_c^3}{R_s^3} \qquad 5.8$$

where θ is the fraction adsorption loading also defined as:

$$\theta = \frac{q(t)}{q_e} \qquad 5.9$$

For fresh adsorbent, when $\theta = 0$, the rate of adsorption gives:

$$\frac{\partial q}{\partial t} = \eta_o F k C_s \qquad 5.10$$

The factor F in the net rate of adsorption is defined as a function of θ and is the ratio of the adsorption rate for θ equal to $q(t)/q_e$ to that for θ equal to zero, and is calculated by dividing Equation (5.3) by (5.10) to give:

$$F = \frac{\eta_C / \eta_0}{\left(\frac{1}{1-\theta}\right) + 3\eta_C \Phi_S^2 \left(\frac{1-(1-\theta)^{1/3}}{(1-\theta)^{1/3}}\right)} \qquad 5.11$$

In the situation where diffusion is rate limiting, the Thiele modulus is very large, and Equation (5.11) becomes:

$$F = \frac{3D_{eff}}{R_s^2 k \eta_0 \rho \left(\frac{1-(1-\theta)^{1/3}}{(1-\theta)^{1/3}}\right)} \qquad 5.12$$

Under proper stirring conditions, the external mass transfer resistance can be ignored. This means that C_B, the concentration in the bulk solution is equal to the concentration at the interface of the bead and solution C_B^{int}. In turn, C_B^{int} is equal to the concentration in the bead at the solution-bead interface (C_S). This has been demonstrated in sodium diffusion experiments for batch systems (Section 3.2.8) assuming copper having the same distribution coefficient as sodium. Equation (5.12) can therefore be modified to:

$$\frac{\partial q}{\partial t} = \frac{3D_{eff}C_B}{R_s^2\rho\left(\frac{1-(1-\theta)^{\frac{1}{3}}}{(1-\theta)^{\frac{1}{3}}}\right)} \qquad 5.13$$

5.3.1.1 Application to batch systems

Figure 5.2 shows the schematic representation of the parameters put into the model. The experimental adsorption rate capacity of the beads is measured from the mass balance of the initial metal concentration C_{Bi} and the metal concentration C_{Bt} at any other finite time interval in the bulk solution. This analysis is continued until the metal concentration remains constant. The solution of the partial differential equation (Equation (5.13) is solved numerically, using a Euler algorithm, after discretization $\frac{\partial q}{\partial t}$ as:

$$\Delta q = \frac{\partial q}{\partial t}\Delta t \qquad 5.14$$

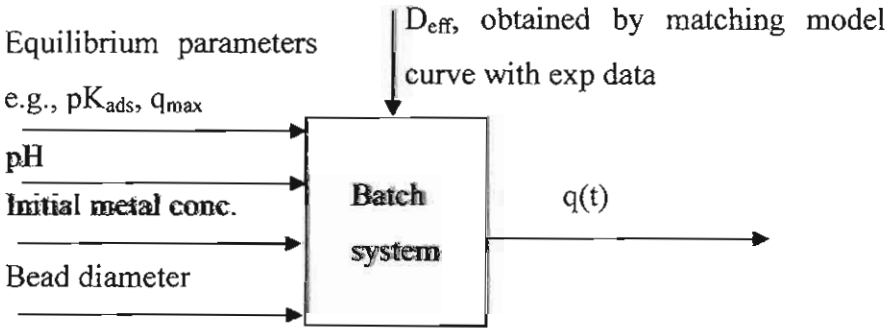

Figure 5.2: Model representation of particle model with input and output variables.

The parameter, θ, in the adsorption rate of Equation (5.13) changes as a function of time. During adsorption the fraction of the metal loading to the total capacity, $q(t)/q_e$, varies from the initial start of adsorption until equilibrium is reached. The time dependent adsorption is measured experimentally, and the theoretical value of q_e (Equation (4.13) is used. The only unknown parameter is the diffusion coefficient and that is determined by fitting the model to the experimental data.

5.3.2 Adsorption column model

In the particle model described in Section 5.3.1, the external mass transfer resistance was considered negligible. However, in a column, the velocity of the liquid is relatively small so the external mass transfer resistance has to be taken into account. This has been done by considering mass transport through the film layer around the beads. A uniformly packed bed with negligible axial and radial dispersion and uniform velocity is assumed. The adsorption rate through the beads is only equated to the rate of transfer through the film layer (Swan *et al.*, 1975).

$$\frac{\partial q}{\partial t} = k_L a(C_B - C_S) = \eta_0 F k C_S \qquad 5.15$$

Eliminating the concentration at the beads surface and re-arranging:

$$\frac{\partial q}{\partial t} = \frac{k_L a\, \eta_0 F k}{k_L a + \eta_0 F k} C_B \qquad 5.16$$

substituting for the factor F, and when θ is not tending to unity Equation (5.16) becomes:

$$\frac{\partial q}{\partial t} = \frac{k_L a \dfrac{3D_{eff}}{R_s^2 \rho \left(\dfrac{1-(1-\theta)^{1/3}}{(1-\theta)^{1/3}} \right)}}{k_L a + \dfrac{3D_{eff}}{R_s^2 \rho \left(\dfrac{1-(1-\theta)^{1/3}}{(1-\theta)^{1/3}} \right)}} C_B \qquad 5.17$$

In many research studies, the mass transfer coefficient has been predicted using empirical correlations (Kawamura *et al.*, 1997; Ko *et al.*, 2001). In this study, the semi-empirical relation as given by Bird *et al.* (1960) was used:

$$Sh = 2.0 + 0.60\, Re^{1/2} Sc^{1/3} \qquad 5.18$$

in which Re is the dimensionless Reynolds number ($d_p v\rho/\mu$), Sc is the dimensionless Schmidt number ($\mu/D_w\rho$), and Sh is the dimensionless Sherwood number ($k_L d_p/D_w$),

5.3.2.1 Adsorption column simulation

In simulating the adsorption column, the column was divided into N number of units as shown in Figure 5.3. Each unit is considered as a continuously stirred tank reactor (CSTR) where the beads in each unit are assumed to be loaded with the same amount of metal. The changes in the sliced-column concentration were determined in discrete time steps equal to $1/N$ of the residence time (typical values of $N = 35$ were used). The adsorption rate was calculated using Equation (5.17) and the change in concentration in each CSTR was subsequently determined, similar to the batch experiments (Section 5.3.1), replacing the adsorption time by the residence time of the CSTR. This was done in such a way that the exit concentration of the 1st CSTR equals the inlet concentration of the 2nd one, the exit concentration of the 2nd CSTR that of the inlet concentration of the 3rd and so forth. The fraction of adsorption rate capacity θ, at each CSTR of the column is obtained by the equilibrium parameters as described in Section 4.5.3.2, including the equilibrium constant (K_{ads}) and the maximum capacity (q_{max}). The effective diffusion coefficient is determined by matching the model curve with experimental data.

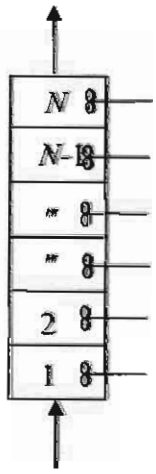

Figure 5.3: Simulation of adsorption column.

5.5 Experimental

Batch kinetic adsorption studies were carried out with copper(II), zinc(II), cadmium(II), and lead(II) ions using beads produced and characterized using the method presented in Sections 2.2.3 and 3.3.4. Only copper(II) was used in the packed bed column filled with cross-linked beads. The adsorption studies were limited to a pH of 7.0 for all the metal ions in order to avoid precipitation.

5.5.1 Chemicals

The following metal salts were used for the experiment; anhydrous $CuSO_4$, (>99.9%, Merck), $Pb(NO_3)_2$, (>99.9%, Aldrich), $CdSO_4$ (>99.9%, Aldrich), hydrated $ZnSO_4.7H_2O$ (>99%, Aldrich), and $NiSO_4.6H_2O$ (>99.9%, Aldrich). Hydrochloric acid (>99%) and sodium hydroxide (>99%) were purchased from Aldrich Chemicals. Distilled water was produced in the laboratory with a Pure Water distiller (Ultima 888 water distiller). Solution pH was measured with a pH meter (Hanna HI 8421 and Corning Scholar 425).

5.5.2 Microscope-analysis

In this analysis, 250 mL of a 100-300 mg/L of copper solution was prepared into a 500 mL Erlenmeyer flask, 6 g of wet chitosan beads were added and the flask was placed in a Labcon incubator with a shaker rotating at 120 rpm at a temperature of 25 ± 0.5°C. At certain intervals of time a few beads, negligible with respect to the total amount of beads, were removed from the copper solution and were placed in liquid nitrogen for 10 seconds. Next, the beads were cut into half with a scalpel blade, placed in a microscopic slide and viewed with a stereo microscope (Nikon SMZ-1) connected to a Digital Camera (Philips-Nikon-Coolpix 955).

5.5.3 Batch adsorption

The batch experimental kinetic studies were carried out using a 500 mL Erlenmeyer flask with 6.0 g wet beads weighed into the flask and 250 mL of 0.12-1.57 mmol/L metal was added. The Erlenmeyer flask was placed in a Labcon incubator at a temperature of 25 ± 0.5°C with a shaker rotating at 120 rpm. The metal solution pH was kept constant with 0.1 M HNO_3 or 0.1 M NaOH solutions. During adsorption, 4 mL of metal solution samples are taken at specific

time intervals, filtered through 0.45 μm membrane filter and analyzed with an atomic absorption spectrometer (Varian SpectrAA-10). After 24 hours, when equilibrium was reached, the wet beads were vacuum filtered through Whatman-glass filters (Grade GF/C), and then rinsed with distilled water before being dried in the oven at 80°C for 24 h to determine the dry mass of chitosan.

5.5.4 Column adsorption and desorption

114 g of LC(0.9)(2.5) beads were packed into a cylindrical column of ID 2.54 cm and of height 40.5 cm constructed of transparent polystyrene. The volume of the beads in the column was 132 mL with a void fraction of 31%. The schematic diagram of the adsorption column is shown in Figure 5.4. A plastic mesh of 100 μm was placed at both ends of the cylinder to contain the beads inside the cylinder. The beads were vacuum filtered before being loaded to the column, and also a vacuum line was connected to the column to allow excess water to be drained from the column. 0.13 mmol/L (8.1 mg/L) of copper(II) solution was fed into the column (initial pH 5.5), with a peristaltic pump (Watson Marlow 313S) at an average flow rate of 7.2 mL/min. The pH was not controlled during adsorption; however, the pH at the influent and effluent lines was continuously measured. The effluent solutions were collected at different intervals and measured for copper concentration using an atomic absorption spectrometer (Varian SpectrAA-10).

When the effluent concentration was approximately the same as the influent concentration, the column was considered to be fully loaded with copper(II) and desorption was carried out. Before desorption, the beads were washed by pumping 4 L of distilled water through the column at 7.2 mL/min and after that, the column was vacuum filtered again to remove all the water at the surface of the beads before desorption with 0.1 M HCl at 7.2 mL/min. After desorption, the beads were washed with distilled water to remove excess acid followed by a washing step with 0.1M sodium hydroxide to return the pH to 6.5 and 7.0. After these procedures, the column was washed with distilled water to remove excess sodium hydroxide and vacuum filtered before another cycle of adsorption. These cycles of adsorption and desorption were repeated.

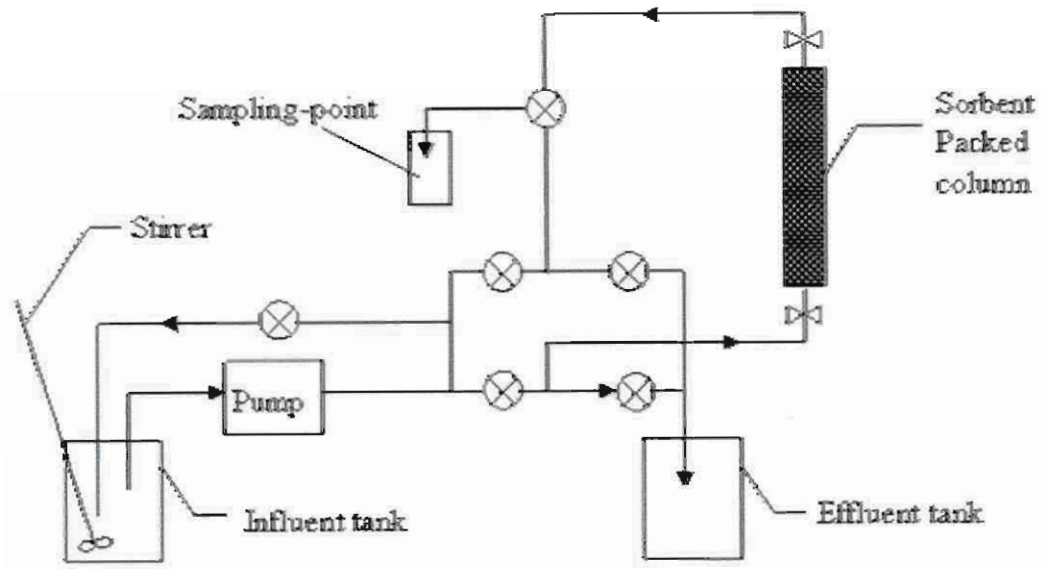

Figure 5.4: Schematic diagram of the continuous flow column arrangement used for copper(II) adsorption.

5.6 Results and discussion

5.6.1. Microscope-study

Figure 5.5 shows microscopic images from fresh and copper loaded beads. When beads are placed in a solution of copper(II) ions, the color of the beads usually turn green after adsorption. This was also observed by Rhazi *et al.* (2002). This color change relating to adsorption was used to follow adsorption of copper into the bead with time. There is a sharp interface between metal loaded portion and the active core in the bead as shown in Figure 5.5. This proves that the assumption of a fast adsorption rate is valid, and the application of Equation (5.14) is justified.

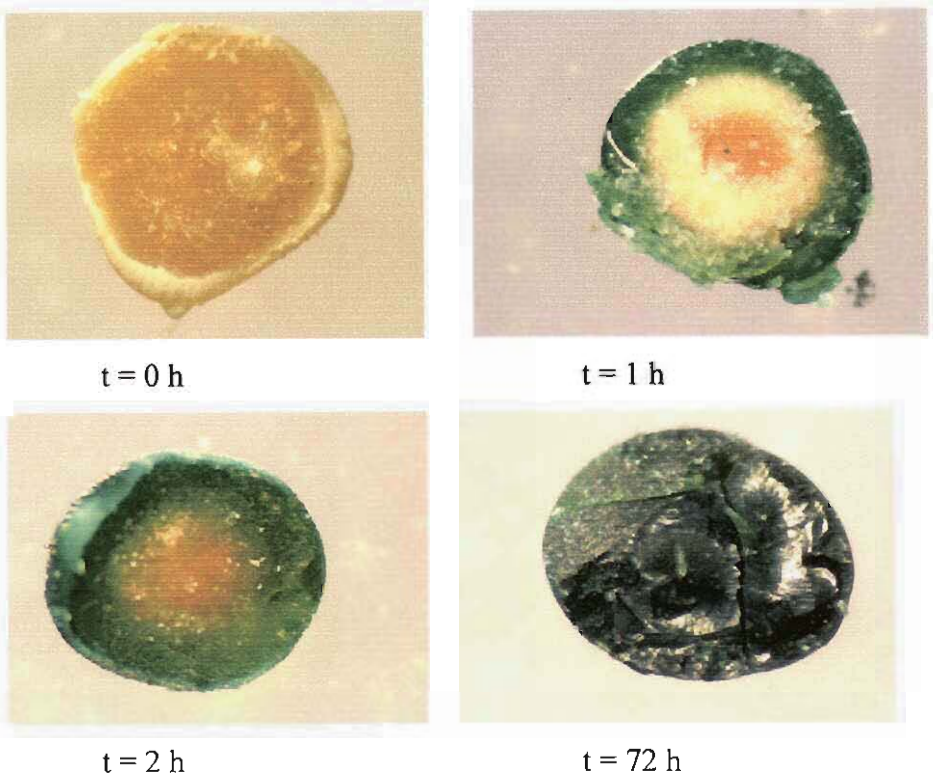

Figure 5.5: Microscope images showing the progressive adsorption of copper onto chitosan beads.

5.6.2 Application of kinetic model to batch experimental results

In this study, all the kinetic data from the batch adsorption were used in modeling Equation (5.13). Copper(II) ions were used to investigate the influence of sorbent modification, such as the DCL and particle size, on adsorption rate. The results and discussion for adsorption at different copper concentrations and the influence of cross-linking are presented in Section 5.6.2.1 and 5.6.2.2 respectively. The influence of particle size on adsorption rate can be found in Section 5.6.2.3. Section 5.6.3 gives a discussion on the kinetics with other metals such as zinc(II), cadmium(II), and lead(II) ions. The results and discussion for the column experiments are presented in Sections 5.6.4-5.6.7.

5.6.2.1 Adsorption kinetics at different copper concentrations

Figure 5.6 shows the kinetics of adsorption at different copper concentrations, the experimental data is presented in Appendix I (Table I-1). The initial adsorption rate increases as the copper concentration increases. The experimental data were fitted with the model (shown as lines) using Equation (5.13) and the values of the effective diffusion coefficient were obtained according to best fit. The effective diffusion coefficients determined are in the range between $(2.5\text{-}4.0)\cdot10^{-11}$ m^2/s as illustrated in Table 5.1. The values of the diffusion coefficients are one order of magnitude lower than the diffusion of copper in water $7.43\cdot10^{-10}$ m^2/s (Gerente *et al.*, 2000) and are also comparable to the value found for cadmium adsorption on cross-linked chitosan beads (Erosa *et al.*, 2001) which is $(0.5\text{-}10)\cdot10^{-11}$ m^2/s and for molybdate and vanadate adsorption onto chitosan beads (Guibal *et al.*, 1998). These values were found to decrease with concentration.

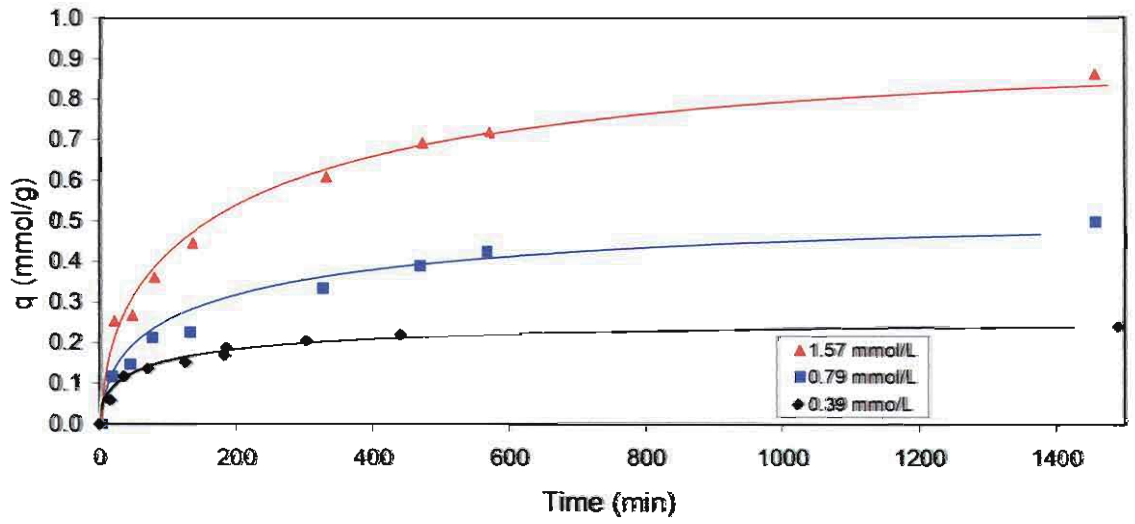

Figure 5.6: Copper adsorption kinetics on LC(1.8)(2.5) beads at a pH 5.8.

Table 5.1: Effective diffusion coefficients determined from the adsorption of copper at pH 5.8.

Conc. (mmol/L)	0.39	0.75	1.57
D_{eff}, 10^{-11} (m^2/s)	4.0 (±0.2)	2.8 (±0.1)	2.5 (±0.1)

5.6.2.2 Influence of cross-linking

Figure 5.7 shows the adsorption rate data for beads that were cross-linked at different glutaraldehyde concentrations. The experimental results are also available in Tables I-2 – I-4 (Appendix I). The initial rate of adsorption for the non-cross-linked and 2.5% cross-linked beads increases faster than the adsorption from the 4.0% cross-linked beads. From Table 5.2, the values of the DCL, water content, and their corresponding effective diffusion coefficients were compared, and from the result, it can be seen that the effective diffusion coefficient increases with increasing water content and thus decreases with an increased DCL. A study by Monteiro and Airoldi (1999) has shown that cross-linking involves inter-chain links between the amine groups of chitosan and the aldehyde groups of glutaraldehyde, and for this reason, metal ion diffusion is hindered with increasing cross-linking as it involves more amine groups and aldehyde groups. Similar results on the effect of cross-linking were observed with regard to the equilibrium performance as reported in Section 4.6.3.2.

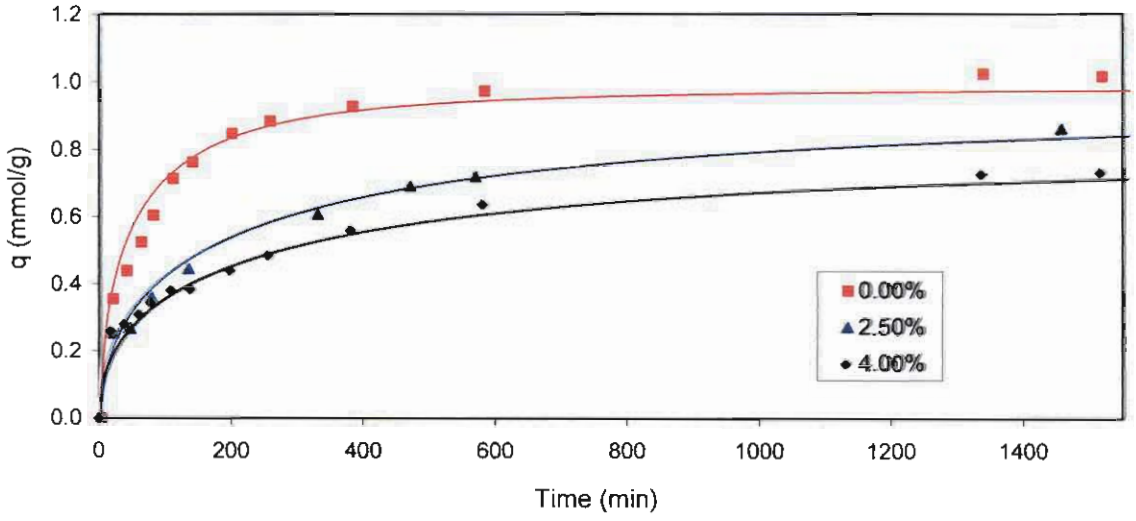

Figure 5.7: Influence of glutaraldehyde concentration on copper adsorption rate.

Table 5.2: Influence of glutaraldehyde concentration on the kinetics of adsorption with 1.57 mmol/L copper on 3.8 mm beads at a pH 6.

Glutaraldehyde (%)	0.0	2.5	4.0
D_{eff}, 10^{-11} (m^2/s)	12.1 (±0.4)	9.9 (±0.3)	8.0(±0.3)
DCL (%)	0.0	18.4	34.7
Water content (%w/w)	96.0	94.9	90.0

5.6.2.3 Influence of bead sizes

Figure 5.8 shows the adsorption rate of beads with different particle sizes, and in Table 5.3 the corresponding diffusion coefficients are given. From the figure, a decrease in the adsorbent particle size results in a decrease in the time required to reach equilibrium, i.e. the initial rate is slightly larger for 3.8 mm beads than for 0.9 and 1.8 mm beads. These observations are different from what has already been found by most researchers who observed a decrease in adsorption rates with an increase in particle sizes (Rorrer *et al.*, 1993; Huang *et al.*, 1996; Erosa *et al.*, 2001; Mohan *et al.*, 2001).

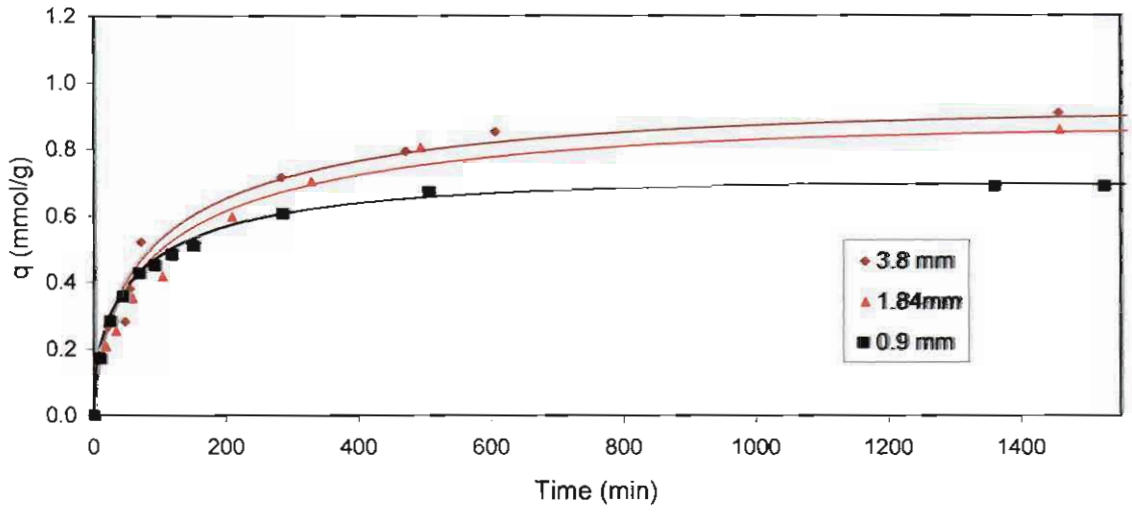

Figure 5.8: Influence of adsorbent particles on adsorption rate.

However, from these studies there is a trend in similarity between the DCL and the value of diffusion coefficients as shown in Table 5.3. This trend is also comparable to the results found in Section 5.6.2.1, an increase in the value of DCL results in a decrease in the value of the effective diffusion coefficient. Also from Table 5.3, the percent water content of the beads decreases with an increase in the DCL, and in this study, the 3.8 mm bead was found to have the largest water content and also the largest diffusion coefficient because the effect of cross-linking is the lowest. It can thus be concluded that the extent of cross-linking plays a part in adsorption and diffusion properties.

Table 5.3: Influence of adsorbent particles on adsorption property using 1.57 mmol/L of copper at a pH 6.

Diameter (mm)	0.9	1.8	3.8
D_{eff}, 10^{-11} (m^2/s)	2.5 (±0.25)	4.8 (±0.3)	9.9 (±0.4)
DCL (%)	32.7	30.6	18.4
Water (%w/w) (±0.1)	90.1	93.4	94.9

5.6.3 Adsorption kinetics of cadmium(II), lead(II) and zinc(II) on LC(3.8)(2.5) beads

Batch kinetics rate experiments were also carried out at different concentrations of cadmium, lead and zinc and their adsorption rate curves are given in Appendix J (Figures J-1 to J-3). The particle model of Equation (5.13) was used and there was a good fit between the model curve and the experimental data. Average diffusion coefficients determined from cadmium, lead and zinc are $6.4 \cdot 10^{-11}$ m^2/s, $6.1 \cdot 10^{-11}$ m^2/s, and $4.4 \cdot 10^{-11}$ m^2/s respectively. These values are also in the same order of magnitude to the value found for molybdate or vanadate adsorption on cross-linked chitosan beads (Guibal *et at.*, 1998). The values of the diffusion coefficients determined are one order of magnitude lower than the diffusion of copper in water at $7.43 \cdot 10^{-10}$ m^2/s (Gerente *et al.*, 2000).

5.6.4 Column adsorption

The experimental breakthrough curve for the adsorption of copper in a column packed with chitosan beads is shown in Figure 5.9, and Tables K-1 – K-2 (Appendix K) give the experimental column results. Equation (5.17), describing the continuous adsorption process in a column, was used to describe experimental breakthrough curves with the input data given in Table 5.4. The maximum capacity (q_{max}) and the equilibrium constant (K_{ads}) are those determined from equilibrium results using the pH-model in Section 4.5.3.2. The value of the external mass transfer coefficient was determined from the empirical correlation involving the Reynolds and Schmidt numbers of Equation (5.18). It was found to be $4.3 \cdot 10^{-6}$ m/s. The model was fitted by adjusting the value of the diffusion coefficient until a good agreement was obtained, and in this case, the effective diffusion was $8.0 \cdot 10^{-11}$ m^2/s when compared to other

values presented in Figure 5.9. This value is slightly higher than the value found in the batch results given in Table 5.3.

Table 5.4: Model parameters used in the prediction of experimental data.

Parameters	Values
Solution pH	5.6
n and m	1.0
Mass of wet beads (g)	114
Density (ρ) (kg/m^3)	1100
Equilibrium constant (K_{ads})	0.00114
Adsorbent capacity (mmol/g)	3.8
Specific surface area (a) (m^2/kg)	67.7
External mass transfer coefficient (k) (m/s)	4.3×10^{-6}
Copper diffusion coefficient in water (D_{copper}) (m^2/s)	7.43×10^{-10}

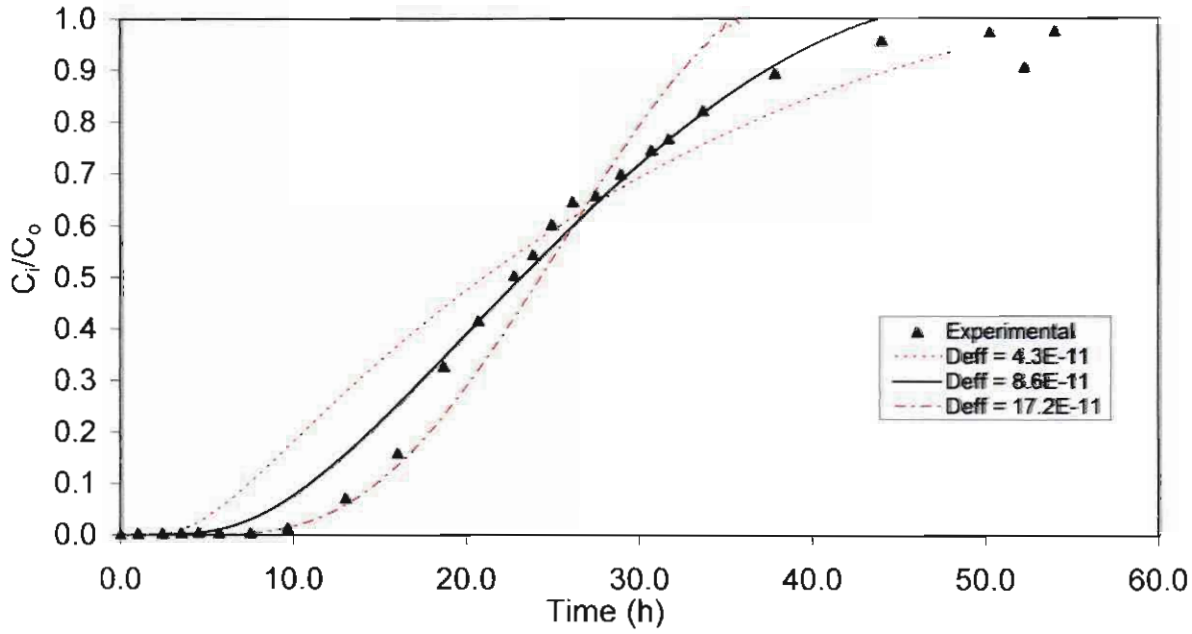

Figure 5.9: Breakthrough curves for copper adsorption onto LC(0.9)(2.5) chitosan beads.

Although there is slight deviation between the model curve (as shown by the line) and the experimental data (as shown by the triangles) at 0.5-30% of the breakthrough, the model described the experimental breakthrough curve fairly well. This deviation can be attributed to

the fluctuation of pH in the column. A pH of 5.6 was applied in the model which is the steady pH in the column after about 19 h service times as shown in Figure 5.10. Below 19 h service time, the model underestimated the real situation in the column because the column pH was above 5.6, so higher copper uptake was achieved.

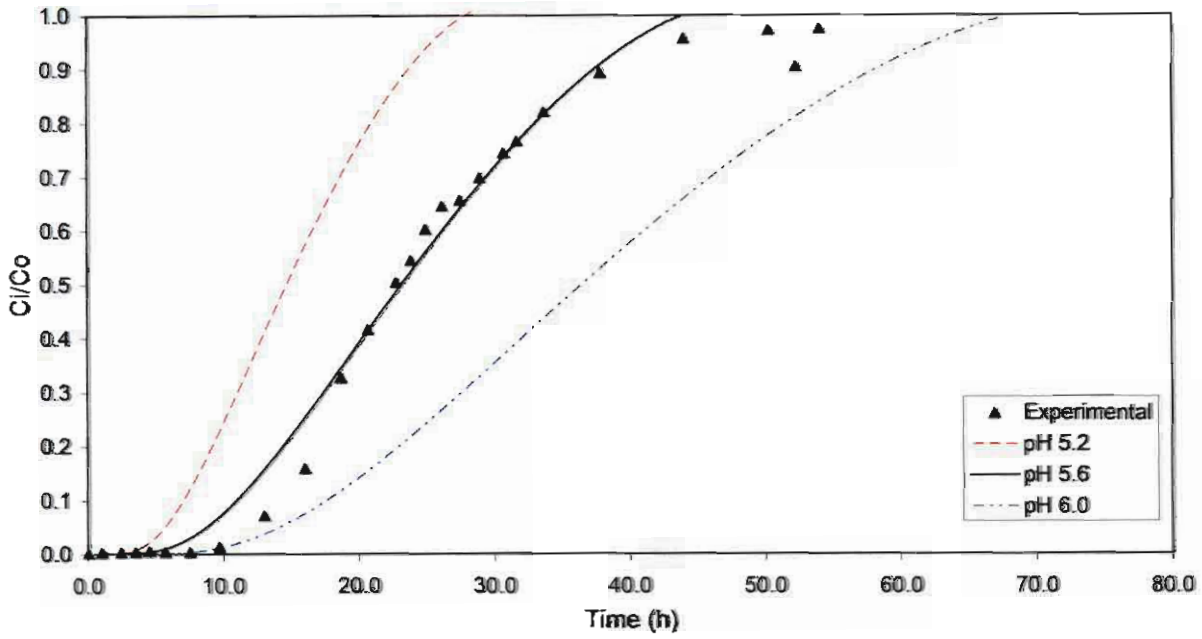

Figure 5.10: Breakthrough curves for copper adsorption onto chitosan beads at different pH.

5.6.5 Multiple cycles

Figure 5.11 depicts the breakthrough curves in a repeated use of the beads through several cycles of adsorption and desorption. The first breakthrough curve that was achieved with the fresh beads was steeper, and it was achieved in a shorter time. After more than 40 bed volumes, the effluent copper concentration began to rise from the base of the column and column saturation was reached after about 220 bed volumes.

After the first cycle of adsorption and desorption, an improved adsorption was observed from the breakthrough curves of the second- and third-cycles of adsorption, despite the loss in mass of the beads as shown in Table 5.5. In the first cycle of adsorption, only about 23% of the adsorbent capacity was used due to the relatively short contact time between the solution and the adsorbent. The improvement in the column performance at the second- and third-cycles of adsorption may be caused by the acid treatment during desorption that causes pore opening at

the surface of the beads, thereby increasing the diffusion rate to the internal adsorption sites. In this case, the used adsorbent capacities in the second- and third-cycles of adsorption were 97% and 74% respectively.

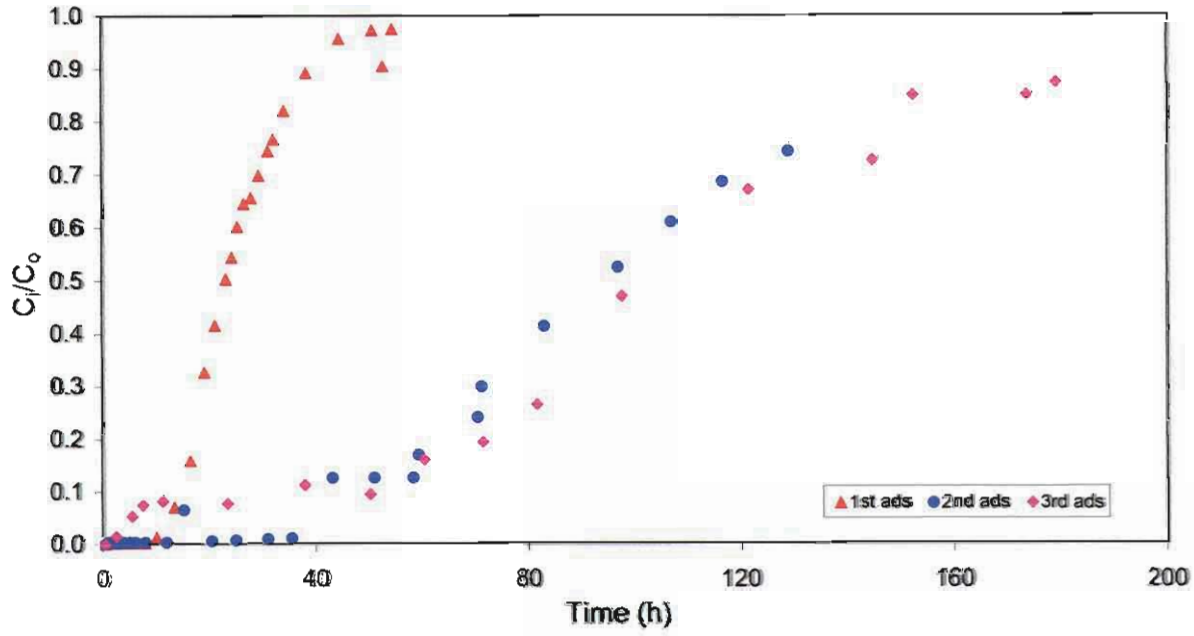

Figure 5.11: Breakthrough curve for different copper adsorption cycles.

Fourth and fifth cycles of adsorption and desorption were carried out as well (not shown in Figure 5.10), and the adsorption performances deteriorated significantly in comparison to previous cycles. It appears that the adsorbent capacity had deteriorated after the third cycle due to mass loss during several acid treatments. The beads lost 21-25% of their initial mass and only 44-48% of their adsorbent capacity was utilized in cycles 4 and 5. These findings are presented in Table 5.5.

Table 5.5: Parameter used at different cycles of adsorption with flow rate of 7.2 mL/min, inlet solution pH 5.5 and inlet copper concentration of 0.13 mmol/L.

Adsorption cycle	Mass of wet beads (g)	% mass loss	% adsorbent capacity used
1st	114.0	0.0	23
2nd	97.7	14.3	97
3rd	91.3	19.9	74
4th	88.5	21.8	48
5th	85.4	25.0	44

The effluent pH profiles during the adsorption cycles are shown in Figure 5.12. The initial pH of the influent was 5.5. As can be seen, from the first cycle, the effluent pH rose to around 7.5 and then dropped to around pH 5.6 where it remained steady for the remaining period of the column operation. Similar pH changes were noticed during the second and third adsorption cycles.

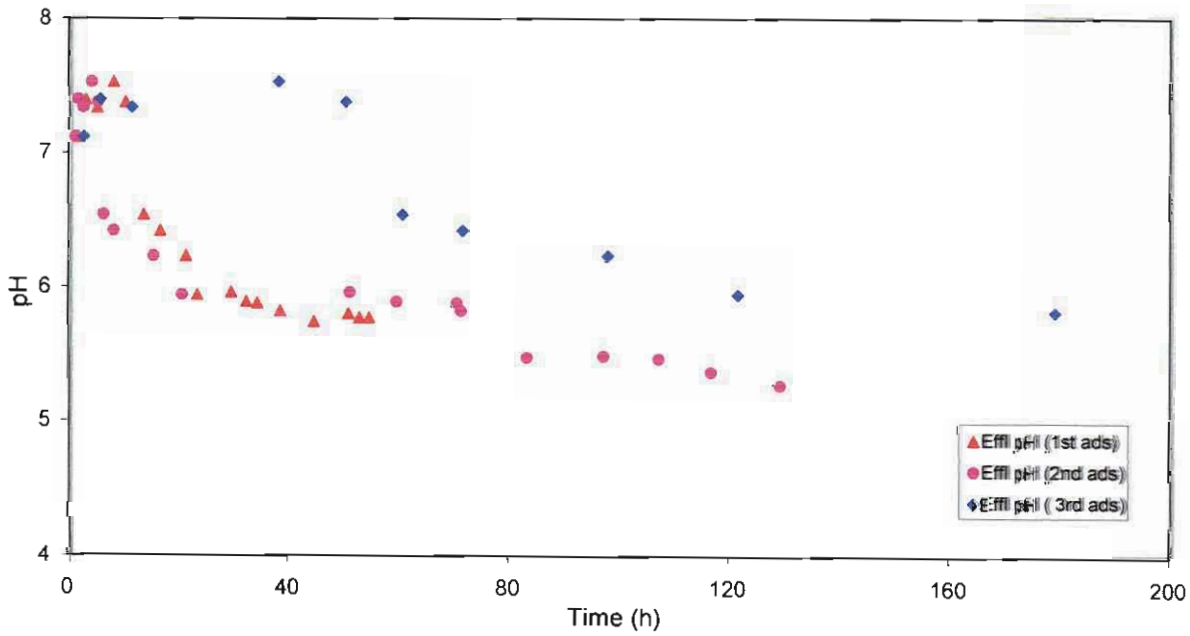

Figure 5.12: Column pH changes over time during the first, second and third cycles of adsorption.

5.6.6 Comparison

A direct comparison with literature data is troublesome, as most materials found in literature are of a different biomass. Only Guibal *et al.* (1999) has previously described the use of chitosan beads for molybdate adsorption. In order to be able to compare results, column simulations were performed with chitosan beads using Equation (5.18) describing the column adsorption process. Experimental conditions were similar to those found in literature, however, a pH of 5.7 was used in the simulation. The number of bed volumes (BV) treated when the exit concentration of copper is 10% and 50% of the initial concentration is shown for each method in Table 5.6. According to the results, chitosan beads seem to perform relatively well in comparison to most other adsorbents. Only *Sargassum* biomass and bone char performed much better than chitosan beads. Since only small amounts of chitosan are present in the beads, the capacity of the beads is relatively low and the performance of the beads can be increased if the concentration of chitosan content in the bead is increased.

Table 5.6: Comparison of chitosan beads column breakthrough with other adsorbents using model simulation with values in bed volume (BV).

Adsorbent	10% adsorbent	50% adsorbent	10% chitosan beads	50% chitosan beads	
Peanut hull	53	77	360	405	[a]
Bone char	537	691	50	81	[b]
Activated carbon	177	236	277	295	[c]
Macro-fungus, Pycnoporus sanguineus	3	5	55	62	[d]
Biomass (*Sargassum*)	1082	2884	66	286	[e]
Immobilized fungal biomass	14	31	231	406	[f]

[a] Johnson et al. *(2002); [b] Ko* et al. *(2001); [c] Monser and Adhoum (2002); [d] Zulfadhly* et al. *(2001); [e] Da Silva* et al. *(2002); [f] Kapoor & Viraraghavan (1998)*

5.6.7 Column regeneration

Figure 5.13 shows the breakthrough curves for the regeneration of copper during the adsorption-desoprtion cycles. A larger amount of copper was regenerated during the second cycle due to the large amount of copper that was also adsorbed at that cycle as shown in Figure 5.11. Table 5.7 shows the amount of copper at each cycle that was desorbed at a given time. The process has proved to be efficient for copper regeneration because copper that was adsorbed at a low concentration of 8.1 mg/L was desorbed into an average concentration >1000 mg/L. From the analysis, it was observed that 1.1 liters of 0.1 M acid is required to desorb more than 91%. At 0.01 M HCl, the desorption concentration was found to be lower by a factor of 10 (figure not shown). Desorption is also regarded as a simple operation because it requires only a fraction of the total cycle time. In the second adsorption step, with a higher copper uptake, it took less than 5% of the cycle time to recover about 99% of the copper adsorbed. The procedures for bringing the pH from about 1.2, after desorption, to between 6.5 and 7.0 with NaOH requires a lot of time because a large volume of hydroxide solution is used, followed by rigorous rinsing with distilled water to stabilize the pH in the neutral range to avoid copper precipitation during adsorption.

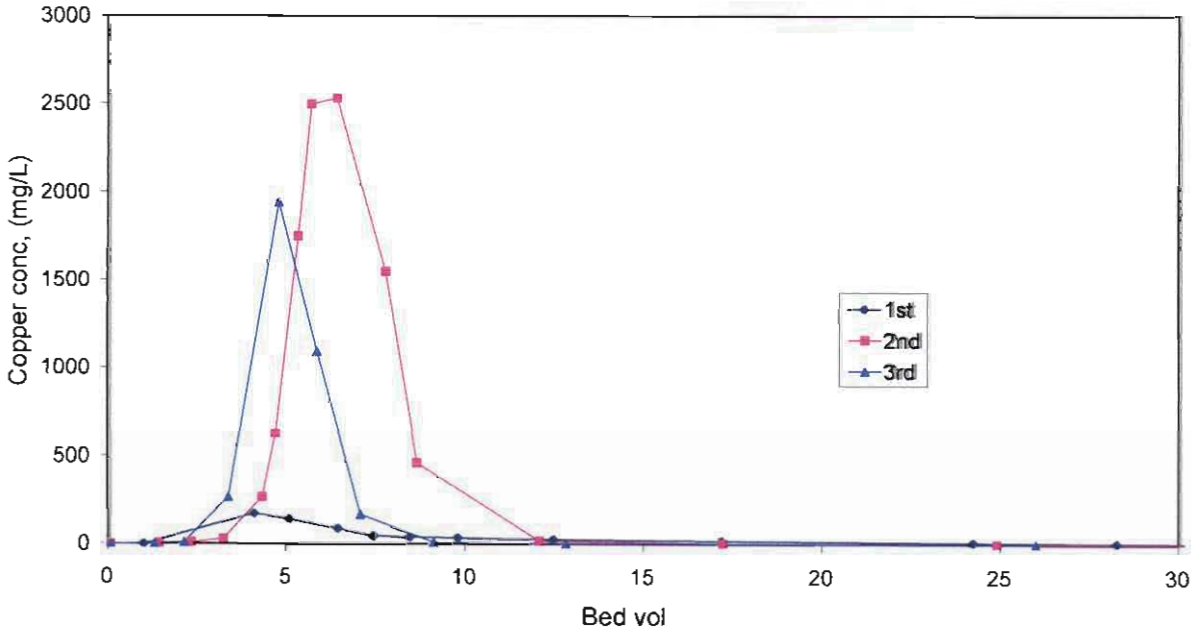

Figure 5.13: Regeneration curves for copper using 0.1M HCl solution

Table 5.7: Desorption parameters

Adsorption cycle	Vol of 0.1 M HCl acid used (L)	% recovery
1st	1.3	94
2nd	1.1	99
3rd	1.1	91

5.7 Conclusions

A shrinking core model was used to describe the kinetics of metal adsorption in the chitosan beads. This model included the assumption of instantaneous adsorption inside the bead, which was confirmed by a microscopic study, showing a sharp interface between fresh and loaded adsorbent as a function of conversion. The shrinking core based, single particle model was tested with dynamic batch experiments, with the effective diffusion coefficient being the single fitting parameter. This model was able to describe the metal adsorption kinetics very well, and from the model, the effective diffusion coefficients were determined for copper, lead, cadmium and zinc adsorption and were in the range $(2.5\text{-}12.1)\cdot10^{-11}$ m^2/s, which is an order smaller than the diffusion coefficient of the metal in water. The diffusion coefficient for copper was influenced by the adsorbent modification, and mainly dependent on the water content in the bead, where a large diffusion coefficient correlated with a high water content.

The single particle model was extended to include external diffusion limitations, which are often present in adsorption columns, and the column was simulated as a CSTR's in series contactor in the absence of axial and radial dispersion. This model, despite the assumption of a constant pH in the column, described the experimental breakthrough curves fairly accurately, using the experimentally determined adsorption equilibrium parameters.

Five consecutive adsorption-desorption cycles were carried out and, despite the loss of some chitosan material, an improved efficiency in the second and third cycle was observed. The fourth and fifth cycle, however, showed a decreased efficiency, and the chitosan beads were physically damaged after the fifth cycle.

From the column desorption studies, it was observed that adsorbent can be regenerated at a concentration of about a thousand fold of the initial concentration, making further processing of the metal streams economically promising.

List of symbols and subscripts

a	specific surface area (m^2/kg)
C	metal concentration (mol/L)
C_B	bulk metal concentration (mol/L)
C^{int}_B	interface concentration (mol/L)
C_e	equilibrium metal concentration in solution (mol/L)
C_s	metal concentration at the bead surface (mol/L)
DCL	degree of cross-linking (dimensionless) (-)
D_{eff}	effective diffusivity of metal within the bead (m^2/s)
D_w	bulk liquid diffusion coefficient in water (m^2/s)
D	mean bead diameter (m)
F	ratio of the adsorption rate when $\theta=0$ to the rate for $\theta=\theta$
k	reaction (adsorption) rate constant ($m^3/s \cdot kg$ adsorbent)
k_L	external mass transfer coefficient (m/s)
q_{max}	maximum adsorption loading (mol/g)
q_{eq}	equilibrium adsorption loading (mol/g)
q(t)	adsorption loading rate (mol/g)
r	rate of metal adsorption (mol/s·kg adsorbent)
r_C	rate of metal adsorption at the inner core of bead (mol/s·kg adsorbent)
r_D	rate of metal diffusion (mol/s·kg adsorbent)
Re	Reynolds number ($Dv\rho/\mu$), dimensionless (-)
R_S	bead radius (m)
R_C	active core radius (m)
t	time (s)
v	bulk fluid velocity in the column (m/s)
Sc	Schmidt number ($\mu/D_w\rho$), dimensionless (-)
Sh	Sherwood number ($k_L D/D_w$), dimensionless (-)
η	effectiveness factor (-)

θ	fractional adsorbent loading, $q(t)/q_{eq}$ (-)
μ	viscosity (kg/m·s)
ρ	bead density (dry mass/wet volume) (kg/m^3)
ρ_f	fluid density (kg/m^3)
Φ	Thiele modulus (dimensionless) (-)
B	bulk fluid
C	in the core
f	fluid
0	for fresh beads
S	at particle surface
max	maximum

References

Bird R.B., Stewart, W.E. & Lightfoot, E.N. 1960. Transport phenomena, John Wiley and Son, New York.

Chen, J.P., Yoon, J.T. & Yiacoumi, S. 2003. Effect of chemical and physical properties of influent on copper sorption onto activated carbon fixed-bed column. *Carbon*, 41, 1635-1644.

Da Silva, E.A., Cossich, E.S., Tavares, C.R.G., Filho, L.C. & Guirardello, R. 2002. Modeling of copper(II) biosorption by marine alga *Sargassum* sp. in fixed-bed column. *Process Biochemistry*, 38, 791-799.

Erosa, D.M.S., Medina, T.I.S., Mendoza, R.N., Rodriguez, M.A. & Guibal, E. 2001. Cadmium sorption on chitosan sorbents: Kinetic and equilibrium studies, *Hydrometallurgy*, 61, 157-167.

Fogler, S.H. 1999. Elements of chemical reaction engineering. Third Edition, Publisher; Prentice-Hall Internation, Inc. 686-806.

Gerente, C., Mesnil, P. C.M., Jean-Francois, Y.A. & Le Cloirec, P. 2000. Removal of metal ions from aqueous solution on low cost natural polysaccharides. Sorption mechanism and approach. *Reactive and Functional Polymers,* 46, 135-144.

Guibal, E., Milot, C. & Roussy, J. 1999. Molybdate sorption by cross-linked chitosan beads: Dynamic studies. *Water Environment Research,* 71, 1-17.

Guibal, E., Milot, C. & Tobin, J.M. 1998. Metal-anion sorption by chitosan beads: Equilibrium and kinetic studies. *Industrial Engineering Chemical Research,* 37, 1454-1463

Hetzikioseyian, A., Tsezos, M. & Mavituna, F. 2001. Application of simplified rapid equilibrium models in simulating experimental breakthrough curves from fixed bed biosorption reactors. *Hydrometallurgy,* 59, 395-406.

Huang, C., Chung,Y. & Lion, M. 1996. Adsorption of Cu(II) and Ni(II) by pelletized biopolymer. *Journal of Hazardous Materials,* 45, 265-277.

Jansson-Charrier, M., Guibal, E., Roussy, J., Delanghe, B. & Le Cloirec, P. 1996 Vanadium (IV) sorption by chitosan: Kinetics and Equilibrium. *Water Research,* 30 (2), 465-475.

Johnson, P.D., Watson, M.A., Brown, J. & Jefcoat, I.A. 2002. Peanut hull pellets as a single use sorbent for the capture of Cu(II) from wastewater. *Waste Management,* 22, 471-480.

Kapoor, A. & Viraraghavan, T. 1998. Removal of heavy metals from aqueous solution using immobilized fungal biomass in continuous mode. *Water Research,* 32(6), 1968-1977.

Ko, D.C.K., Porter, J.F. & McKay, S.P. 2001. Film-pore diffusion model for the fixed-bed sorption of copper and cadmium ions onto bone char. *Water Resource,* 35(16), 3876-3886.

Kawamura, Y., Yoshida, H., Asai, S. & Tanibe, H. 1997. Breakthrough curve for adsorption of mercury (II) on polyaminated highly porous chitosan beads. *Water Science and Technology,* 35 (7), 97-105.

Mohan, D., Gupta, V.K., Srivastava, S.K. & Chander, S. 2001. Kinetics of mercury adsorption from wastewater using activated carbon derived from fertilizer waste. *Colloids and Surfaces, A Physical and Engineering Aspects,* 177, 169-181.

Monteiro, O.A.C. & Airoldi, C. 1999. Some studies of cross-linking chitosan-glutaraldehyde interaction in a homogeneuous system. *International Journal of Biological Macromolecules,* 29, 119-128

Monser, L. & Adhoum, N. 2002. Modified activated carbon for the removal of copper, zinc chromium and cyanide from wastewater. *Separation and Purification Technology,* 26, 137-146.

Nestle, N. & Kimmich, R. 1996. Heavy metal uptake of alginate gels studied by MNR microscopy. *Colloids and Surfaces, A: Physical and Engineering Aspects,* 115, 141-147.

Rhazi, M., Desbrieres, J., Tolaimate, A., Rinaudo, M., Vottero, P., Alagui, A. & El Meray, M. 2002. Influence of the nature of metal ions on the complexation with chitosan. Application to the treatment of liquid waste. *European Polymer Journal,* 38, 1523-1530.

Rorrer, G.L, Hein, T. & Way, D.J. 1993. Synthesis of porous-magnetic chitosan beads for removal of cadmium ions from waste water. *Industrial Engineering Chemical Research,* 32, 2170-2178.

Swan, G.A., McElrath, K.O., Baricos, W.H., Cohen, W. & Chambers, R.P. 1975. Heavy metal removal from aqueous media. In: I. Zwiebel and N.H. Sweed (eds.), *AIChE Symposium series: adsorption and ion exchange*, 152 (71), 96-103.

Wu, F.C., Tsang, R.L. & Juang, R.S. 2001. Kinetic modeling of liquid-phase adsorption of reactive dyes and metal ions on chitosan. *Water Research,* 35 (3), 613-608.

Zulfadhly, Z., Mashitah, M.D. & Bhatia, S. 2001. Heavy metal removal in a fixed-bed column by the macro fungus *Pycnoporus sanguineus*. *Environmental Pollution,* 112, 463-470.

Chapter 6 Conclusions, prospects and recommendations

6.1 Conclusions

The chitosan flakes that were synthesized from the exoskeleton of the *Jasus lalandii* had a molecular weight and degree of deacetylation of $9.4 \cdot 10^4$ g/mol and 83% respectively. The molecular weight decreased slightly to $7.8 \cdot 10^4$ g/mol when the flakes were converted to non-cross-linked beads.

Beads were prepared with a size of 0.9–3.8 mm and a concentration of 0-4vol% glutaraldehyde was used to stabilize the beads in acidic media. The non-cross-linked beads had an amine concentration of 4.9 mmol/g and this value decreased with increasing glutaraldehyde concentration and decreasing bead size. The degree of cross-linking was determined by comparing the amine concentration of the different beads, and the degree of cross-linking, which varied between 0 and 35%, therefore also increased with an increasing glutaraldehyde concentration and decreasing bead diameter. The water content in the beads increased with a decreasing degree of cross-linking and varied between 90 and 96%. The beads were stable at a pH of 2 when the degree of cross-linking was larger than 18%.

For modeling purposes, the pK_a of the chitosan was also determined, and was found to be 6.0 for the non-cross-linked beads; a value that is in agreement with the literature. The pK_a decreased with an increase in the degree of cross-linking so that the pK_a value for beads with a 35% degree of cross-linking was found to be 4.3. It was also found that the water in the beads was assessable for inert metals and that the distribution coefficient between the water in the beads and the bulk water was close to unity.

An equilibrium model that takes the effect of pH on the adsorption into account was used. From this model, together with the experimental results, it was determined that one hydroxide ion in the free solution and one amine group of the chitosan are involved in the metal complexation. It was shown that the DCL affects the equilibrium constant, and an increase in the DCL was found to decrease the equilibrium constant. The adsorption capacity was determined from the equilibrium model, and the values that were obtained were in close agreement with the amine concentration, determined in the characterization of the beads. The particle size had no significant influence on the adsorption equilibrium parameters.

Photographs from microscopic images from the adsorption of copper at fixed intervals revealed a shrinking core of the un-reacted particle and a shrinking core model was able to describe the uptake rates for all the metals studied in batch systems. The effective diffusion coefficients were calculated from the model and the calculated diffusion coefficients in the case for Copper(II), Cadmium(II), Lead(II) and Zinc(II) were $(2\text{-}12)\cdot10^{-11}$, $(6\text{-}10)\cdot10^{-11}$, $(4\text{-}7)\cdot10^{-11}$, and $(3\text{-}6)\cdot10^{-10}$ m^2/s respectively. It was found that the diffusion properties were influenced by the modification of the material and the diffusion coefficient decreased with an increase in the degree of cross-linking.

The application of the column model to experimental breakthrough curves shows a slight deviation with the model and this is attributed to the fluctuation of pH in the column. Column regeneration carried out with copper showed that up to three or four cycles of adsorption and desorption are possible, and the adsorbed metals can be concentrated into a high metal concentration.

The adsorption capacities of the produced chitosan were excellent compared to available literature values and benchmark materials, and recovery of the metal was successful. However, before chitosan can be introduced in the process industry, the bead stability has to be improved.

6.2 Prospects

The economic promise of chitosan in waste water remediation stems from the fact that it can be obtained from fishery waste. Most of the chitosan in the market today is currently produced from crab, lobster, shrimp, prawn, crawfish and krill shells discarded from canning industries in America, Japan, India, and Australia. Many countries, such as South Africa, Nigeria and Mexico, produce large amounts of unexploited shell waste material. A research report by Van der Westhuizen (2003), shows that 2000 tons of South African rock lobster alone is sold in the market yearly. A report by Ravi (2000) indicated that chitinous solid waste fraction of the average Indian landing of shell fish ranges from 60 000 to 80 000 tons. The reported and estimated global marine resources to currently seem to be in the order of between 10 and 100 million tons.

Fishery waste can be readily converted to chitosan. The disadvantage however is the large amounts of chemicals are involved in the processes of such conversion. According to No and Meyer (1997), it requires 6.2 kg of HCl and 1.8 kg of NaOH to produce 1 kg of 70% deacetylated chitosan from shrimp shells – this in addition to process water (0.5 t) and cooling water (0.9 t). The market value is as a result still very high relative to the costs of conventional adsorbents. The current price of chitosan as obtained from Biopolymer Engineering in the USA and France Chitin were US$25/kg and €25/kg respectively in 2005. The costs of production, and therefore the price of chitosan can be significantly reduced if large quantities are produced.

Another factor limiting the use of chitosan is its solubility in a low pH environment. This characteristic makes metal recovery through the use of acid troublesome. This limitation has been improved by cross-linking the material.

However, the capacity of chitosan for metal adsorption has been found to be equivalent to, or higher than that of other adsorbents such as activated carbon, cation exchange resin (Ambelite 200Na) and marine algae. Chitosan has many useful characteristics which other adsorbents do not have, the amine groups in chitosan can be used to modify the material by adding other compounds in order to improve adsorption performance or to increase its selectivity for certain metals. It can also be modified to suit the specific pH range required for the adsorption of a particular metal. It can be transformed into other applications such as water soluble polymers, modified flakes, modified gel beads, and membranes.

Although the use of gel beads for metal remediation has proved to be very efficient, especially with regard to column applications, large industrial applications have not been reported. This research has shown that chitosan beads in a column can be applied in a small scale pilot plant to remove low concentrations of metal ions from wastewater. The disadvantage of this process is the loss in the mass of beads during several regenerations. For the column process to be industrially feasible, the stability of the beads has to be improved in order to increase the number of possible regeneration cycles.

6.3 Recommendations

The recommendation of this study is therefore to investigate the possibility of increasing the stability of the beads, or by using other modifications of chitosan. In addition, a detailed technical and economical evaluation is recommend as a prerequisite for the entry of chitosan based adsorbent material into the competitive world of the chemical and mineral processing industry.

References

No, H.K. & Meyer, S.P. 1997. Preparation of chitin and chitosan. Chitin Hand Book. Edited by Muzzarilli, RAA & Peter, MG. European chitin society. 475-489.

Ravi-Kumar, N.V.M. 2000. A review of chitin and chitosan applications. *Reactive and Functional Polymers*, 46(1), 1-27.

Van der Wethuizen, O. 2003. Internal project report submitted to the School of Chemical and Minerals Engineering, North-West University, Potchefstroom.

APPENDIX A: Water quality standard, Government legislation on effluent discharge, Effect of heavy metals on environment.

Table A-1: Some General and Special Standards for Effluent (DWAF, 1998).

Parameter	General standard	Special standard
Colour, odour, or taste	No detectable colour, odour or taste	No detectable colour, odour or taste
pH	5.5-9.5	5.5-7.5
Temperature (°C)	<35	<25
OA (mg/L)	<10	<5
COD (mg/L)	<75	<30
Conductivity	<75 mS/m above that of intake water	15% above that of intake water
Suspended solids (mg/L)	<25	<10
Soap oil and grease (mg/L)	<2.5	nil
Sodium (mg/L)	<90 above that of intake water nil	<50 above that of intake water 1.5
Nitrate as N (mg/L)	0.50	0.50
Total Chromium, Cr (mg/L)	0.1	0.02
Phenolic compound as phenols (mg/L)	0.1	0.1
Lead (as Pb) mg/L	1.0	1.0
Copper (mg/L)	5.0	5.0
Zinc (mg/L)	0.05	0.05
Cadmium, as Cd (mg/L)	not specified	not specified
Nickel (mg/L)	0.5	0.1
Arsenic (mg/L)	not specified	0.3
Iron (mg/L)	0.5	0.5
Cyanide as CN^-	0.05	0.05
Mercury as Hg (mg/L)	0.05	0.05
Selenium as Se (mg/L)		

Table A-2: South Africa environmental laws affecting waste water emissions and health and safety in the industry (Data dynamic, 2004/www.ddyn.com).

Act	Principal focus	Problems targeted
Water Services and Regulations Act (1997)	Protection of water environment and effluent standard	Water quality and water reuse
Environmental Conservation and Regulation Act (1989)	Environmental protection	Protection of natural and social environment
Health Act (1977)	Control of pollution	Effect of pollutants on health
Occupational Health and Safety Act and Regulations (1993)	Ensuring adequate health and safety levels	Workers health and safety

Table A-3: Principal Constituents and Concentrations in the Untreated Effluent from Metal Finishing Processes (Buckley, 1987).

Constituent	Conc. (mg/L)	Constituent	Conc. (mg/L)
Fe^{2+}	1-10	CN^{-1}	1-50
Cu^{2+}	5-50	SO_4^{-2}	15-25
Ni^{2+}	2-15	Cl^{-1}	1-250
Cr^{6+}	10-120	CO_3^{-2}	10-50
Cr^{3+}	0.1-1.0	SIO_3^{-2}	30-50
Zn^{2+}	10-50	PO_4^{-3}	20-50
Cd^{2+}	10-50	organics	0.1-1.0
Sn^{2+}	0.1-20		

Table A-4: Heavy metals and the effects on the environment.

Metal		Effects
Copper	Low concentration	Imparts a strong astringent taste to water and staining of laundry and plumbing fittings
	High concentration	Gastrointestinal disturbances and possible liver, kidney and red blood cell damages. Severe poisoning with possible fatalities. Causes severe taste and staining problems.
Cadmium		In humans, long-term exposure can cause renal disfunction. High exposure can lead to obstructive lung disease and has been linked to lung cancer. It can also produce bone defect (osteomalacia, osteoporosis) in humans and animals. The metal can be linked to high blood pressure and effects on the myocardium in animals.
Zinc		At sufficiently high concentration it can cause gastrointestinal disturbances, zinc imparts an astringent taste, and opalescent or milk appearance to water.
Lead		High level of exposure may result in toxic biochemical effects in humans, which in turn cause problems in the synthesis of haemoglobin, effects on the kidney, gastrointestinal track, joints and reproductive system, and acute or chronic damage to the nervous system. At intermediate concentrations it can have small, subtle, subclinical effects, particularly on neuropsychological development in children.
Nickel		Short-term exposure to nickel is not known to cause any health problem, but long-term exposure can cause decrease in body weight, heart and liver damage, and skin irritation.

Table A-5: Summary of the practical applications of chitin derivative products.

Area	Chitin-based product	Application
Medicine	Chitin Chitin fiber Chitosan-collagen composite	Wound dressings Wound sutures Artificial skin
Cosmetics	Chitosan Hydroxyalkyl chitosan Liquid chitin	Cream and other skin-care products Hair stiffeners
Technical applications	Chitin membranes Depolymerized chitosan	Loudspeakers Adsorption of endotoxins and nucleic acid
Environmental	Chitosan and chitosan salts	Flocculation for purification Of protein-containing wastewater. Removal of metal ion
Agriculture	Chitosan	Compostation accelerator
Food technology	Chitosan	Food additive
Biotechnology	Chitosan	Porous particles for bioreactors immobilization of enzyme and cells
Chemistry	Chitosan Alkali chitin	Carrier of catalysts Intermediate for the synthesis of chitin derivative

APPENDIX B: Experimental procedures for dye absorption to measure DDA.

Dye absorption method using UV spectrophotometer.

A stock solution of the dye was prepared by dissolving 0.1750 g dye in 1 L of 0.1 M acetic acid. The precise molarity of this stock dye solution was determined from the absorbance value measured at 484 nm after diluting 10-fold with 0.1 m acetic acid solution. The absorption coefficient (ε) of C.I. Acid orange 7 in 0.1 M acetic acid at 484 nm is 22.500 cm^2/mol. Chitosan flakes were sieved through 100μm before being used. 0.1 g was accurately weighed into 1 L of 0.1 M acetic acid to dissolve. Aliquots (10 mL) of the stock dye solution were added to each of the ten 100 mL volumetric flasks and approximately 40 mL of 0.1 M acetic acid were added to each. The following volumes of chitosan solution were added to the volumetric flasks: 0, 2.0, 4.0, 6.0, 8.0, 10.0, 12.5, 15.0, 20.0, 25.0 mL and each solution was made up to the mark with 0.1 M acetic acid. The absorbance values were measured at 484 nm using 0.1 M acetic acid as a reference solution, with a Cary 50 Conc spectrophotometer connected to computer using Cary Win UV software. A graph of absorbance versus the volume of chitosan solution added was plotted. Two intersecting straight lines were observed, and the point of intersection gives the volume of chitosan solution that was equivalent in terms of amine groups concentration, to 10 mL of the stock dye solution of a known molarity. The equation for the calculation of the degree of N-acetylation was that given by Robert (1997).

APPENDIX C: Determination of α and amine concentration from titration results.

The total concentration of chitosan available for adsorption can be obtained from the analysis of titration data. Chitosan being a weak base, the pH in aqueous solution is slightly higher than that of a neutral solution. Chitosan beads, ground with a Teflon homogenizer were made into a solution of V_o mL. A pH probe electrode was inserted into the solution of chitosan and stirred continuously to attain equilibrium. The suspension was titrated with V_a of C_a standard hydrochloric acid. The initial equilibrium pH of chitosan solution before titration begins is pH_{ie} and the final equilibrium pH when ΔV mL of acid was added is pH_{fe}.

If a gram of chitosan was used, therefore, the amount of $[H^+]$ needed for equilibrium pH adjustment when ΔV mL of acid was added is;

$$(10^{-pH_{ie}} - 10^{-pH_{fe}})(\frac{V_o + \Delta V}{1000}) \text{ mol/g} \qquad \text{(i)}$$

ΔV is the change in volume of acid added at each interval of titration. The mol of acid per gram of bead added at this interval is,

$$\text{mol of } [H^+]/g = (\Delta V.C_a)/1000$$

The degree of protonation at this particular interval point of titration is;

$$\alpha_i = \frac{\left[\Delta VC_a - \left((10^{-pH_{ie}} - 10^{-pH_{fe}})(\frac{V_o + \Delta V}{1000})\right)\right]_i}{[-NH_2]_{Total}/g} \qquad \text{(ii)}$$

The equilibrium reaction of chitosan in aqueous solution is

$$-NH_2 + H^+ \Leftrightarrow -NH_3^+$$

therefore, the degree of protonation is

$$\alpha_i = \left[\frac{[H^+]}{10^{-pK_a} + [H^+]}\right]_i \qquad \text{(iii)}$$

The total amount of chitosan will definitely be the total mol of acid to neutralize the amino sites, this will come from the summation of all the moles of acid needed to affect pH changes at equilibrium from the onset (*i*) of titration to equivalent point (*e*). The total concentration of chitosan will be, from Equations (i) and (iii);

$$[-NH_2]_{Total}/g = \frac{\sum_i^e \left(\Delta V C_a - \left((10^{-pH_{ie}} - 10^{-pH_{fe}})(\frac{V_o + \Delta V}{1000}) \right) \right)}{\sum_i^e \left(\frac{[H^+]}{10^{-pK_a} + [H^+]} \right)} \qquad \text{(iv)}$$

This equation is used to calculate the DDA and DCL.

APPENDIX D: Titration results; beads cross-linked in 2.5% glutaraldehyde solution.

Table D-1: Titration experimental data.

Mass of chitosan beads	10.0	g
Total volume	1.0	L
Concentration of HCl	1.0	mol/L
pKa	4.3	
Diameter of bead	3.8	mm
Mol of chitosan/g	0.0042	mol/g

Burette reading (mL)	Acid added (mmol)	pH	α
9.0	0.0	8.90	0.071
9.3	0.3	6.78	0.095
9.4	0.4	5.78	0.190
9.8	0.8	5.55	0.238
10.0	1.0	5.35	0.310
10.3	1.3	4.96	0.404
10.7	1.7	4.82	0.476
11.0	2.0	4.7	0.547
11.3	2.3	4.61	0.618
11.6	2.6	4.53	0.690
11.9	2.9	4.48	0.760
12.2	3.2	4.43	0.855
12.6	3.6	4.21	0.925
12.9	3.9	3.88	0.984
13.2	4.2	3.52	0.986
13.5	4.5	2.65	0.988
13.7	4.7	2.37	0.990
14.0	5.0	2.10	0.997
14.3	5.3	1.92	0.998
14.5	5.5	1.83	0.999

APPENDIX E: Set out of Set I and Set II experiments.

Table E-1: Detailed illustration of Set I and Set II experiments.

Set I (adsorption)			Set II (adsorption)		
pH adjustment at equilibrium	Beads	Model	Initial pH (no pH adjustment at equilibrium)	Beads	Model
5-6	LC(3.8)(0.0) LC(3.8)(2.5) LC(3.8)(4.0) LC(0.9)(2.5) LC(1.8)(2.5)	Langmuir and Equilibrium models	2-5	LC(3.8)(0.0) LC(3.8)(2.5) LC(3.8)(4.0) LC(0.9)(2.5) LC(1.8)(2.5) CC(3.8)(0.0) CC(3.8)(2.5)	Equilibrium model
Set I (no desorption)			Set II (desorption)		
			Initial pH	Beads	
			1-3	LC(3.8)(2.5)	

APPENDIX F: Experimental equilibrium results plus Langmuir and equilibrium mode parameters

Metal loading capacity (mg/g) =

$$\frac{(\text{Initial metal concentration} \times \text{vol}) - (\text{Final metal concentration} \times \text{vol})}{\text{mass of dry beads}}$$

The Langmuir model was linearized as:

$\frac{C_{eq}}{q_e} = \frac{1}{q_m b} + \frac{C_e}{b}$ and the plot of the term in the left hand side versus the second term in right hand side were regressed and used to determined

the Langmuir parameters.

Table F-1: Adsorption isotherm of copper adsorption on LC(3.8)(2.5) beads at a pH 6

Proposed model parameters

Equil. pH	6.0	
pKa	4.3	
DOP	0.10	
$[H^+]$	0.001	mmol/L
Kads	0.0026	
b	2.19	L/mmol
qmax	4.2	mmol/g

Langmuir parameters

q_m	3.4	mmol/g
b	2.7	L/mmol
r^2	0.99	

Init.[Cu2+] (mg/L)	Final [Cu2+] (mg/L)	Vol (mL)	M of Cu ads (mg)	M of dBe (g)	qe (Exp) (mg/g)	qe, Langmuir (mg/g)	M of SO_4^{2-} ads. (mg)	Final [Cu2+] (mmol/L)	qe (Exp) (mmol/g)	qe, Lang (mmol/g)	qe, pH Model (mmol/g)
0	0.00	0.00	0.000	0.000	0.000	0.000	0.00	0.000	0.000	0.000	0.000
10.00	0.51	10.00	0.095	0.010	9.722	4.588	0.14	0.008	0.153	0.072	0.059
40.00	3.33	10.00	0.367	0.013	28.037	26.525	0.55	0.052	0.442	0.418	0.350
80.00	10.40	10.00	0.696	0.011	65.960	64.350	1.05	0.164	1.039	1.013	0.896
120.00	21.60	10.00	0.984	0.011	90.871	98.739	1.49	0.340	1.431	1.555	1.450
160.00	36.00	10.00	1.240	0.010	119.397	123.192	1.87	0.567	1.880	1.940	1.882
200.00	62.10	10.00	1.379	0.010	143.104	145.983	2.08	0.978	2.254	2.299	2.316
250.00	80.10	10.00	1.699	0.011	153.998	154.864	2.57	1.261	2.425	2.439	2.495
300.00	122.80	10.00	1.772	0.011	163.329	167.056	2.68	1.934	2.572	2.631	2.750
350.00	174.20	10.00	1.758	0.010	181.53	174.666	2.66	2.743	2.859	2.751	2.914

Table F-2: Adsorption isotherm of copper adsorption on LC(3.8)(2.5) beads at a pH 5.5

Adsorption on cross-linked beads at pH 5.5

Propssed model parameters

Equil. pH	5.5	
pKa	4.3	
DOP	0.12	
$[H^+]$	0.0032	mmol/L
Kads	0.0026	
b	0.56	L/mmol
qmax	4.2	mmol/g

Langmuir parameters

qm	3.3	mmol/g
b	0.71	L/mmol
r^2	0.94	

Init.[Cu2+] (mg/L)	Final [Cu2+] (mg/L)	Vol (mL)	M of Cu ads (mg)	M of dBe (g)	qe (Exp) (mg/g)	qe, Langmuir (mg/g)	M of SO42- ads. (mg)	Final [Cu2+] (mmol/L)	qe (Exp) (mmol/g)	qe, Lang (mmol/g)	qe, pH Model (mmol/g)
10.00	1.43	10.00	0.09	0.014	6.072	4.697	0.130	0.023	0.096	0.074	0.048
40.00	10.20	10.00	0.30	0.014	21.436	28.224	0.450	0.161	0.338	0.444	0.316
80.00	17.99	10.00	0.62	0.016	38.805	43.667	0.937	0.283	0.611	0.688	0.520
120.00	35.20	10.00	0.85	0.015	56.715	67.210	1.282	0.554	0.893	1.058	0.888
160.00	45.20	10.00	1.15	0.015	75.269	76.784	1.735	0.712	1.185	1.209	1.062
200.00	70.50	10.00	1.30	0.016	83.521	93.632	1.958	1.110	1.315	1.475	1.410
250.00	91.10	10.00	1.59	0.015	103.108	102.738	2.402	1.435	1.624	1.618	1.625
300.00	118.50	10.00	1.82	0.016	115.716	111.305	2.744	1.866	1.822	1.753	1.848
355.00	168.30	11.00	2.05	0.016	127.986	121.252	3.105	2.650	2.016	1.909	2.136

Table F-3: Adsorption isotherm of copper adsorption on LC(3.8)(2.5) beads at a pH 5.0

Proposed model parameters

Equil. pH	5.0	
pKa	4.3	
DOP	0.17	
$[H^+]$	0.010	mmol/L
Kads	0.0026	
b	0.17	L/mmol
qmax	4.2	mmol/g

Langmuir parameters

qm	2.1	mmol/g
b	0.39	L/mmol
r^2	0.94	

Init.[Cu2+] (mg/L)	Final [Cu2+] (mg/L)	Vol (mL)	M of Cu ads (mg)	M of dBe (g)	qe (Exp) (mg/g)	qe, Langmuir (mg/g)	M of SO42- ads. (mg)	Final [Cu2+] (mmol/L)	qe (Exp) (mmol/g)	qe, Lang (mmol/g)	Qe, pH Model (mmol/g)
10.00	4.20	10.00	0.06	0.014	4.044	3.399	0.088	0.066	0.064	0.054	0.040
40.00	23.10	10.00	0.17	0.015	11.630	16.564	0.255	0.364	0.183	0.261	0.210
80.00	41.20	10.00	0.39	0.016	24.853	26.637	0.587	0.649	0.391	0.419	0.357
120.00	65.30	10.00	0.55	0.015	35.398	37.331	0.827	1.028	0.557	0.588	0.533
160.00	95.00	10.00	0.65	0.015	43.478	47.529	0.983	1.496	0.685	0.748	0.724
200.00	119.30	10.00	0.81	0.015	53.117	54.153	1.220	1.879	0.836	0.853	0.862
250.00	150.30	10.00	1.00	0.015	67.351	61.011	1.507	2.367	1.061	0.961	1.019
300.00	187.40	10.00	1.13	0.015	74.206	67.525	1.702	2.951	1.169	1.063	1.183
350.00	244.20	11.00	1.16	0.014	80.617	75.079	1.759	3.846	1.270	1.182	1.395

Table F-4: Adsorption isotherm of copper adsorption on non-cross-linked beads at a pH 6

Proposed model parameters

Equil. pH	6.0	
pKa	6.0	
DOP	0.17	
$[H^+]$	0.001	mmol/L
Kads	0.004	
b	6.3	L/mmol
qmax	5.3	mmol/g

Langmuir parameters

qm	4.2	mmol/g
b	3.4	L/mmol
r^2	0.98	

Init.[Cu2+] (mg/L)	Final [Cu2+] (mg/L)	Vol (mL)	M of Cu ads (mg)	M of dBe (g)	qe (Exp) (mg/g)	qe, Langmuir (mg/g)	M of SO42- ads. (mg)	Final [Cu2+] (mmol/L)	qe (Exp) (mmol/g)	qe, Lang (mmol/g)	qe, pH Model (mmol/g)
10.00	1.00E-03	10.00	0.100	0.014	6.992	0.036	0.151	0.000	0.110	0.001	0.000
40.00	1.00E-03	10.00	0.400	0.015	27.397	0.036	0.605	0.000	0.431	0.001	0.000
80.00	1.00E-03	10.00	0.800	0.016	49.999	0.036	1.209	0.000	0.787	0.001	0.000
120.00	1.80E+00	10.00	1.182	0.016	75.682	49.501	1.787	0.028	1.192	0.780	0.515
160.00	6.40E+00	10.00	1.536	0.017	90.545	108.637	2.322	0.101	1.426	1.711	1.321
200.00	9.90E+00	10.00	1.901	0.018	108.018	130.146	2.874	0.156	1.701	2.050	1.685
240.00	2.13E+01	10.00	2.187	0.017	127.798	161.424	3.306	0.335	2.013	2.542	2.308
280.00	4.71E+01	10.00	2.329	0.014	164.350	182.260	3.521	0.742	2.588	2.870	2.801
320.00	6.20E+01	10.00	2.580	0.014	186.686	187.051	3.900	0.976	2.940	2.946	2.925
400.00	8.47E+01	10.00	3.153	0.017	182.814	191.311	4.766	1.334	2.879	3.013	3.039
500.00	1.94E+02	10.00	3.062	0.016	194.561	198.253	4.629	3.052	3.064	3.122	3.232
700.00	3.27E+02	10.00	3.731	0.019	200.926	200.553	5.640	5.148	3.164	3.158	3.298

APPENDIX G: Experiment results for equilibrium constant determination: Example of calculations

Beads used for adsorption = LC(3.8)(2.5)

Initial metal concentration, Co, = 200 mg/L

Final metal concentration, Ce, = 95 mg/L

Volume of solution = 0.247 L

Mass of dry beads = 0.215 g

$$\text{Mass of Cu adsorbed } (q_e)\,\text{mol/g} = \frac{(200-95)\times 0.246}{63.5\times 1000\times 0.215} = 0.00189\text{mol/g}$$

Equilibrium pH = 5.57

Degree of protonation (α) =0.22

Maximum capacity qmax = 0.0042 mol/g

n = 1

$$K = \frac{q_e}{n(1-\alpha)(q_{max}-q_e)^n C_e} = \frac{(0.00189)}{1(1-0.22)(0.0042-0.00189)^{\times 1}\times(\frac{95}{63.5\times 1000})} = 701.14\text{mol/g}$$

Log K = 2.84

Table G-1: Adsorption-desorption and equilibrium constant measurements with copper adsorption onto LC(3.8)(2.5) beads.

Equil. pH	Co (g/L)	Ce (g/L)	Vol (L)	M of Cu ads (mg)	Cu2+ aqu (mol/L)	Cu ads (mol)	M of dBe (g)	Cu2+ ads (mol/g)	DOP	[-NH2] (mmol/g)	K	log K
6.31	0.050	0.010	0.249	9.9E-03	1.58E-04	1.6E-04	2.16E-01	7.2E-04	1.5E-01	3.0E-03	6.3E+03	3.80
5.88	0.150	0.033	0.248	2.9E-02	5.16E-04	4.6E-04	3.47E-01	1.3E-03	1.9E-01	2.3E-03	1.9E+03	3.29
5.86	0.150	0.039	0.247	2.8E-02	6.07E-04	4.3E-04	3.59E-01	1.2E-03	1.9E-01	2.4E-03	1.6E+03	3.22
5.84	0.100	0.027	0.248	1.8E-02	4.23E-04	2.8E-04	3.53E-01	8.1E-04	1.9E-01	2.7E-03	2.4E+03	3.37
5.80	0.100	0.028	0.247	1.8E-02	4.38E-04	2.8E-04	3.72E-01	7.6E-04	2.0E-01	2.8E-03	2.3E+03	3.36
5.76	0.040	0.009	0.010	3.1E-04	1.41E-04	4.9E-06	5.82E-03	8.4E-04	2.0E-01	2.7E-03	2.2E+03	3.35
5.60	0.100	0.040	0.010	6.0E-04	6.22E-04	9.5E-06	6.48E-03	1.5E-03	2.1E-01	2.1E-03	1.1E+03	3.04
5.57	0.200	0.095	0.246	2.6E-02	1.49E-03	4.1E-04	2.15E-01	1.9E-03	2.2E-01	1.8E-03	6.7E+02	2.83
5.55	0.080	0.034	0.010	4.6E-04	5.28E-04	7.3E-06	5.63E-03	1.3E-03	2.2E-01	2.3E-03	1.1E+03	3.03
5.53	0.200	0.089	0.246	2.7E-02	1.40E-03	4.3E-04	2.19E-01	2.0E-03	2.2E-01	1.7E-03	8.1E+02	2.91
5.49	0.250	0.133	0.245	2.9E-02	2.09E-03	4.5E-04	1.82E-01	2.5E-03	2.2E-01	1.3E-03	4.8E+02	2.68
5.41	0.120	0.052	0.010	6.7E-04	8.21E-04	1.1E-05	6.11E-03	1.7E-03	2.3E-01	1.9E-03	1.1E+03	3.05
5.40	0.250	0.146	0.243	2.5E-02	2.30E-03	4.0E-04	2.13E-01	1.9E-03	2.3E-01	1.8E-03	4.5E+02	2.66
5.40	0.200	0.121	0.010	7.9E-04	1.91E-03	1.2E-05	6.03E-03	2.0E-03	2.3E-01	1.7E-03	6.5E+02	2.81
5.35	0.160	0.088	0.010	7.2E-04	1.38E-03	1.1E-05	5.79E-03	2.0E-03	2.4E-01	1.7E-03	8.2E+02	2.91
5.35	0.240	0.166	0.010	7.4E-04	2.61E-03	1.2E-05	6.24E-03	1.9E-03	2.4E-01	1.8E-03	4.0E+02	2.60
5.32	0.300	0.172	0.244	3.1E-02	2.70E-03	4.9E-04	2.14E-01	2.3E-03	2.4E-01	1.5E-03	5.8E+02	2.77
5.27	0.300	0.188	0.242	2.7E-02	2.95E-03	4.3E-04	2.24E-01	1.9E-03	2.4E-01	1.7E-03	3.7E+02	2.57
5.13	0.320	0.175	0.010	1.4E-03	2.76E-03	2.3E-05	1.18E-02	1.9E-03	2.5E-01	1.7E-03	4.2E+02	2.62
5.09	0.100	0.072	0.651	1.8E-02	1.13E-03	2.9E-04	4.06E-01	7.1E-04	2.6E-01	2.6E-03	2.4E+02	2.39

5.06	0.100	0.068	0.488	1.6E-02	1.06E-03	2.5E-04	3.82E-01	6.5E-04	2.6E-01	2.6E-03	2.3E+02	2.37
4.90	0.000	0.126	0.143	1.8E-02	1.98E-03	2.8E-04	3.55E-01	8.0E-04	3.0E-01	2.4E-03	1.7E+02	2.23
4.84	0.100	0.061	0.360	1.4E-02	9.55E-04	2.2E-04	3.83E-01	5.8E-04	2.8E-01	2.6E-03	2.3E+02	2.37
4.84	0.000	0.030	0.375	1.1E-02	4.67E-04	1.8E-04	8.21E-01	2.1E-04	3.2E-01	2.7E-03	1.7E+02	2.23
4.84	0.000	0.022	0.534	1.2E-02	3.43E-04	1.8E-04	7.96E-01	2.3E-04	3.2E-01	2.7E-03	2.5E+02	2.40
4.82	0.000	0.350	0.067	2.3E-02	5.51E-03	3.7E-04	2.53E-01	1.5E-03	4.1E-01	1.6E-03	1.6E+02	2.22
4.72	0.000	0.165	0.074	1.2E-02	2.59E-03	1.9E-04	2.55E-01	7.5E-04	4.4E-01	1.9E-03	1.5E+02	2.18
4.70	0.000	0.090	0.086	7.8E-03	1.42E-03	1.2E-04	2.52E-01	4.9E-04	4.5E-01	2.0E-03	1.7E+02	2.22
4.64	0.100	0.069	0.151	1.0E-02	1.09E-03	1.6E-04	4.07E-01	4.0E-04	3.0E-01	2.7E-03	1.4E+02	2.14
4.63	0.000	0.676	0.035	2.4E-02	1.06E-02	3.7E-04	2.42E-01	1.5E-03	5.0E-01	1.3E-03	1.1E+02	2.04
4.62	0.000	0.040	0.270	1.1E-02	6.34E-04	1.7E-04	7.85E-01	2.2E-04	3.5E-01	2.6E-03	1.3E+02	2.12
4.60	0.000	0.108	0.076	8.2E-03	1.70E-03	1.3E-04	2.20E-01	5.8E-04	3.6E-01	2.3E-03	1.5E+02	2.17
4.60	0.000	0.438	0.033	1.5E-02	6.89E-03	2.3E-04	2.13E-01	1.1E-03	3.6E-01	2.0E-03	7.9E+01	1.89
4.56	0.000	0.270	0.040	1.1E-02	4.25E-03	1.7E-04	2.29E-01	7.5E-04	3.7E-01	2.2E-03	8.1E+01	1.91
4.30	0.000	0.431	0.041	1.8E-02	6.78E-03	2.8E-04	3.47E-01	7.9E-04	4.3E-01	2.0E-03	6.0E+01	1.78
4.29	0.000	0.431	0.037	1.6E-02	6.79E-03	2.5E-04	3.59E-01	6.9E-04	4.3E-01	2.0E-03	5.1E+01	1.71
4.28	0.000	0.094	0.090	8.4E-03	1.48E-03	1.3E-04	8.19E-01	1.6E-04	4.3E-01	2.3E-03	4.8E+01	1.68
4.20	0.000	0.126	0.057	7.1E-03	1.98E-03	1.1E-04	7.80E-01	1.4E-04	4.5E-01	2.2E-03	3.3E+01	1.51
4.17	0.000	0.107	0.071	7.7E-03	1.69E-03	1.2E-04	7.36E-01	1.6E-04	4.8E-01	2.1E-03	4.6E+01	1.67
3.90	0.000	0.978	0.004	3.4E-03	1.54E-02	5.4E-05	2.19E-01	2.5E-04	7.7E-01	9.1E-04	1.8E+01	1.25
3.87	0.000	0.248	0.009	2.1E-03	3.91E-03	3.4E-05	7.83E-01	4.3E-05	8.0E-01	8.3E-04	1.3E+01	1.12
3.79	0.000	0.232	0.011	2.7E-03	3.65E-03	4.2E-05	7.58E-01	5.5E-05	8.2E-01	7.5E-04	2.0E+01	1.31

Table G-2: Adsorption and equilibrium constant measurements with copper adsorbed onto LC(0.9)(2.5) beads.

Equil. pH	Co (g/L)	Ce (g/L)	Vol (L)	M of Cu ads (mg)	Cu2+ aqu (mol/L)	Cu ads (mol)	M of dBe (g)	Cu2+ ads (mol/g)	DOP	[-NH2] (mmol/g)	K	log K
5.61	0.0400	0.0115	10.000	2.9E-01	1.80E-04	4.5E-06	1.22E-02	3.7E-04	2.1E-01	2.9E-03	7.1E+02	2.85
5.66	0.0800	0.0243	10.000	5.6E-01	3.82E-04	8.8E-06	1.33E-02	6.6E-04	1.3E-01	2.1E-03	8.1E+02	2.91
5.57	0.1200	0.0489	10.000	7.1E-01	7.70E-04	1.1E-05	1.30E-02	8.6E-04	1.2E-01	2.0E-03	5.7E+02	2.75
5.48	0.1600	0.0738	10.000	8.6E-01	1.16E-03	1.4E-05	1.25E-02	1.1E-03	1.4E-01	1.7E-03	5.4E+02	2.73
5.55	0.2000	0.0912	10.000	1.1E+00	1.44E-03	1.7E-05	1.30E-02	1.3E-03	1.6E-01	1.5E-03	6.1E+02	2.79
5.38	0.2400	0.1326	10.000	1.1E+00	2.09E-03	1.7E-05	1.38E-02	1.2E-03	1.8E-01	1.5E-03	3.8E+02	2.58
5.369	0.2800	0.1613	10.000	1.2E+00	2.54E-03	1.9E-05	1.30E-02	1.4E-03	1.8E-01	1.4E-03	4.1E+02	2.62
5.29	0.3200	0.2081	10.000	1.1E+00	3.27E-03	1.8E-05	1.25E-02	1.4E-03	1.8E-01	1.4E-03	3.1E+02	2.49
5.193	0.4000	0.2754	10.000	1.2E+00	4.33E-03	2.0E-05	1.32E-02	1.5E-03	1.9E-01	1.3E-03	2.6E+02	2.42

Table G-3: Adsorption and equilibrium constant measurements using LC(1.8)(2.5) beads.

Equil. pH	Co (g/L)	Ce (g/L)	Vol (L)	M of Cu ads (mg)	Cu2+ aqu (mol/L)	Cu ads (mol)	M of dBe (g)	Cu2+ ads (mol/g)	DOP	[-NH2] (mmol/g)	K	log K
5.84	0.04	0.01	10.000	3.1E-01	1.40E-04	4.89E-06	5.82E-03	8.4E-04	1.9E-01	2.6E-03	2.3E+03	3.37
5.50	0.075	0.03	10.000	4.2E-01	5.26E-04	6.55E-06	5.63E-03	1.2E-03	2.2E-01	2.2E-03	1.0E+03	3.00
5.60	0.1	0.04	10.000	6.1E-01	6.20E-04	9.55E-06	6.48E-03	1.5E-03	2.1E-01	2.0E-03	1.2E+03	3.08
5.47	0.12	0.06	10.000	6.1E-01	9.29E-04	9.61E-06	6.11E-03	1.6E-03	2.3E-01	1.9E-03	9.0E+02	2.95
5.35	0.16	0.09	10.000	6.8E-01	1.45E-03	1.07E-05	5.79E-03	1.8E-03	2.4E-01	1.6E-03	7.8E+02	2.89
5.40	0.2	0.12	10.000	7.9E-01	1.91E-03	1.24E-05	6.03E-03	2.1E-03	2.3E-01	1.5E-03	7.1E+02	2.85
5.22	0.24	0.16	10.000	8.0E-01	2.52E-03	1.26E-05	6.24E-03	2.0E-03	2.5E-01	1.5E-03	5.4E+02	2.73

Table G-4: Adsorption and equilibrium constant measurements using LC(3.8)(0.0) beads.

Equil. pH	Co (g/L)	Ce (g/L)	Vol (L)	M of Cu ads (mg)	Cu2+ aqu (mol/L)	Cu ads (mol)	M of dBe (g)	Cu2+ ads (mol/g)	DOP	[-NH2] (mmol/g)	K	log K
6.06	160	6.4000	0.010	1.5E+00	1.01E-04	2.42E-05	1.70E-02	1.4E-03	1.7E-01	3.2E-03	9.9E+03	4.00
6.01	200	9.9000	0.010	1.9E+00	1.56E-04	2.99E-05	1.76E-02	1.7E-03	1.8E-01	3.0E-03	6.4E+03	3.81
5.8	240	16.5000	0.010	2.2E+00	2.60E-04	3.52E-05	1.71E-02	2.1E-03	2.0E-01	2.6E-03	3.9E+03	3.59
5.64	280	25.2000	0.010	2.5E+00	3.97E-04	4.01E-05	1.40E-02	2.9E-03	2.1E-01	1.9E-03	3.8E+03	3.57
5.55	320	40.5000	0.010	2.8E+00	6.37E-04	4.40E-05	1.36E-02	3.2E-03	2.2E-01	1.6E-03	3.1E+03	3.50
5.45	400	52.0000	0.010	3.5E+00	8.18E-04	5.48E-05	1.70E-02	3.2E-03	2.3E-01	1.6E-03	2.4E+03	3.39
5.16	500	151.8000	0.010	3.5E+00	2.39E-03	5.48E-05	1.51E-02	3.6E-03	2.5E-01	1.3E-03	1.2E+03	3.08
5.04	700	285.9000	0.010	4.1E+00	4.50E-03	6.52E-05	1.78E-02	3.7E-03	2.6E-01	1.2E-03	6.7E+02	2.83

Table G-5: Adsorption and equilibrium measurements constant using LC(3.8)(4.0) beads.

Equil. pH	Co (g/L)	Ce (g/L)	Vol (L)	M of Cu ads (mg)	Cu2+ aqu (mol/L)	Cu ads (mol)	M of dBe (g)	Cu2+ ads (mol/g)	DOP	[-NH2] (mmol/g)	K	log K
5.75	0.12	0.03	0.010	8.6E-04	5.39E-07	1.35E-08	1.65E-02	8.2E-07	2.0E-01	3.0E-03	5.0E+02	2.70
5.60	0.16	0.06	0.010	9.7E-04	9.92E-07	1.53E-08	1.64E-02	9.3E-07	2.1E-01	3.0E-03	3.1E+02	2.50
5.64	0.2	0.07	0.010	1.3E-03	1.11E-06	2.04E-08	1.56E-02	1.3E-06	2.1E-01	3.0E-03	3.9E+02	2.59
5.50	0.24	0.09	0.010	1.5E-03	1.47E-06	2.31E-08	1.80E-02	1.3E-06	2.2E-01	3.0E-03	2.9E+02	2.47
5.42	0.28	0.13	0.010	1.5E-03	1.98E-06	2.43E-08	1.82E-02	1.3E-06	2.3E-01	2.9E-03	2.3E+02	2.36
5.31	0.32	0.19	0.010	1.3E-03	2.92E-06	2.12E-08	1.68E-02	1.3E-06	2.4E-01	2.9E-03	1.5E+02	2.17
5.27	0.4	0.24	0.010	1.6E-03	3.78E-06	2.51E-08	1.70E-02	1.5E-06	2.4E-01	2.9E-03	1.4E+02	2.13
5.09	0.6	0.44	0.010	1.6E-03	6.96E-06	2.48E-08	1.47E-02	1.7E-06	2.6E-01	2.8E-03	8.6E+01	1.93

Table G-6: Adsorption and equilibrium constant measurements using LC(3.8)(2.5) beads in copper and 0.25M sodium nitrate solutions

Equil. pH	Co (g/L)	Ce (g/L)	Vol (L)	M of Cu ads (mg)	Cu2+ aqu (mol/L)	Cu ads (mol)	M of dBe (g)	Cu2+ ads (mol/g)	DOP	[-NH2] (mmol/g)	K	log K
6.35	40	1.22	0.010	3.9E-01	1.92E-05	6.11E-06	1.78E-02	3.4E-04	1.5E-01	2.9E-03	6.1E+03	3.78
6.05	80	6.55	0.010	7.3E-01	1.03E-04	1.16E-05	1.97E-02	5.9E-04	1.7E-01	2.7E-03	2.1E+03	3.33
5.85	120	21.2	0.010	9.9E-01	3.34E-04	1.56E-05	2.02E-02	7.7E-04	1.9E-01	2.4E-03	9.4E+02	2.97
5.80	160	37.2	0.010	1.2E+00	5.86E-04	1.93E-05	1.99E-02	9.7E-04	2.0E-01	2.3E-03	7.3E+02	2.86
5.66	200	75.2	0.010	1.2E+00	1.18E-03	1.97E-05	1.99E-02	9.9E-04	2.1E-01	2.2E-03	3.7E+02	2.57
5.57	250	110.4	0.010	1.4E+00	1.74E-03	2.20E-05	2.11E-02	1.0E-03	2.2E-01	2.2E-03	2.8E+02	2.44
5.49	300	162.2	0.010	1.4E+00	2.55E-03	2.17E-05	2.13E-02	1.0E-03	2.2E-01	2.2E-03	1.8E+02	2.27
5.46	350	204.4	0.010	1.5E+00	3.22E-03	2.29E-05	2.07E-02	1.1E-03	2.3E-01	2.1E-03	1.6E+02	2.22
5.46	400	231.1	0.010	1.7E+00	3.64E-03	2.66E-05	2.04E-02	1.3E-03	2.3E-01	1.9E-03	1.9E+02	2.27
5.38	450	287.1	0.010	1.6E+00	4.52E-03	2.57E-05	2.00E-02	1.3E-03	2.3E-01	2.1E-03	1.4E+02	2.13

Table G-7: Adsorption and equilibrium constant measurements using LC(3.8)(2.5) beads in copper and 0.1M sodium nitrate solutions.

Equil. pH	Co (g/L)	Ce (g/L)	Vol (L)	M of Cu ads (mg)	Cu2+ aqu (mol/L)	Cu ads (mol)	M of dBe (g)	Cu2+ ads (mol/g)	DOP	[-NH2] (mmol/g)	K	log K
6.23	10	0.44	0.010	9.6E-02	6.93E-06	1.51E-06	1.54E-02	9.8E-05	1.6E-01	3.5E-03	4.1E+03	3.61
6.07	40	2.06	0.010	3.8E-01	3.24E-05	5.97E-06	1.56E-02	3.8E-04	1.7E-01	3.2E-03	3.7E+03	3.57
5.98	80	12.3	0.010	6.8E-01	1.94E-04	1.07E-05	1.83E-02	5.8E-04	1.8E-01	3.0E-03	1.0E+03	3.01
6.11	120	22.2	0.010	9.8E-01	3.50E-04	1.54E-05	1.56E-02	9.9E-04	1.7E-01	2.7E-03	1.1E+03	3.02
5.75	160	60.4	0.010	1.0E+00	9.51E-04	1.57E-05	1.55E-02	1.0E-03	2.0E-01	2.5E-03	4.2E+02	2.62
5.63	200	84.3	0.010	1.2E+00	1.33E-03	1.82E-05	1.60E-02	1.1E-03	2.1E-01	2.4E-03	3.5E+02	2.55
5.55	250	119	0.010	1.3E+00	1.87E-03	2.06E-05	1.69E-02	1.2E-03	2.2E-01	2.3E-03	2.8E+02	2.45
5.45	300	162.5	0.010	1.4E+00	2.56E-03	2.17E-05	1.66E-02	1.3E-03	2.3E-01	2.2E-03	2.3E+02	2.36
5.34	350	206.5	0.010	1.4E+00	3.25E-03	2.26E-05	1.64E-02	1.4E-03	2.4E-01	2.2E-03	2.0E+02	2.29

Table G-8: Adsorption and equilibrium constant measurements using LC(3.8)(2.5) beads in copper and 0.01M sodium nitrate solutions

Equil. pH	Co (g/L)	Ce (g/L)	Vol (L)	M of Cu ads (mg)	Cu2+ aqu (mol/L)	Cu ads (mol)	M of dBe (g)	Cu2+ ads (mol/g)	DOP	[-NH2] (mmol/g)	K	log K
6.09	20	1.8	0.010	1.8E-01	2.83E-05	2.87E-06	1.37E-02	2.1E-04	1.7E-01	3.3E-03	2.2E+03	3.35
6.02	50	5.78	0.010	4.4E-01	9.10E-05	6.96E-06	1.27E-02	5.5E-04	1.8E-01	3.0E-03	2.0E+03	3.30
6.02	80	10	0.010	7.0E-01	1.57E-04	1.10E-05	1.20E-02	9.2E-04	1.8E-01	2.7E-03	2.2E+03	3.33
5.94	120	16	0.010	1.0E+00	2.52E-04	1.64E-05	1.44E-02	1.1E-03	1.8E-01	2.5E-03	1.8E+03	3.26
5.74	160	42.1	0.010	1.2E+00	6.63E-04	1.86E-05	1.23E-02	1.5E-03	2.0E-01	2.2E-03	1.1E+03	3.02
5.58	200	65.1	0.010	1.3E+00	1.03E-03	2.12E-05	1.25E-02	1.7E-03	2.2E-01	2.0E-03	8.5E+02	2.93
5.52	250	87.1	0.010	1.6E+00	1.37E-03	2.57E-05	1.43E-02	1.8E-03	2.2E-01	1.9E-03	7.0E+02	2.84
5.42	300	144.6	0.010	1.6E+00	2.28E-03	2.45E-05	1.27E-02	1.9E-03	2.3E-01	1.8E-03	4.8E+02	2.68

Table G-9: Adsorption and equilibrium constant measurements using LC(3.8)(2.5) beads in copper and 0.001M sodium nitrate solutions

Equil. pH	Co (g/L)	Ce (g/L)	Vol (L)	M of Cu ads (mg)	Cu2+ aqu (mol/L)	Cu ads (mol)	M of dBe (g)	Cu2+ ads (mol/g)	DOP	[-NH2] (mmol/g)	K pH	log K (g/L)
5.88	20	2.63	0.010	1.7E-01	4.14E-05	2.74E-06	1.28E-02	2.1E-04	1.9E-01	3.2E-03	1.6E+03	3.20
5.98	50	6.56	0.010	4.3E-01	1.03E-04	6.84E-06	1.20E-02	5.7E-04	1.8E-01	3.0E-03	1.9E+03	3.27
5.86	80	12.2	0.010	6.8E-01	1.92E-04	1.07E-05	1.27E-02	8.4E-04	1.9E-01	2.7E-03	1.6E+03	3.21
5.94	120	16.8	0.010	1.0E+00	2.65E-04	1.63E-05	1.36E-02	1.2E-03	1.8E-01	2.5E-03	1.8E+03	3.27
5.73	160	52.3	0.010	1.1E+00	8.24E-04	1.70E-05	1.04E-02	1.6E-03	2.0E-01	2.1E-03	9.6E+02	2.98
5.61	200	65.4	0.010	1.3E+00	1.03E-03	2.12E-05	1.30E-02	1.6E-03	2.1E-01	2.0E-03	7.9E+02	2.90
5.43	250	81.5	0.010	1.7E+00	1.28E-03	2.65E-05	1.55E-02	1.7E-03	2.3E-01	1.9E-03	6.9E+02	2.84
5.37	300	154.5	0.010	1.5E+00	2.43E-03	2.29E-05	1.24E-02	1.8E-03	2.3E-01	1.8E-03	4.2E+02	2.62

Table G-10: Adsorption and equilibrium constant measurements using CC(3.8)(2.5) beads.

Equil. pH	Co (g/L)	Ce (g/L)	Vol (L)	M of Cu ads (mg)	Cu2+ aqu (mol/L)	Cu ads (mol)	M of dBe (g)	Cu2+ ads (mol/g)	DOP	[-NH2] (mmol/g)	K pH	log K (g/L)
5.68	120	48.20	0.010	7.2E-01	7.59E-04	1.13E-05	1.65E-02	6.8E-04	1.8E-01	2.6E-03	3.5E+02	2.55
5.87	160	65.20	0.010	9.5E-01	1.03E-03	1.49E-05	1.32E-02	1.1E-03	1.8E-01	2.2E-03	5.0E+02	2.70
5.50	200	126.80	0.010	7.3E-01	2.00E-03	1.15E-05	1.29E-02	9.0E-04	2.0E-01	2.3E-03	1.9E+02	2.29
5.39	250	172.40	0.010	7.8E-01	2.71E-03	1.22E-05	1.26E-02	9.7E-04	2.4E-01	2.2E-03	1.7E+02	2.22
5.28	350	258.30	0.010	9.2E-01	4.07E-03	1.44E-05	1.25E-02	1.2E-03	2.5E-01	2.0E-03	1.4E+02	2.16
5.50	200	102.3	0.010	9.8E-01	1.61E-03	1.54E-05	2.01E-02	7.7E-04	2.1E-01	2.4E-03	2.0E+02	2.30
5.39	300	164.2	0.010	1.4E+00	2.59E-03	2.14E-05	2.04E-02	1.0E-03	2.3E-01	2.1E-03	1.9E+02	2.28
5.57	400	210.8	0.010	1.9E+00	3.32E-03	2.98E-05	2.08E-02	1.4E-03	2.4E-01	1.8E-03	2.4E+02	2.38

Table G-11: Adsorption and equilibrium constant measurements using CC(3.5)(0.0) beads.

Equil. pH	Co (g/L)	Ce (g/L)	Vol. (L)	M of Cu ads (mg)	Cu2+ aqu (mol/L)	Cu ads (mol)	M of dBe (g)	Cu2+ ads (mol/g)	DOP	[-NH_2] (mmol/g)	K	log K
5.69	37.6	4.30	0.010	3.3E-01	6.77E-05	5.24E-06	1.80E-02	2.9E-04	2.1E-01	2.6E-03	1.6E+03	3.22
5.62	69.1	10.60	0.010	5.9E-01	1.67E-04	9.21E-06	1.72E-02	5.4E-04	2.1E-01	2.4E-03	1.3E+03	3.12
5.49	125.1	21.60	0.010	1.0E+00	3.40E-04	1.63E-05	2.04E-02	8.0E-04	2.2E-01	2.2E-03	1.1E+03	3.03
5.55	165.2	35.10	0.010	1.3E+00	5.53E-04	2.05E-05	1.87E-02	1.1E-03	2.2E-01	2.0E-03	1.0E+03	3.01
5.35	197.6	54.60	0.010	1.4E+00	8.60E-04	2.25E-05	1.94E-02	1.2E-03	2.3E-01	1.9E-03	7.2E+02	2.86
5.39	230	67.50	0.010	1.6E+00	1.06E-03	2.56E-05	1.94E-02	1.3E-03	2.3E-01	1.8E-03	7.1E+02	2.85
5.23	271.5	101.30	0.010	1.7E+00	1.60E-03	2.68E-05	1.74E-02	1.5E-03	2.5E-01	1.6E-03	6.2E+02	2.79
5.12	358.6	174.4	0.010	1.8E+00	2.75E-03	2.90E-05	1.80E-02	1.6E-03	2.6E-01	1.5E-03	4.0E+02	2.60

APPENDIX H: Shrinking core equations

Particle model

In an article by San *et al.* (1975) a particle rate theory is presented for the adsorption of metal ions using spherical particles. A shrinking core model is assumed (Figure H-1). In the shrinking core model the diffusion in the beads is the rate-limiting step. The adsorption is beginning in the outermost layers of the beads. When the capacity of the outer layer is reached, the copper is adsorbed onto the next layer.

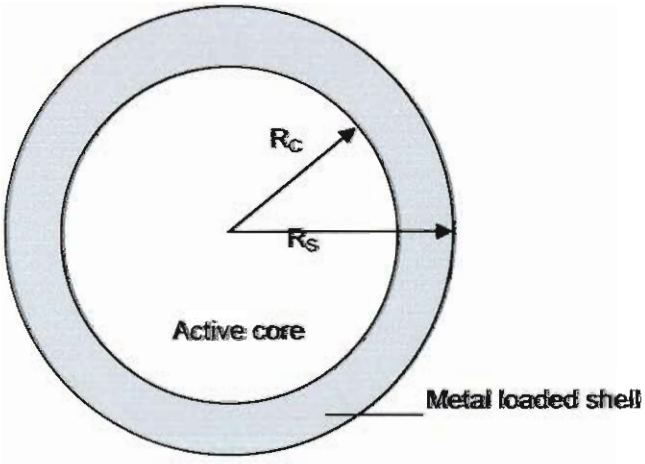

Figure H-1: A bead according to the shrinking core model

The outer shell, which is fully adsorbed with copper 'grows', and the core without copper 'shrinks'. The model is based on the assumption that the rate of diffusion through the outer fully loaded shell is equal to the rate of adsorption in the active core.

The rate of the adsorption may then be given by the relationship

$$\frac{\partial Q}{\partial t} = \eta_0 F k C_S \qquad \text{(v)}$$

In which:			
	Q	adsorption loading	mol/kg
	k	adsorption rate constant	m^3/s·kg adsorbent
	C_S	metal concentration at the bead surface	mol/m^3

The factor F is the ratio of the adsorption rate for a partly loaded bead over the adsorption rate for a fresh bead. η_0 is the effectiveness factor for fresh adsorbent. It is derived in a way similar to that for a heterogeneous catalysed first order reaction in a porous catalyst.

$$\eta_0 = \frac{1}{\Phi_S}\left(\frac{1}{\tanh 3\Phi_S} - \frac{1}{3\Phi_S}\right) \qquad \text{(vi)}$$

With the adsorption Thiele modulus

$$\Phi_S = \frac{R_S}{3}\left(\frac{k\rho}{D_{eff}}\right)^{1/2} \qquad \text{(vii)}$$

In which:			
	R_S	bead radius	m
	D_{eff}	effective diffusivity of metal within the bead	m^2/s
	ρ	bead density (dry mass/wet volume)	kg/m^3

The rate of diffusion through the beads is:

$$r_D = \frac{4\pi R^2 D_{eff} \cdot \partial C/\partial R}{4/3\,\pi R_S^3 \rho} = \frac{3D_{eff} R_S R_C (C_S - C_C)}{\rho R_S^3 (R_S - R_C)} \qquad \text{(viii)}$$

C_C	metal concentration in the core	mol/m^3
R_C	core radius	m

The rate of reaction in the inner core can be described with the following equation:

$$r_C = \frac{4/3\,\pi R_C^3 \rho \eta_C k C_C}{4/3\,\pi R_S^3 \rho} = \frac{R_C^3 \eta_C k C_C}{R_S^3} \qquad \text{(ix)}$$

The effectiveness factor for the unloaded core

$$\eta_C = \frac{1}{\Phi_C}\left(\frac{1}{\tanh 3\Phi_C} - \frac{1}{3\Phi_C}\right) \qquad \text{(x)}$$

The Thiele modulus for the unloaded core:

$$\Phi_C = \frac{R_C}{3}\left(\frac{k\rho}{D_{eff}}\right)^{1/2} \qquad \text{(xi)}$$

It was assumed that the rate of diffusion equals the rate of reaction. Equaling both equations and elimination the core concentration C_C gives:

$$r_D = r_C = \frac{\partial Q}{\partial t} = \frac{\eta_C k C_S}{\frac{R_S^3}{R_C^3} + \frac{3\eta_C \Phi_S^2 (R_S - R_C)}{R_C}} \qquad \text{(xii)}$$

A new variable is introduced, θ, which is the adsorption loading fraction, defined as q/q_{max}. It follows that $1-\theta=R_C^3/R_s^3$. Inserting this in Equation (xii) gives:

$$\frac{\partial Q}{\partial t} = \frac{\eta_C k C_S}{\frac{1}{1-\theta} + \frac{3\eta_C \Phi_S^2\left(1-(1-\theta)^{1/3}\right)}{(1-\theta)^{1/3}}} \qquad \text{(xiii)}$$

For fresh beads, when θ=0, the equation gives:

$$\frac{\partial Q}{\partial t} = \eta_0 k C_S \qquad \text{(xiv)}$$

The factor F (defined as the adsorption rate divided by the rate at θ=0) can now be calculated by dividing Equation (xiii) by Equation (xiv)

$$F = \frac{\eta_C / \eta_0}{\left(\frac{1}{1-\theta}\right) + 3\eta_C \Phi_S^2 \left(\frac{1-(1-\theta)^{1/3}}{(1-\theta)^{1/3}}\right)} \qquad \text{(xv)}$$

When diffusion becomes rate limiting, the Thiele modulus (Φ_S) becomes infinite.
As long as θ is not becoming unity:

$$F = \frac{3D_{eff}}{R_s^2 \cdot k \cdot \eta_0 \cdot \rho \left(\frac{1-(1-\theta)^{1/3}}{(1-\theta)^{1/3}}\right)} \qquad \text{(xvi)}$$

When in the lab a batch experiment is performed in which the Erlenmeyer is shaken properly, external diffusion can assumed not to be rate limiting. The metal concentration at the particle surface is the same as the concentration in the bulk. The adsorption rate equation then becomes:

$$\frac{\partial Q}{\partial t} = \eta_0 Fk \cdot C_B = \frac{3D_{eff} \cdot C_B}{R_s^2 \cdot \rho \left(\frac{1-(1-\theta)^{1/3}}{(1-\theta)^{1/3}}\right)} \qquad \text{(xvii)}$$

Column model I

When adsorption is done using beads packed in a column, the assumption that the copper concentration at the bead surface is equal to that in the bulk is no longer valid. A static layer will form around the beads by which the concentration at the bead surface will be smaller than in the bulk. The thickness of the layer depends on the velocity of the liquid phase.

The rate of adsorption equals the rate of diffusion through the beads and equals the diffusion through the static layer around the beads:

$$\frac{\partial Q}{\partial t} = \eta_0 Fk \cdot C_S = k_L a(C_B - C_S) \qquad \text{(xviii)}$$

with: k_L external mass transfer coefficient m/s

a	specific surface area	m^2/kg

Eliminating the concentration at the bead surface (C_S):

$$\frac{\partial Q}{\partial t} = \frac{k_L a \cdot \eta_0 Fk}{k_L a + \eta_0 Fk} C_B \qquad \text{(xix)}$$

Combining with Equation (xvi) gives:

$$\frac{\partial Q}{\partial t} = \frac{k_L a \dfrac{3D_{eff}}{R_s^2 \cdot \rho \left(\dfrac{1-(1-\theta)^{1/3}}{(1-\theta)^{1/3}} \right)}}{k_L a + \dfrac{3D_{eff}}{R_s^2 \cdot \rho \left(\dfrac{1-(1-\theta)^{1/3}}{(1-\theta)^{1/3}} \right)}} C_B \qquad \text{(xx)}$$

APPENDIX I: Batch kinetic experiments

$$\text{Mass of Cu adsorbed (mg)} = [Cu]_o - [Cu]_t \times Vol$$

$$\text{Adsorption loading (mg/g)} = \frac{\text{mass of Cu adsorbed (mg)}}{\text{gram dry beads (g)}} = \frac{[Cu]_o - [Cu]_t \times Vol}{g}$$

where $[Cu]_o$ = initial copper concentration

$[Cu]_t$ = copper concentration at time t

Table I-1: Adsorption kinetics of copper at concentrations of 25, 50 and 100 mg/L on LC(1.8)(2.5) beads at a pH 5.8

Time (min)	[Cu] mg/L	+/-	Vol (mL)	+/-	Mass of Cu in solt (mg)	+/-	Mass of Cu adsorbed (mg)	+/-	Ads. loading (mg/g)	Ads loading (mmol/g)
0	25	1.25	250	0.2	6.25	0	0	0.000	0.000	0.000
15	19.54	0.977	250	0.2	4.885	0.561	1.365	0.138	3.709	0.058
35	14.35	0.718	246	0.2	3.530	0.356	2.720	0.274	7.390	0.116
70	10.37	0.519	242	0.2	2.510	0.253	3.740	0.377	10.163	0.160
95	8.38	0.419	238	0.2	1.994	0.201	4.256	0.429	11.563	0.182
125	7.99	0.400	234	0.2	1.870	0.189	4.380	0.442	11.902	0.187
185	8.08	0.404	230	0.2	1.858	0.187	4.392	0.443	11.932	0.188
245	7.64	0.382	226	0.2	1.727	0.174	4.523	0.456	12.290	0.194
440	4.99	0.250	222	0.2	1.108	0.112	5.142	0.519	13.972	0.220
1490	2.81	0.141	218	0.2	0.613	0.062	5.637	0.569	15.317	0.241

Time (min)	[Cu] mg/L	+/-	Vol (mL)	+/-	Mass of Cu in solt (mg)	+/-	Mass of Cu adsorbed (mg)	+/-	Ads. loading (mg/g)	Ads loading mmol/g
0	50	2.50	250	0.2	12.500	0.000	0.000	0.000	0.000	0.000
15	41.6	2.08	250	0.2	10.400	1.153	2.100	0.212	5.766	0.091
30	36.27	1.81	246	0.2	8.922	0.899	3.578	0.361	9.823	0.155
55	30.8	1.54	242	0.2	7.454	0.752	5.046	0.509	13.855	0.218
100	29.24	1.46	238	0.2	6.959	0.702	5.541	0.559	15.213	0.240
149	26.08	1.30	234	0.2	6.103	0.615	6.397	0.645	17.564	0.277

205	23.8	1.19	230	0.2	5.474	0.552	7.026	0.709	19.291	0.304
325	20.34	1.02	226	0.2	4.597	0.464	7.903	0.797	21.699	0.342
495	15.85	0.79	222	0.2	3.519	0.355	8.981	0.906	24.659	0.388
1447	9.71	0.49	218	0.2	2.117	0.214	10.383	1.048	28.508	0.449

Time (min)	[Cu] mg/L	+/-	Vol (mL)	+/-	Mass of Cu in solt (mg)	+/-	Mass of Cu adsorbed (mg)	+/-	Ads. loading (mg/g)	Ads. loading (mg/g)
0	100.0	5	250	0.2	25	0	0	0	0	0
15	80.7	4.035	250	0.2	20.175	2.275	4.825	0.486	13.219	0.208
30	77.6	3.882	246	0.2	19.099	1.925	5.901	0.595	16.166	0.255
55	69.5	3.474	242	0.2	16.814	1.695	8.186	0.825	22.427	0.353
100	64.4	3.221	238	0.2	15.332	1.546	9.668	0.975	26.488	0.417
149	55.8	2.79	234	0.2	13.057	1.317	11.943	1.204	32.720	0.515
205	48.7	2.435	230	0.2	11.201	1.130	13.799	1.392	37.805	0.595
325	38.5	1.925	226	0.2	8.701	0.878	16.299	1.644	44.655	0.703
490	28.7	1.435	222	0.2	6.371	0.643	18.629	1.880	51.037	0.804
1455	15.2	0.76	218	0.2	3.314	0.334	21.686	2.189	59.415	0.936

Table I-2: Adsorption kinetics of copper at a concentration of 100 mg/L onto (LC(3.8)(0.0) beads at a pH 6.

Time (min)	[Cu] mg/L	+/-	Vol (mL)	+/-	Mass of Cu in solt (mg)	+/-	Mass of Cu adsorbed (mg)	+/-	ads. Loading (mg/g)	+/-	Ads load (mmol/g
0	100	5	250	0.2	25.00	0.00	0.00	-	0.00	0.00	0.00
17	65.7	3.285	250	0.2	16.43	2.08	8.58	0.86	22.56	0.10	0.36
38	58.4	2.92	246	0.2	14.37	1.45	10.63	1.07	27.97	0.10	0.44
60	50.9	2.545	242	0.2	12.32	1.24	12.68	1.28	33.36	0.10	0.53
78	43.7	2.185	238	0.2	10.40	1.05	14.60	1.47	38.40	0.10	0.60
108	33.2	1.66	234	0.2	7.77	0.78	17.23	1.74	45.33	0.10	0.71
137	28.6	1.43	230	0.2	6.58	0.66	18.42	1.86	48.46	0.10	0.76
197	20.1	1.005	226	0.2	4.54	0.46	20.46	2.06	53.81	0.10	0.85
255	16.4	0.82	222	0.2	3.64	0.37	21.36	2.16	56.19	0.10	0.88
380	11.9	0.595	218	0.2	2.59	0.26	22.41	2.26	58.94	0.10	0.93
580	7.1	0.355	214	0.2	1.52	0.15	23.48	2.37	61.77	0.10	0.97
1335	1.6	0.08	210	0.2	0.34	0.03	24.66	2.49	64.88	0.10	1.02
1515	2.6	0.13	206	1.2	0.54	0.06	24.46	2.59	64.35	0.11	1.01

Table I-3: Adsorption kinetics of copper at a concentration of 100 mg/L on LC(3.8)(2.5) beads at a pH 6.

Time (min)	[Cu] mg/L	+/-	Vol (mL)	+/-	Mass of Cu in solt (mg)	+/-	Mass of Cu adsorbed (mg)	+/-	ads. Loading (mg/g)	+/-	Ads loading mmol/g
0	100	5	250	0.2	25.00	0.00	0.00	-	0.00	0.00	0.00
18	75.2	3.76	250	0.2	18.80	2.21	6.20	0.62	17.01	0.10	0.27
44	75	3.75	246	0.2	18.45	1.86	6.55	0.66	17.97	0.10	0.28
76	66.9	3.345	242	0.2	16.19	1.63	8.81	0.89	24.17	0.10	0.38
132	59.3	2.965	238	0.2	14.11	1.42	10.89	1.10	29.87	0.10	0.47
328	32.5	1.625	234	0.2	7.61	0.77	17.40	1.75	47.72	0.10	0.75
468	24.1	1.205	230	0.2	5.54	0.56	19.46	1.96	53.38	0.10	0.84
567	19.3	0.965	226	0.2	4.36	0.44	20.64	2.08	56.62	0.10	0.89
1454	9.5	0.475	222	0.2	2.11	0.21	22.89	2.31	62.80	0.10	0.99

Table I-4: Adsorption kinetics of copper at a concentration of 100 mg/L on LC(0.9)(2.5) bead at a pH 6.

Time (min)	[Cu] mg/L	+/-	Vol (mL)	+/-	Mass of Cu in solt (mg)	+/-	Mass of Cu adsorbed (mg)	+/-	Ads. loading (mg/g)	Ads. loading (mmo/g)
0	100	5	250	0.2	25.000	0.000	0.000	0.000	0.000	0.000
10	79.3	3.965	250	0.2	19.825	2.257	5.175	0.522	10.911	0.172
25	66.9	3.345	246	0.2	16.457	1.659	8.543	0.861	18.012	0.284
44	58.7	2.935	242	0.2	14.205	1.432	10.795	1.088	22.760	0.358
69	51.1	2.555	238	0.2	12.162	1.226	12.838	1.295	27.069	0.426
92	48.9	2.445	234	0.2	11.443	1.154	13.557	1.367	28.585	0.450
118	45.5	2.275	230	0.2	10.465	1.056	14.535	1.466	30.646	0.483
150	42.8	2.14	226	0.2	9.673	0.976	15.327	1.546	32.316	0.509
285	36.3	1.815	222	0.2	8.059	0.813	16.941	1.709	35.720	0.563
505	32.1	1.605	218	0.2	6.998	0.706	18.002	1.817	37.957	0.598
1360	23.56	1.178	214	0.2	5.042	0.509	19.958	2.014	42.081	0.663
1525	23.38	1.169	210	0.2	4.910	0.496	20.090	2.028	42.359	0.667

Table I-5: Adsorption kinetic of copper at a concentration of 100 mg/L on LC(3.8)(4.0) beads at a pH 6.

Time (min)	[Cu] mg/L	+/-	Vol (mL)	+/-	Mass of Cu in solt (mg)	+/-	Mass of Cu adsorbed (mg)	+/-	Ads. loading (mg/g)	+/-	Ads loading (mmol/g)
0	100	5	250	0.2	25.00	0.00	0.00	-	0.00	0.00	0.00
17	70.7	3.535	250	0.2	17.68	2.15	7.33	0.74	16.41	0.10	0.26
38	69.4	3.47	246	0.2	17.07	1.72	7.93	0.80	17.76	0.10	0.28
60	67.2	3.36	242	0.2	16.26	1.64	8.74	0.88	19.58	0.10	0.31
78	64.3	3.215	238	0.2	15.30	1.54	9.70	0.98	21.72	0.10	0.34
108	60.9	3.045	234	0.2	14.25	1.44	10.75	1.08	24.08	0.10	0.38
137	61.4	3.07	230	0.2	14.12	1.42	10.88	1.10	24.37	0.10	0.38
197	55.4	2.77	226	0.2	12.52	1.26	12.48	1.26	27.96	0.10	0.44
255	50.6	2.53	222	0.2	11.23	1.13	13.77	1.39	30.84	0.10	0.49
380	41.9	2.095	218	0.2	9.13	0.92	15.87	1.60	35.55	0.10	0.56
580	32.6	1.63	214	0.2	6.98	0.70	18.02	1.82	40.38	0.10	0.64
1335	21.1	1.055	210	0.2	4.43	0.45	20.57	2.08	46.08	0.10	0.73
1515	20.9	1.045	206	1.2	4.31	0.46	20.69	2.19	46.36	0.11	0.73

APPENDIX J: Curves of adsorption kinetics for lead, cadmium and zinc

Experimental curves from the adsorption of cadmium, lead and zinc, and the model curves with lines.

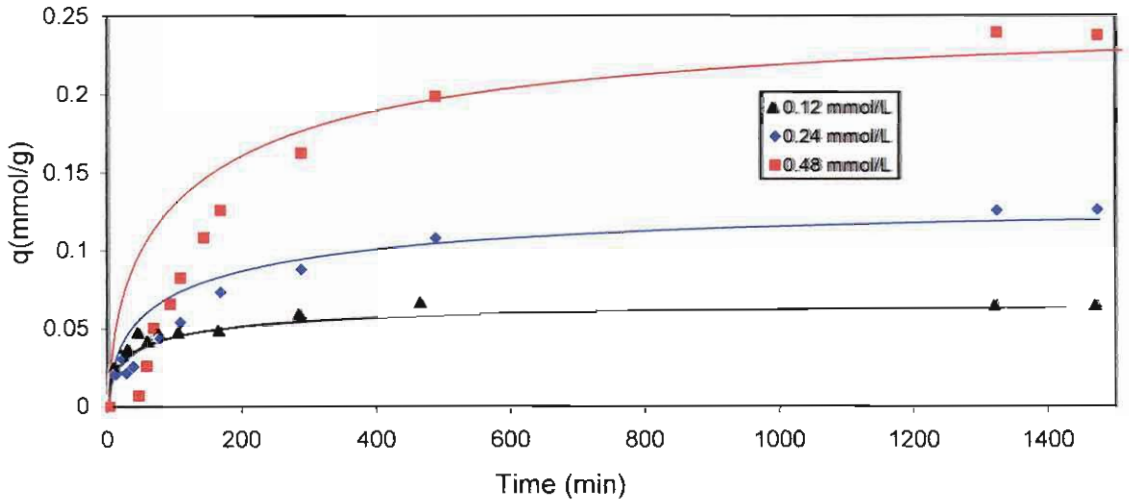

Figure J-1: Lead(II) adsorption rate onto chitosan beads.

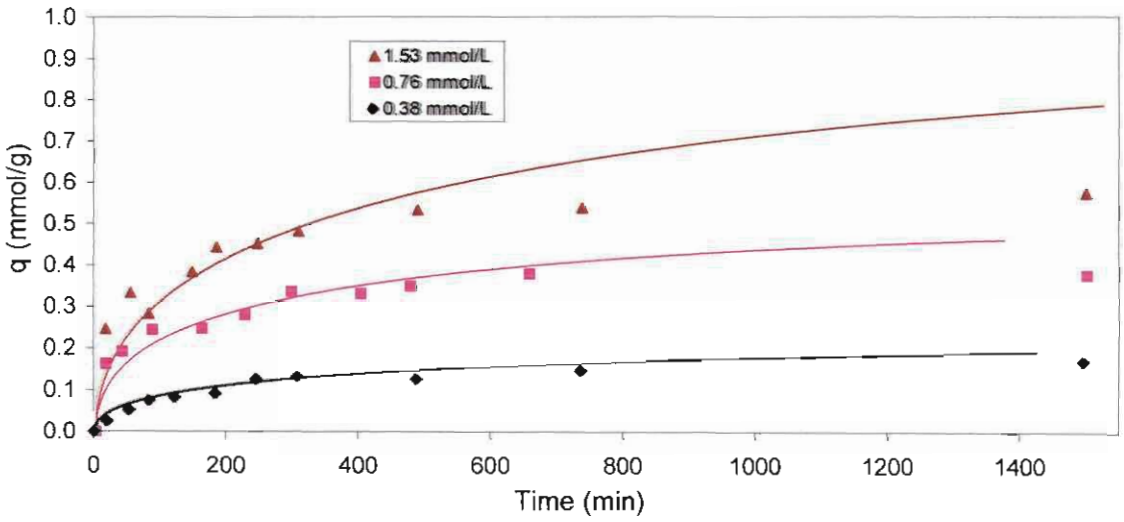

Figure J-2: Zinc(II) ions adsorption rate onto chitosan beads.

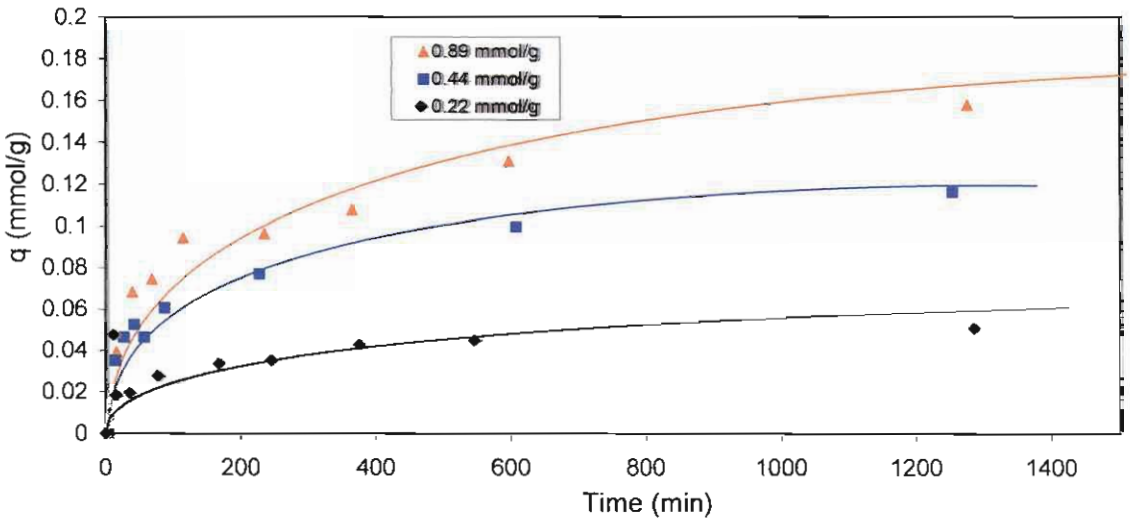

Figure J-3: Cadmium(II) ion adsorption rate onto chitosan beads.

APPENDIX K: Column adsorption and desorption results

Table K-1: First adsorption and desorption cycle data from column

Inlet pH		5.5	
Diameter of column		2.54	cm
Height of column		40.5	cm
Cross sectional area		4.67782857	cm^2
Volume of the column		189.452057	cm^3
Empty mass of column A		188.66	g
Mass of wet beads + column A		302.28	g
Pump flow rate thru the column		7.2	mL/min
Measured void vol		64	mL
Measured bed vol		128.684	mL
Initial $[Cu^{2+}]$	Ave	8.1	mg/L
Density		1100	kg/m^3
Mass of wet beads		114	g

Adsorption

Time min	Time hr	No of Bed volume	Outlet $[Cu^{2+}]$ (mg/L)	C/Co	Outlet pH
0.00	0.00	0.00	0	0	
60.00	1.00	3.78	0.02	0.0024691	7.12
145.00	2.42	9.14	0.025	0.0030864	7.4
210.00	3.50	13.24	0.03	0.0037037	
270.00	4.50	17.02	0.04	0.0049383	7.34
340.00	5.67	21.44	0.03	0.0037037	
450.00	7.50	28.37	0.03	0.0037037	7.53
580.00	9.67	36.57	0.11	0.0135802	7.38
780.00	13.00	49.18	0.58	0.0716049	6.54
960.00	16.00	60.53	1.29	0.1592593	6.42
1120.00	18.67	70.62	2.65	0.3271605	
1240.00	20.67	78.18	3.37	0.4160494	6.23
1365.00	22.75	86.07	4.08	0.5037037	5.94
1430.00	23.83	90.16	4.41	0.5444444	
1495.00	24.92	94.26	4.88	0.6024691	
1568.00	26.13	98.87	5.23	0.645679	
1648.00	27.47	103.91	5.32	0.6567901	
1735.00	28.92	109.40	5.66	0.6987654	5.96
1840.00	30.67	116.02	6.03	0.7444444	
1900.00	31.67	119.80	6.21	0.7666667	5.89

2020.00	33.67	127.37	6.36	0.7851852	5.88
2270.00	37.83	143.13	6.89	0.8506173	5.82
2640.00	44.00	166.46	7.45	0.9197531	5.74
3015.00	50.25	190.10	7.71	0.9518519	5.8
3135.00	52.25	197.67	7.33	0.9049383	5.77
3240.00	54.00	204.29	7.9	0.9753086	5.77

Desorption

Time (min)	Time (h)	No Bed volume	Vol (L)	Outlet $[Cu^{2+}]$ (mg/L)	Out pH
0.00	0.00	0.00	0	0.99	3.24
14.00	0.86	0.10	0.06		3.20
60.00	3.67	0.43	171.6	0.97	3.16
75.00	4.59	0.54	142.6	0.97	3.17
95.00	5.81	0.68	86.8		7.34
110.00	6.73	0.79	46.6	0.97	3.07
125.00	7.65	0.90	38.7	0.97	2.23
145.00	8.88	1.04	35	0.95	1.54
185.00	11.32	1.33	26.38		1.32
255.00	15.61	1.84	18.25		1.23
360.00	22.04	2.59	10.62	0.99	1.23
420.00	25.71	3.02	7.21	0.99	1.27
630.00	38.56	4.54	1.24	1	1.25
960.00	58.76	6.91	0.34	1.04	1.28
1155.00	70.70	8.32	0.43	1	1.27
1195.00	73.15	8.60	0.34	1	1.26

Table K-2: Second adsorption and desorption cycle data from column

Diameter of column		2.54	cm
Inlet pH		5.5	
Height of column		40.5	cm
Cross sectional area		4.68	cm^2
Volume		189.45	cm^3
Empty mass of column A		188.66	g
Mass of wet beads + column A		285.88	g
Pump flow rate thru the column		7.2	mL/min
Measured void vol		64	mL
Measured bed vol		128.684	mL
Initial $[Cu^{2+}]$	Ave	8.1	mg/L
Density		1100	kg/m^3
Mass of wet beads		97.2	g

Adsorption

Time (min)	Time (h)	No Bed volume	Vol (L)	Outlet $[Cu^{2+}]$ (mg/L)	Out pH
0.00	0.00	0.00	0.00	0	
30.00	0.50	2.21	0.21600	0.03	7.12
65.00	1.08	4.79	0.46800	0.03	7.4
88.00	1.47	6.48	0.63360	0.03	
120.00	2.00	8.84	0.86400	0.04	7.34
154.00	2.57	11.35	1.10880	0.02	
210.00	3.50	15.47	1.51200	0.03	7.53
280.00	4.67	20.63	2.01600	0.03	7.38
340.00	5.67	25.05	2.44800	0.03	6.54
450.00	7.50	33.16	3.24000	0.03	6.42
690.00	11.50	50.85	4.96800	0.03	
885.00	14.75	65.21	6.37200	0.03	6.23
1200.00	20.00	88.43	8.64000	0.05	5.94
1470.00	24.50	108.32	10.58400	0.06	
1830.00	30.50	134.85	13.17600	0.08	
2100.00	35.00	154.75	15.12000	0.09	
2560.00	42.67	188.64	18.43200	0.26	
3030.00	50.50	223.28	21.81600	0.43	5.96
3480.00	58.00	256.44	25.05600	0.97	
3540.00	59.00	260.86	25.48800	1.3	5.89
4200.00	70.00	309.49	30.24000	1.84	5.88

4245.00	70.75	312.81	30.56400	2.28	5.82
4955.00	82.58	365.13	35.67600	3.15	5.47
5790.00	96.50	426.66	41.68800	3.99	5.48
6390.00	106.50	470.87	46.00800	4.64	5.46
6960.00	116.00	512.87	50.11200	5.23	5.36
7710.00	128.50	568.14	55.51200	5.67	5.26

Desorption

Time (min)	No of Bed volume	Vol (L)	Inlet $[Cu^{2+}]$ (mg/L)	Outlet $[Cu^{2+}]$ (mg/L)	Inlet pH	Out pH
0.00	0.00		0	0	1.08	
15.00	1.35	0.12	0	4.4	1.09	
25.00	2.26	0.20	0	9.3	1.07	3.16
35.00	3.16	0.28	0	29.4	1.07	3.17
47.00	4.24	0.37	0	265.3	1.07	7.34
51.00	4.61	0.40	0	625.2	1.07	3.07
58.00	5.24	0.46	0	1750	1.06	2.23
62.00	5.60	0.49	0	2495	1.06	1.54
70.00	6.32	0.55	0	2530	1.06	1.32
85.00	7.68	0.67	0	1550	1.05	1.23
95.00	8.58	0.75	0	460.2	1.09	1.23
133.00	12.01	1.05	0	18.57	1.05	1.27
190.00	17.16	1.50	0	2.85		1.25
275.00	24.83	2.17	0	1.68	1.09	1.28
385.00	34.76	3.04	0	1.35	1.09	1.27
480.00	43.34	3.79	0	0.8		1.26

Table K-3: Third adsorption and desorption cycle data from column

Diameter of column		2.54	Cm
Inlet pH		5.5	
Height of column		40.5	cm
Cross sectional area		4.6778286	cm^2
Volume		189.45206	cm^3
Empty mass of column A		188.66	g
Mass of wet beads + column A		280.02	g
Pump flow rate thru the column		7.2	mL/min
Measured void vol		64	mL
Measured bed vol		128.684	mL
Initial $[Cu^{2+}]$	Ave	8.1	mg/L

Density	1100	kg/m^3
Mass of wet beads	91.36	g

Desorption

Time hr	No Bed volume	Inlet $[Cu^{2+}]$ (mg/L)	Outlet $[Cu^{2+}]$ (mg/L)	Outlet pH
0.00	0.00	8.1	0	
2.08	9.80	8.1	0.13	7.12
5.08	23.92		0.46	7.4
7.08	33.33		0.64	
10.83	50.97	8.2	0.7	7.34
23.00	108.21	8.12	0.66	
37.50	176.43	8.14	0.96	7.53
49.75	234.07	8.1	0.81	7.38
60.08	282.69	8.12	1.38	6.54
71.00	334.05		1.66	6.42
81.25	382.27		2.26	
97.25	457.55		4	6.23
120.87	568.67		5.72	5.94
144.25	678.68		6.2	
151.82	714.28		7.23	
173.08	814.34			
178.58	840.22	8.19	7.43	5.81